

Western Michigan University
Civil and Construction Engineering Department

**A Sensor Network System for the Health Monitoring
of the Parkview Bridge Deck**

By:

Osama Abudayyeh, Ph. D., P.E.
Professor and Associate Dean
Department of Civil and Construction Engineering
College of Engineering and Applied Sciences
Western Michigan University
Kalamazoo, MI 49008-5314

Sponsored by Michigan Department of Transportation

Technical Report Number RC-1536

January 2010

Technical Report Documentation Page

1. Report No. RC 1536	2. Government Accession No.	3. MDOT Project Manager Steve Kahl, P.E.	
4. Title and Subtitle A Sensor Network System for the Health Monitoring of the Parkview Bridge Deck		5. Report Date January 31, 2010	
7. Author(s) Dr. Osama Abudayyeh, P.E. Principal Investigator		6. Performing Organization Code	
9. Performing Organization Name and Address Western Michigan University 1903 W. Michigan Ave, Kalamazoo, MI		8. Performing Org Report No.	
12. Sponsoring Agency Name and Address Michigan Department of Transportation Construction and Technology Division PO Box 30049, Lansing MI 48909		10. Work Unit No.	
		11. Contract Number :	
		11(a). Authorization Number:	
15. Supplementary Notes		13. Type of Report and Period Covered Final Report, 2005-2010	
		14. Sponsoring Agency Code	
16. Abstract <p>Bridges are a critical component of the transportation infrastructure. There are approximately 600,000 bridges in the United State according to the Federal Highway Administration. Four billion vehicles traverse these bridges daily. Regular inspection and maintenance are essential components of any bridge management program to ensure structural integrity and user safety. Even though intensive bridge inspection and maintenance are being performed nationwide, the outcomes are not necessarily impressive. It has been reported that of the 600,000 bridges, 12% have been deemed structurally deficient, and another 13% have been declared functionally obsolete. Consequently, 25% of the nations' bridges require immediate attention or repair and may present safety challenges. This suggests a need for effective, continuous monitoring systems so that problems can be identified at early stages and economic measures can be taken to avoid costly replacement and/or bridge failures. Therefore, there is a need for bridge health monitoring technologies and systems to enable continuous monitoring and real time data collection.</p> <p>A sensor-based bridge health monitoring system was developed and deployed for the newly constructed Parkview Bridge in Kalamazoo, Michigan. This system adopted rapid bridge construction techniques using precast concrete technology. Today, these sensor networks, also known as health monitoring systems (SHM), can be used to develop models to determine how a structure is behaving internally. Sensors were installed at strategic locations and connected to a remote computer workstation via telephone lines. Continuous bridge condition data are being collected in real time, archived in the laboratory computer workstation, and analyzed to assess the structural performance and integrity. This continuous information can greatly increase bridge safety for its users by providing early warning signs before a failure occurs.</p> <p>Furthermore, a methodology for assessing the savings in time and cost associated with adopting Rapid Bridge Construction (RBC) techniques was developed and used in this research project. A comparison study was carried out to assess the performance of RBC technique at the Parkview Bridge. The RBC technique was found to save bridge construction time and consequently realize savings in extra travel time. This travel time saving is significant enough that it justifies the relatively high initial cost of the RBC technique.</p>			
17. Key Words: Sensor Network, Structural Health Monitoring, Rapid Bridge Construction, Vibrating Wires Strain Gauges, Load Testing, Full-Depth Deck Panels		18. Distribution Statement No restrictions. This document is available to the public through the Michigan Department of Transportation.	
19. Security Classification (report) Unclassified	20. Security Classification (Page) Unclassified	21. No of Pages 95 (excluding the CD of Appendix D)	22. Price

ABSTRACT

Bridges are critical components of the transportation infrastructure. There are approximately 600,000 bridges in the United State according to the Federal Highway Administration. Four billion vehicles traverse these bridges daily. Regular inspection and maintenance are essential components of any bridge management program to ensure structural integrity and user safety. Even though intensive bridge inspection and maintenance are being performed nationwide, the outcomes are not necessarily impressive. It has been reported that of the 600,000 bridges, 12% have been deemed structurally deficient and another 13% have been declared functionally obsolete. Consequently, 25% of the nations' bridges require immediate attention or repair and may present safety challenges. This suggests a need for effective, continuous monitoring systems so that problems can be identified at early stages and economic measures can be taken to avoid costly replacement and/or bridge failures. Therefore, there is a need for bridge health monitoring technologies and systems to enable continuous monitoring and real time data collection.

A sensor-based bridge health monitoring system was developed and deployed for the newly constructed Parkview Bridge in Kalamazoo, Michigan. This system adopted rapid bridge construction techniques using precast concrete technology. Today, these sensor networks, also known as health monitoring systems (SHM), can be used to develop models to determine how a structure is behaving internally. Sensors were installed at strategic locations and connected to a remote computer workstation via telephone lines. Continuous bridge condition data are being collected in real time, archived in the laboratory computer workstation, and analyzed to assess the structural performance and integrity. This continuous information can greatly increase bridge safety for its users by providing early warning signs before a failure occurs.

Furthermore, a methodology for assessing the savings in time and cost associated with adopting Rapid Bridge Construction (RBC) techniques was developed and used in this research project. A comparison study was carried out to assess the performance of RBC technique at the Parkview Bridge. The RBC technique was found to save bridge construction time and consequently realize savings in extra travel time. This travel time saving is significant enough that it justifies the relatively high initial cost of the RBC technique.

ACKNOWLEDGEMENTS

This project was sponsored by the Michigan Department of Transportation (MDOT (Contract # 04-0090/Z3 – SPR # 101688). The assistance of Mr. Steve Kahl of the Michigan Department of Transportation (MDOT) Construction and Technology Support is greatly appreciated. Also, the support from Ms. Bobbi Welke, Mr. Pete Pfeiffer, Ms. Zhizhen Liu, Ms. Janine Cooper, and Mr. Jim Woods of the MDOT Southwest Region Office is acknowledged and greatly appreciated. Any opinions, findings, conclusions, or recommendations expressed in this material are those of the authors and do not necessarily reflect the views of MDOT or Western Michigan University.

DISCLAIMER

The contents of this report reflect the views of the authors who are responsible for the facts and the accuracy of the data presented herein. The contents do not necessarily reflect the official views or policies of the Michigan Department of Transportation, nor Western Michigan University. This report does not constitute a standard, specification, or regulation. Trade or manufacturers' names, which may appear in this report, are cited only because they are considered essential to the objectives of the report. The United States (U.S.) government and the State of Michigan do not endorse products or manufacturers.

PROJECT TEAM

Principal Investigator:

Osama Abudayyeh, Ph. D., P.E. (December 2005 – January 2010)
Department of Civil and Construction Engineering
Western Michigan University, Kalamazoo, MI

Co-Principal Investigators:

Ikhlas Abdel-Qader, Ph.D., P.E. (December 2005 – January 2010)
Associate Professor
Department of Electrical and Computer Engineering
Western Michigan University, Kalamazoo, MI

Hubo Cai, Ph. D., P.E. (July 2008 – June 2009)
Assistant Professor
Department of Civil and Construction Engineering
Western Michigan University, Kalamazoo, MI

Sherif Yehia, Ph. D., P.E. (December 2005 – June 2008)
Associate Professor
Department of Civil and Construction Engineering
Western Michigan University, Kalamazoo, MI

TABLE OF CONTENTS

ABSTRACT

ACKNOWLEDGEMENTS

DISCLAIMER

PROJECT TEAM

LIST OF TABLES

LIST OF FIGURES

EXECUTIVE SUMMARY

1.0 INTRODUCTION

2.0 CONCRETE BRIDGE HEALTH MONITORING

2.1 Structural Health Monitoring Systems (SHM)

2.2 State-of-the-Art in SHM Instrumentation

3.0 SCOPE AND OBJECTIVES

4.0 PARKVIEW BRIDGE HEALTH MONITORING SYSTEM

4.1 An Overview of Parkview Bridge

4.2 Parkview Bridge SHM Instrumentation Selection and Configuration

4.3 Sensor Hardware Installation – Field Construction Considerations

4.4 The Parkview Bridge SHM Data Structure

5.0 ASSESSMENT OF THE RAPID BRIDGE CONSTRUCTION TECHNIQUE

5.1 Advantages and Disadvantages of RBC

5.2 Time Study Methodology

5.3 Time Study Results and Discussions

6.0 LOAD TESTING

6.1 Load Testing Objectives and Approaches

6.2 Load Testing Scenarios

6.3 Load Configuration

6.4 Load Testing Procedure

6.5 Top Fiber Stresses from Deflection Measurements

6.6 Field Measurements Validation

6.7 Load Test 1 - Before Opening

6.8 Load Test 2 – After Opening

6.9 Discussion of the Results

7.0 ONE-YEAR HEALTH MONITORING

7.1 SHM Initial Configuration Setup

7.2 SHM Sensor Data Collection and Representation

7.3 Discussion of Results

8.0 CONCLUSIONS

9.0 RECOMMENDATIONS FOR FUTURE WORK

10.0 REFERENCES

APPENDIX A: LIST OF ACRONYMS, ABBREVIATIONS, AND SYMBOLS

APPENDIX B: SENSOR CONSTRUCTION SPECIFICATIONS

APPENDIX C: LOAD TEST SPREADSHEETS AND FORMULAS

APPENDIX D: SENSOR STRESS CHARTS AND DATA (CD-ROM)

LIST OF TABLES

TABLE 1: Health Monitoring Case Study Summary

TABLE 2: Advantages and Disadvantages of Sensors

TABLE 3: Fiber Optic vs. Vibrating Wire Sensors

TABLE 4: Sensors Used for Longitudinal Load Stress Monitoring (Group 1)

TABLE 5: Sensors Used for Transverse Load Stress Monitoring (Group 2)

TABLE 6: Sensors Used for Stress Monitoring at Joints between Panels (Group 3)

TABLE 7: Sensors Used for Stress Monitoring Along Cast-in-Place Grout (Group 4)

TABLE 8: Specifications of the Lovers Lane Bridge and the Parkview Bridge

TABLE 9: Parkview Bridge WBS: Conventional vs. Rapid Construction Methods

TABLE 10: Tabular Schedule Report – Conventional Bridge Construction

TABLE 11: Tabular Schedule Report – Rapid Bridge Construction

TABLE 12: Element-by-Element Comparison of Conventional vs. Rapid Construction

TABLE 13: Testing Scenarios

TABLE 14: Actual Loaded Truck Weights

TABLE 15: Deck Dead Load Stresses from Design Calculations (psi)

TABLE 16: Load Test 1 Summary of Deflections

TABLE 17: Live Load Stresses Based on Deflections - South Side Panels (psi)

TABLE 18: Live Load Stresses Based on Deflections - North Side Panels (psi)

TABLE 19: Total Stresses Based on Deflections - South Side Panels (psi)

TABLE 20: Total Stresses Based Deflections - North Side Panels (psi)

TABLE 21: Load Test 2 Summary of Deflections

TABLE 22: Live Load Stresses from Deflections - South Side Panels (psi)

TABLE 23: Live Load Stresses from Deflections - North Side Panels (psi)

TABLE 24: Live Load Stresses from Sensors - South Side Panels (psi)

TABLE 25: Live Load Stresses from Sensors - North Side Panels (psi)

TABLE 26: Total Stresses Based on Deflection Measurements – South (psi)

TABLE 27: Total Stresses Based on Deflection Measurements - North (psi)

TABLE 28: Total Stresses Based on Sensor Readings – South (psi)

TABLE 29 Total Stresses Based on Sensor Readings – North (psi)

TABLE 30: Maximum and Minimum Stresses - North (psi)

TABLE 31: Maximum and Minimum Stresses – South (psi)

LIST OF FIGURES

- FIGURE 1: Completed Parkview Bridge
- FIGURE 2: Schematic view of the Parkview Bridge SHM system configuration
- FIGURE 3: Parkview Bridge deck layout
- FIGURE 4: The components and wiring of the sensor network.
- FIGURE 5: Conventional bridge construction schedule
- FIGURE 6: Rapid bridge construction schedule (without construction delays)
- FIGURE 7: Detour and intersection
- FIGURE 8: Flow chart for the bridge load testing process
- FIGURE 9: Load testing locations
- FIGURE 10: General configurations for trucks
- FIGURE 11: Validating scenario 1 results from load test 1 (drawn not to scale)
- FIGURE 12: North longitudinal load stress for span two (January)
- FIGURE 13: North longitudinal load temperature for span two (January)
- FIGURE 14: North longitudinal load stresses for span two (1/17/09).
- FIGURE 15: North longitudinal load temperature for span two (1/17/09)
- FIGURE 16: North longitudinal load stresses piers 1, 2 and 3 (January)
- FIGURE 17: North longitudinal load temperature at piers 1, 2, and 3 (January)
- FIGURE 18: North transverse load stresses for span two (January)
- FIGURE 19: North transverse load temperature for span two (January)
- FIGURE 20: Stress monitoring along north panel edge for span two (January)
- FIGURE 21: Temperature monitoring along north panel edge for span two (January)
- FIGURE 22: Stresses along cast-in-place grout for span two (January)
- FIGURE 23: Temperature along cast-in-place grout for span two (January)
- FIGURE 24: Maximum and Minimum Longitudinal Stresses – North Panels
- FIGURE 25: Maximum and Minimum Longitudinal Stresses – South Panels
- FIGURE 26: Maximum and Minimum Transverse Stresses – North Panels
- FIGURE 27: Maximum and Minimum Transverse Stresses – South Panels

EXECUTIVE SUMMARY

Bridges are critical components of the transportation infrastructure. With today's growing travel demands and aging bridge infrastructure in the United States, more and more alterations, repairs, inspections, and construction processes are required to maintain safe usage. There are approximately 600,000 bridges in the United State according to the U.S. Department of Transportation Federal Highway Administration (FHWA 2007). Four billion vehicles traverse these bridges daily (Phares 2005). Regular inspections and maintenance are essential components of any bridge management program to ensure structural integrity and user safety. This is a grand challenge due to the enormous number of existing bridges.

To assess the condition of bridge, a few approaches are commonly used in practice. Visual inspection has a long history in bridge condition assessment and documents any sign of cracking, spalling, leaching, deflection and vibration, accidental damage, and deck surface damages. However, the extent of structural deficiency of a concrete bridge is usually unreliable through visual inspections (Phares 2005). Coring samples provide a supplementary approach, in which small cores are drilled and concrete samples are obtained and tested in a laboratory. Since samples are taken from small selected portions of the concrete, inefficient conclusions might be reached due to the lack of overall behavioral information throughout the concrete structure. Diagnostic testing is another bridge condition assessment technique in which a bridge is exposed to varying loads and its responses measured and analyzed (NCHRP 1998). Diagnostic testing faces many constraints related to cost and traffic interruption. More importantly, diagnostic testing lacks the capability of continuously monitoring the bridge performance, which is the key to determining the remaining bridge service life (Howell 2006).

Even though intensive bridge inspection and maintenance are being performed nationwide, the outcomes are not impressive. It has been reported that of the 600,000 bridges, 12% have been deemed structurally deficient and another 13% have been declared functionally obsolete (FHWA 2008a, BTS 2007a, FHWA 2007). Consequently, 25% of the nation's bridges require immediate attention or repair and may present safety challenges, suggesting a need for effective, continuous monitoring systems so that problems can be identified at early stages and economic measures can be taken to avoid costly replacement and/or bridge failures (Casas 2003). Therefore, there is a need for bridge health monitoring technologies and systems to enable continuous monitoring and real time data collection

A sensor-based bridge health monitoring system was developed and deployed for the newly constructed Parkview Bridge in Kalamazoo, Michigan. This system adopted rapid bridge construction techniques using precast concrete technology. Today, these sensor networks, also known as health monitoring systems (SHM), can be used to develop models to determine how a structure is behaving internally. In this study, sensors were installed at strategic locations to allow for short and long term static analysis of the Parkview Bridge deck. The system was composed of a remotely accessible, on-site data acquisition system and vibrating wire strain gauges (sensors) to monitor both strain and temperature over given time increments. The system relies on a redundant embedded sensor network in the concrete bridge deck to collect and provide static performance data under different loading conditions in order to provide reliable assessment of the condition of the bridge over time. The design and installation of the Health Monitoring equipment was fully completed in December of 2008. Continuous bridge condition

data are being collected in real time, archived in the laboratory computer workstation, and analyzed to assess the structural performance and integrity. The study focused on the design of the data analysis system and on the collection of one year's worth of data to begin the process of creating a base-line performance and deterioration prediction model for the Parkview Bridge deck. Every aspect from design and installation to data collection has gone well. The bridge continues to provide valuable data in ten-minute increments to the Western Michigan University research team. This continuous information can greatly increase bridge safety for its users by providing early warning signs before a failure occurs.

Furthermore, a methodology for assessing the savings in time and cost associated with adopting Rapid Bridge Construction (RBC) techniques was developed and used in this research project. A comparison study was carried out to assess the performance of the RBC technique at the Parkview Bridge. In this study, the performance for all construction activities was recorded, the productivity was calculated, and an as-built CPM schedule was developed. The performance data for the conventional approach were obtained from the Lovers Lane Bridge project, which is spatially and temporally close to the Parkview Bridge, to establish the baseline for the comparison study. Step-by-step and element-by-element comparisons were conducted to identify sources for time savings and to quantify such savings by assessing the travelers' user cost savings that were achieved due to the shortening of the construction duration. The RBC technique was found to save bridge construction time and consequently realize savings in extra travel time. This travel time saving is significant enough that it can suffice the justification of the relatively high initial cost of the RBC technique. Considered together with other advantages of RBC, such as high quality and low maintenance cost, the technique offers a more efficient and economic alternative to the conventional method. More assessment studies such as this one will need to be conducted to fully understand and realize the advantages of RBC techniques.

1.0 INTRODUCTION

Bridges are critical components of the transportation infrastructure. There are approximately 600,000 bridges in the United State according to the U.S. Department of Transportation Federal Highway Administration (FHWA 2007) Four billion vehicles traverse these bridges daily (Phares 2005). Regular inspections and maintenance are essential components of any bridge management program to ensure structural integrity and user safety. This is a grand challenge due to the enormous number of existing bridges.

To assess the condition of bridge, a few approaches are commonly used in practice. Visual inspection has a long history in bridge condition assessment and documents any sign of cracking, spalling, leaching, deflection and vibration, accidental damage, and deck surface damages. However, the extent of structural deficiency of a concrete bridge is usually unreliable through visual inspections (Phares 2005). Coring samples provide a supplementary approach, in which small cores are drilled and concrete samples are obtained and tested in a laboratory. Since samples are taken from small selected portions of the concrete, inefficient conclusions might be reached due to the lack of overall behavioral information throughout the concrete structure. Diagnostic testing is another bridge condition assessment technique in which a bridge is exposed to varying loads and its responses measured and analyzed (NCHRP 1998). Diagnostic testing faces many constraints related to cost and traffic interruption. More importantly, diagnostic testing lacks the capability of continuously monitoring the bridge performance, which is the key to determining the remaining bridge service life (Howell 2006).

Even though intensive bridge inspection and maintenance are being performed nationwide, the outcomes are not impressive. It has been reported that of the 600,000 bridges, 12% have been deemed structurally deficient while another 13% have been deemed functionally obsolete (FHWA 2008a, BTS 2007a, FHWA 2007). Consequently, 25% of the nation's bridges require immediate attention or repair and may present safety challenges, suggesting a need for effective, continuous monitoring systems so that problems can be identified at early stages and economic measures can be taken to avoid costly replacement and/or bridge failures (Casas 2003). Therefore, there is a need for bridge health monitoring technologies to enable continuous monitoring and real time data collection.

This report presents a sensor-based bridge health monitoring system that was designed and developed for the Parkview Bridge in Kalamazoo, Michigan. The report also presents a methodology for assessing the savings in time and cost associated with adopting Rapid Bridge Construction (RBC) techniques in the construction of the Parkview Bridge.

2.0 CONCRETE BRIDGE HEALTH MONITORING

With today's growing travel demands and aging bridge infrastructure in the United States, more and more alterations, repairs, inspections, and construction processes are required to maintain safe usage. Many older bridges still in use today are ill equipped for the unforeseen travel demands and patterns generated by today's standards of transportation, and are reaching their design life expectancy, requiring new construction or repair. Traffic and variable loading

conditions greatly influence the performance, durability, and safety of a bridge structure throughout its service life. In addition to carrying traffic loads, a bridge is exposed to its surrounding environment. Environmental factors such as temperature, humidity, and precipitation can significantly affect the structural integrity and performance of a bridge. The condition of a bridge is never constant and therefore needs to be monitored continuously. Continuous monitoring can provide the basis for determining the deterioration rate and for estimating the remaining service life, thus assisting in making important decisions regarding bridge maintenance.

2.1 Structural Health Monitoring Systems (SHM)

With newer technology available, a wide variety of different sensors have been developed to measure different mechanical properties of a material or composite to determine behavior. Many different types of sensors and gages are used in applications of bridge health monitoring. When monitoring a bridge, two main categories of measurement are often used: kinematic (displacement, strain, acceleration) and environmental (temperature, humidity, and wind) (Phares 2005, Robertson 2005, Sawyer 2005, Xia 2005, Cheung 2004, Casas 2003, Chen 2003, Lewis 2003, Lin 2003, Fu 2002, Shenton 2001, Shah 2000). These two categories of measurement provide valuable information about a structure's behavior over time. To measure these quantities, the most common sensors implemented on bridges today include: fiber optic sensors, vibrating wire strain gages, resistance strain gages, thermocouples, and wireless sensors (Phares 2005, Robertson 2005, Sawyer 2005, Xia 2005, Cheung 2004, Casas 2003, Chen 2003, Lewis 2003, Lin 2003, Fu 2002, Shenton 2001, Shah 2000). Both wire and wireless sensors can be used for monitoring and data collection. Strain gages, vibrating wire gauges, and fiber optic sensors are commonly used to measure strain, temperature, and loads (Casas 2003, Chen 2003, Lewis 2003). In addition, electric displacement and electrical inclinometer transducers are used for displacement and rotations measurements. Data collection can be done on site or remotely by dial-in or wireless communications (Casas 2003, Chen 2003, Lewis 2003, Lin 2003, Fu 2002, Shah 2000). Due to the advancement in sensor technology, many of these sensors can be embedded in concrete at strategic locations, comprising a sensor network. These sensor networks, also known as health monitoring systems (SHM), can be used to develop models to determine how a structure is behaving internally. This continuous information gathering can greatly increase bridge safety for its users by providing early warning signs before a failure occurs. To prevent misleading conclusions through erroneous data, SHMs are composed of redundant sensors for added reliability and assurance.

Among many technologies that have been developed to aid bridge condition assessment, sensor technology has attracted enormous research interest due to its capability of continuously monitoring the bridge condition (Olund 2007, Howell 2006, Ko 2005, Casas 2003). Applications of sensor-based SHM have been expanding in bridge health monitoring to increase safety and help engineers develop models for determining how a structure is behaving internally. At this moment however, only few studies on sensor-based SHM in practice are available. Examples of health monitoring system for bridges include the following:

1. The Confederation Bridge located in Canada between Province of New Brunswick and Prince Edward Island is an example of an elaborate bridge health monitoring system. A 3,281-foot section of the bridge includes 389 transducers to monitor static and dynamic loading along with variable environmental conditions (Cheung 2004). These transducers include strain gages, thermocouples, ice force panels, displacement gages, tilt-meters, and accelerometers. All of these transducers make up the health monitoring system for internal and external factors affecting the bridge over its one hundred years design life expectancy. Due to the geographical location of the bridge, it faces some extreme weather conditions and hazards. Twenty eight ice force panels are located on the piers to determine the amount of pressure exerted by the ice on the pier. Tilt-meters are used to determine if any tilting of the piers is occurring due to the ice pressure. Two underwater sonar systems are used to determine ice thickness around the piers. Furthermore, eight displacement sensors along with twenty vibrating wire strain gauges are used to monitor the bridges deformation over time. Eight pyranometers are used to measure the amount of solar radiation given off by the sun and two hundred and forty three thermocouples to monitor and record temperature variation. Finally, seventy Six accelerometers are used for monitoring accelerations due to seismic activity, wind, and loading. These sensors combined together provide a reliable profile of the bridges behavior in its environment over time.
2. In Oahu, Hawaii, the North Halawa Valley Viaduct was constructed in 1994 using post tensioning, box-girders, spanning up to 361 feet in length. The overall length of the viaduct is 4,921 feet (Robertson 2005). The viaduct's health monitoring system was composed of over 200 instruments to measure and monitor the structure's behavior over time. The North Halawa Valley Viaduct has a health monitoring system that has been collecting data for over nine years. The instrumentation used was to monitor both static short and long term behavior of the structure. The main objectives of this project were to collect data that provided strain, ambient temperature, creep and shrinkage, tendon relaxation, and deflection (Robertson 2005). The types of instruments used included strain gages, thermocouples, span extensometers, tendon load cells, base-line deflection systems, tilt-meters, and data loggers for recording. To fully monitor the behavior of the viaduct, instruments were placed at or near mid spans and supports. To monitor strain, vibrating wire strain gages were embedded and oriented to measure longitudinal strain in the deck and beam sections. For short term monitoring, they collected data every five minutes, and for long term monitoring, every two hours. Eight gages were placed near mid spans while 10 gages were placed at the supports. The gages were placed in the top and bottom fiber of the concrete sections. Top and bottom strain values were then averaged and interpolated to determine the strain at mid depth. These values were then compared with estimated values generated from a finite element modeling. The researchers concluded there was good agreement between the actual and modeled data for short term characteristics. The predictions generated through design for long term differed significantly from observations. The reason for this was due to the unanticipated creep and shrinkage behavior caused by unpredictable weather and material variables. Since actual material characteristics were known through strain gages and load testing, the models then could be adjusted accordingly. Once modeling was determined to be viable, bridge behavior envelopes were determined using the modeling program and measured values.

Upper and lower bounds were estimated from measured data for use with general environmental and material variables. Overall, the vibrating wire strain gages proved to be reliable throughout the testing period. With the information provided, the research collected over nine years provided design engineers good envelopes to use as a guide for further development and design.

Also, Chajes (2000) reported on a study, in which strain gauges were used to remove restricted load limitations on three bridges in Delaware. Casas (2003) described the usage of fiber optic sensors for bridge monitoring including crack detection, strain monitoring, and temperature monitoring. In Addition, Howell (2006) reported the development of an in-service strain monitoring system and its application in a number of bridges in Delaware. Finally, Olund (2007) reported a series of bridge health monitoring studies conducted in Connecticut using the sensor technology, with recommendations of sensor selection and system configuration. Table 1 provides a summary of the characteristics of some examples of these sensor networks that are already in use (Robertson 2005, Cheung 2004, Yang 2003).

TABLE 1: Health Monitoring Case Study Summary

Case Study	Types of Sensors Used*	# of Sensors Used	Sensor Placement	Data Collection Time Increments	Load Type Monitored
Confederation Bridge (Canada)	(1), (2), (3), (4), (5), (6), (7), (8)	389	Deck, Beam, Pier	Variable	Static/Dynamic
Pemiscot County Bridge, Missouri (U.S.)	(1), (3), (4)	64	Deck, Beam	-	Static
North Halawa Valley Viaduct, Hawaii (U.S.)	(1), (4)	200	Deck, Beam	5 minutes/2 hours	Static
Parkview Bridge, Michigan (U.S.)	(1), (4)	184	Deck	10 minutes	Static

*Sensor Types: (1) Vibrating Wire Strain Gage, (2) Fiber Optical, (3) Resistance Strain Gage (4) Thermocouples, (5) Accelerometer, (6) Tilt-meter, (7) Displacement, (8) Ice-Force

These studies demonstrated the applicability of using sensor systems in continuously monitoring the condition of concrete bridges. Observations and findings in these studies laid a foundation for the design and implementation of the sensor network for the Parkview Bridge in Michigan. However, it is worth noting that while the above examples describe the monitoring systems used in providing condition assessment in bridges, they differ from the Parkview Bridge project: the Parkview Bridge was constructed using RBC techniques with full-depth precast deck panels when all the other cases have cast-in-place decks. Such techniques need to be evaluated and are the motivation behind this study, making this SHM study different from the others and posing unique challenges.

2.2 State-of-the-Art in SHM Instrumentation

Monitoring strains at critical locations in the bridge deck can provide crucial information about stress due to loading and temperature. Gathering this information can provide a basis for predicting the behavior of similar bridges. According to recently published literature, the most common types of sensors used in bridge health monitoring are strain sensors (Geokon 2006, Kim 2006, Lynch 2006, OPSens 2006, Roctest 2006, Ravisankar 2005, Daher 2004, Casas 2003, Aktan 2002, Lynch 2001, Merzbacher 1996). Strain sensors measure elements that translate force, pressure, tension, etc., into strain readings. Various types of strain sensors have been successfully used in bridge health monitoring, such as vibrating wire strain gages, electrical resistance strain gages, fiber optic sensors, and wireless sensors. Each one of these sensors is discussed below. The overall advantages and disadvantages of these types of sensors are summarized in Table 2.

- *Vibrating Wire Strain Gages (VWSG)*: According to FHWA, VWSGs are recommended for monitoring long-term strains in concrete (FHWA 2006). VWSG has a body composed of steel tube with flanges or end plates attached to either end. Inside the tube, a steel wire is held in tension between the two end plates. Any strain in concrete causes the plates to move relative to each other, decreasing or increasing the tension in the wire. This tension in the wire is then measured by plucking the wire with an electromagnetic coil and measuring the frequency of the resulting vibration (Boart 2006, Geokon 2006). The amount of time required to perform the pluck/read operation on a sensor is less than one second. Therefore, when numerous sensors are multiplexed to a data acquisition system, it can take several seconds to cycle through all the VWSGs. Due to this limitation, VWSGs are not suitable for dynamic measurements (Aktan 2002).
- *Electrical Resistance Strain Gages*: The design of electrical resistance strain gages is based on the fact that the electrical resistance of a conductor will change when it is subjected to strain in either tension or compression. Since the resistance is directly proportional to the length of the conductor, any change in the length resulting from strain will translate to changes in its resistance. When the conductor is stretched, it elongates and becomes narrower which causes an increase in resistance. A Wheatstone bridge circuit then converts this change in resistance to a voltage that can be recorded (Daher 2004, Aktan 2002).
- *Fiber Optic Sensors*: An emerging technology for strain measurement in concrete is fiber optic sensors (FOSs). The main advantages of these sensors are their high sensitivity as well as their immunity to electromagnetic interference. They can be used to measure a wide variety of parameters including strain, temperature, corrosion, crack formation, and displacement. Two types of FOSs are commonly used for strain monitoring: Fiber Bragg Gratings (FBG) and Fabry-Perot sensors. FBG sensors have a series of engravings, or Bragg gratings in their fiber core. The Bragg gratings reflect back an optical wavelength through diffraction. When there is a change in the grating, the peak wavelength of the reflected light is shifted. Any strain or change in mechanical property can thus be measured (Casas 2003). FBG sensors can be connected in series or multiplexed in order to reduce cable length. Fabry-Perot sensors consist of a tube housing optical fibers that

create a reflective interface. These sensors are very accurate and have a low sensitivity to thermal effects (Merzbacher 1996).

- *Wireless System:* The use of conventional sensors, which depend on using cables to communicate their measurements to a central processing unit, have very high installation costs and the wires themselves might be damaged which will affect the output results. Bearing in mind these disadvantages, many research efforts have focused on developing wireless monitoring systems that have lower initial and installation costs, and can insure a greater degree of reliability in the communication of sensor measurements (Lynch 2001). A wireless sensor network consists of hundreds of small nodes or "motes" which are independent sensing devices (strain gages, accelerometers, and linear voltage displacement transducers) that incorporate a microcontroller (computer on a chip to control electronic device), a power unit, and a communication module (Lynch 2006). A wireless sensor network is designed to work on batteries, limiting the network life span by 5 to 10 years. Hence, it becomes an important design criterion to minimize the overall power consumption so that life span of monitoring can be maximized (Kim 2006).

TABLE 2: Advantages and Disadvantages of Sensors

Sensor	Function	Advantages	Disadvantages
Electrical Resistance Strain Gages	Short Term Monitoring	Operate over a wide range of temperatures	Data read out equipment is expensive
		Inexpensive	Tedious installation, time consuming to install and to connect to data acquisition system
		Suitable for dynamic loads	Affected by electromagnetic interference
		Available in a wide variety of gage lengths	Lead length limitation
		Provides an electrical signal that can be measured with a wide variety of circuits	
Vibrating Wire Gages	Long Term Monitoring	Long term reliability	May require long lengths of wire
		Multiplexing ability	Cannot monitor live loads
		Easy installation	
		Low cost	
		Immune to electromagnetic interference	
		Rugged housing resistant to impact and corrosion	
		Measures temperature as well as strain	

Fiber Optic Sensors	Long Term Monitoring & Short Term Monitoring	Light weight	The fiber wire should be handled carefully and gently
		Small size	Expensive hardware and software
		Multiplexing ability	Long term behavior still under investigation
		Immune to electromagnetic interference	Expensive installation
		Environmental ruggedness	
		Extremely accurate	
Wireless System	Short Term Monitoring	No cables are required for data transfer	Restricted battery life
		Low cost of deployment	Still under investigation
		Each mote works independently	

TABLE 3: Fiber Optic versus Vibrating Wire Sensors

Parameters	Embeddable Fiber Optic Sensor	Vibrating Wire Strain Gage
Gage length	1 to 500 mm	50 to 300 mm
Resolution	0.01% full scale	1 Microstrain
Measurement range	±2000 to ±10000 Microstrain	±2000 to ±3000 Microstrain
Remote operations possibility	Yes	Yes
Working principle	Measuring the change in optical characteristics such as intensity, wave length , phase	Measuring the frequency of a taut wire
Availability for embedment and surface mounting	Yes	Yes
Material of sensor	High strength silica	High strength steel piano wire
Structural response capabilities	Static and dynamic loads	Just static loads
Temperature range	- 20 to 60 °C	-20 to 80°C
Immunity to electromagnetic interface	Yes	Yes
Ability to multiplexing	Yes for long and short term monitoring	Yes for long term monitoring

3.0 SCOPE AND OBJECTIVES

The main objective of the proposed project is to evaluate the condition and structural behavior of the Parkview bridge during fabrication, construction, and after the bridge has been subjected to traffic. In addition, an overall evaluation of the efficiency of the proposed system for rapid bridge deck replacement will be conducted. These objectives can be achieved through the following tasks:

- Study the different types of sensors used for structural health monitoring purposes.
- Investigate current bridge health monitoring systems.
- Select the most applicable, most promising sensors for strain monitoring, and design and develop a sensor network for implementation at the bridge deck.
- Collect, organize, and analyze sensor data over time (1 year for this phase) to develop a long-term health monitoring program for the bridge deck.
- Perform static live load testing on the bridge to evaluate and compare data on structural performance and behavior.
- Assess the effectiveness of the rapid bridge construction technique as compared to conventional methods.

4.0 PARKVIEW HEALTH MONITORING SYSTEM

The Parkview Bridge is the first prefabricated bridge in Michigan to take advantage of rapid bridge construction techniques and sensor network technology. This section will present the SHM instrumentation that was designed and deployed to monitor the performance of the bridge's full-depth deck panels. It is worth noting that the selection of any sensor network system depends on the specifications of the problem at hand, the features of technology available at the time of implementation, the reliability of the sensors, and on the cost of the system.

4.1 An Overview of Parkview Bridge

The Parkview Bridge is located in Kalamazoo, Michigan next to the Engineering Campus at Western Michigan University. It crosses over US-131, a main highway with heavy traffic in Southwest Michigan. After many years of service, this bridge needed a major repair or a complete replacement. A decision was made to replace the existing bridge using rapid bridge construction techniques. The new Parkview Bridge was designed to have four spans and three lanes, with all its major bridge elements including piers, abutments, I-beam girders, and full depth deck panels prefabricated off site. The superstructure is composed of type IV AASHTO girders, and the deck is composed of forty eight, nine-inch thick precast reinforced concrete panels. These panels are categorized as North and South. Once the North and South panels were installed on-site, they were joined by a cast-in-place grouted joint. The deck is post tensioned with an added three inch asphalt wearing surface. As mentioned earlier, this new bridge is the first in Michigan to be constructed using the RBC technique. Figure 1 illustrates the various prefabricated elements of the bridge including multi-section abutments, single segment pier columns, single section pier caps prestressed concrete I-beams girders and post-tensioned full-depth deck panels. The actual construction began on April 7th, 2008, and the bridge was re-opened to traffic on September 8th, 2008.

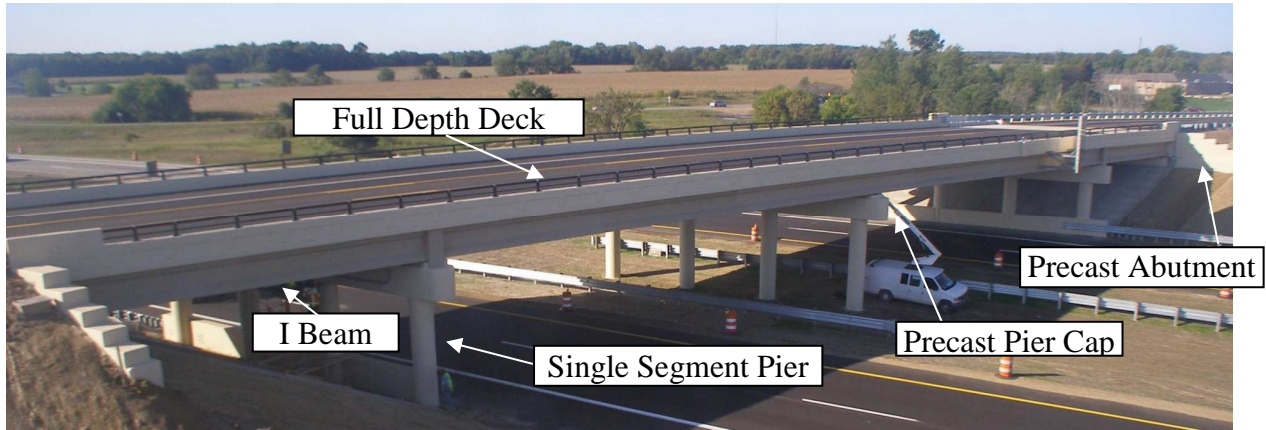


FIGURE 1: Completed Parkview Bridge

4.2 Parkview Bridge SHM Instrumentation Selection and Configuration

Properly placed strain and thermocouple sensors can provide valuable information about structural performance. Additional measuring devices can be used, but only strain and temperature measurements were chosen in this project for efficiency and cost effectiveness. The SHM system is composed of (Geokon 2006):

- 184 Geokon Vibrating-Wire Strain Gauges (sensors) Model VCE-4200 with built-in thermocouples installed in the bridge deck panels,
- 2 Geokon MICRO-10 Data Loggers Model Number 8020-1-1,
- 12 Geokon Multiplexers Model 8032-16-1S,
- 2 modems,
- a remote computer workstation in a laboratory with communication software, and
- necessary wiring for communication and data transfer.

Figure 2 provides a schematic view of the system configuration.

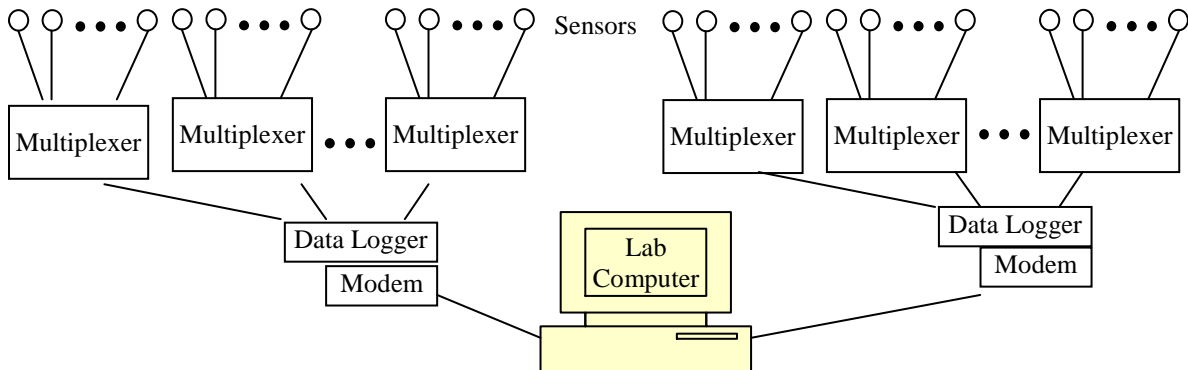


FIGURE 2: Schematic view of the Parkview Bridge SHM system configuration.

In order to effectively monitor the structural performance, sensors must be placed at strategic locations. Four groups of strain and temperature sensors were installed at

1. Mid spans and supports to monitor longitudinal stresses,
2. Mid spans in the transverse direction to monitor lateral stresses,
3. Edges of deck panels to monitor the joints between panels, and
4. Along the two sides of the grouted joint between the North and South panels.

Figure 3 shows the locations of the sensors installed. These sensors are used to capture data throughout the day at ten-minute increments to determine maximum and minimum values of stresses and temperatures recorded. Since the deck and beam act as a composite section after construction, sensors were placed near the top fiber of the section. Due to limitations by the owner, sensors were only placed in the deck. The construction details in terms of plans and specification for the installation of the selected instrumentation are provided in Appendix B.

4.3 Sensor Hardware Installation – Field Construction Considerations

Attaching VWSG sensors to reinforcing bars must follow a few precautions to ensure proper operation. In this study, all sensors were attached to the top reinforcement using zip ties with foam spacers to provide cover. Figure 4 (a) illustrates the details of a properly secured sensor and how this configuration allows for the free flow of concrete mix while protecting the sensor and its wire during casting.

Once the sensors were properly attached to reinforcement, the wires connecting them to multiplexers were loosely coiled around the reinforcement to allow concrete bonding between the wires and the reinforcement and to prevent any damage that might occur to the wire during the placement of concrete. The wires were run to a four inch diameter PVC pull boxes to protect them from the concrete during the pour and to provide accessibility to the wires after the installation of the deck panels at the bridge site. Each wire was labeled to indicate the sensor location and orientation after casting. Figure 4 (b) shows a completed sensor network for a panel along with wire routing and pull box placement. Figure 4 (c) illustrates the exposed pull box underneath the deck panels for access and splicing. Sensor wires were spliced together and run through PVC conduits underneath the deck panels to the data logging equipment.

In this project a combination of 12 multiplexers, 2 data loggers, and two modems were chosen to collect and record sensor data. The equipment was housed in three cabinets to protect the electrical equipment from varying environmental conditions, which were secured to the pier of the bridge as shown in Figure 4 (d). Each data logger contains a modem for remotely communicating with the laboratory computer workstation for data transfer.

4.4 The Parkview Bridge SHM Data Structure

To effectively monitor the bridge performance under varying load conditions, sensors were grouped depending on their locations to address the structural monitoring needs outlined earlier. In this study, four groups of sensors were used to monitor the bridge performance:

- Group 1 – Longitudinal stresses at mid spans and over the piers,
- Group 2 – Transverse stresses at mid spans,
- Group 3 -- Stresses at joints between panels, and
- Group 4 -- Stress at both sides of the cast-in-place grout between North and South panels.

Figure 3 shows the locations and labels of all the sensors in the panels, and provides the group number for each sensor in parenthesis. If a sensor belongs to multiple groups, the numbers are separated by commas.

Group 1 refers to those sensors placed near mid spans and at pier locations, and orientated longitudinally near the traffic lanes to monitor longitudinal stresses. Table 4 summarizes the list of sensor labels that contribute to Group 1 in each panel. Group 2 includes those sensors that are used to monitor the bridge performance under transverse loading. The locations are similar to those in Group 1 but oriented transversely. Table 5 lists all Group 2 sensors. Note that the highlighted sensors in Table 5 were declared non-operational as they were constantly recording data that are out of range and inconsistent with the readings from the surrounding redundant sensors. Group 3 refers to those sensors along the edges of critical panels. The main reason for having this group of sensors is to monitor the bonding and load transfer of deck panels. Theoretically, the deck and girders should behave as a composite section, but environmental factors and loading may cause the composite section to behave as smaller sections if joints fail or show fatigue over time. Table 6 displays the sensors used for this category. Group 4 refers to those sensors that are placed along both sides of the center grout joining North and South panels. They are oriented longitudinally. Table 7 lists all sensors belonging to this group.

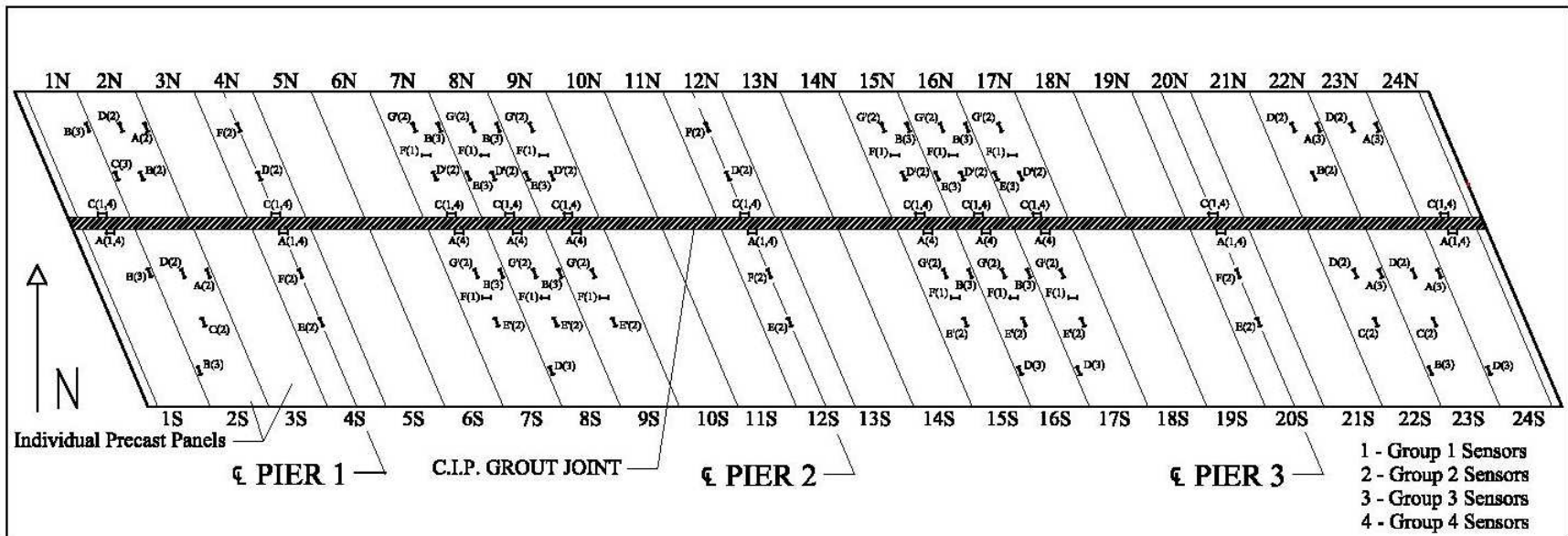
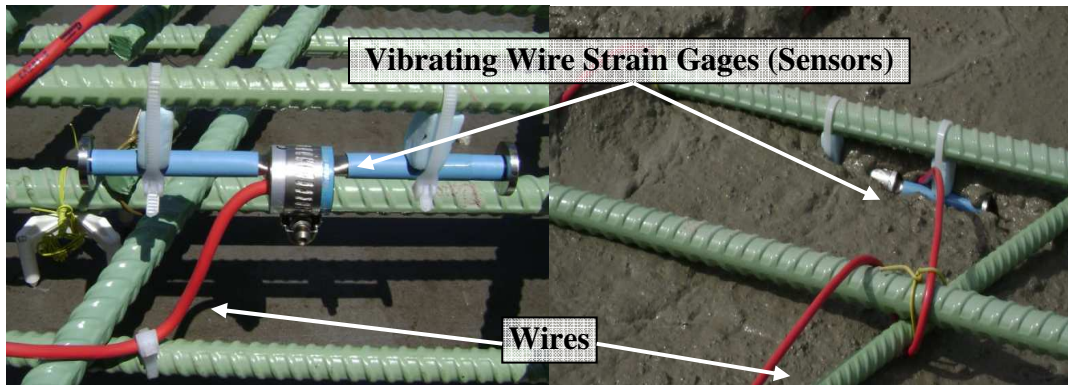


FIGURE 3: Parkview Bridge deck layout.



(a) Properly secured sensor



(b) Conduit placement



(c) Exposed Conduit, Wire, and Splicing.



(d) Cabinets and data logging equipment.

FIGURE 4: The components and wiring of the sensor network.

TABLE 4: Sensors Used for Longitudinal Load Stress Monitoring (Group 1)

Span 1				
North Panel	Sensor	Sensor	South Panel	Sensor
1	N-1-C		1	S-1-A
Pier 1				
4	N-4-C		4	S-4-A
Span 2				
7	N-7-C	N-7-F	7	S-7-F
8	N-8-C	N-8-F	8	S-8-F
9	N-9-C	N-9-F	9	S-9-F
Pier 2				
12	N-12-C		12	S-12-A
Span 3				
15	N-15-C	N-15-F	15	S-15-F
16	N-16-C	N-16-F	16	S-16-F
17	N-17-C	N-17-F	17	S-17-F
Pier 3				
20	N-20-C		20	S-20-A
Span 4				
24	N-24-C		24	S-24-A

TABLE 5: Sensors Used for Transverse Load Stress Monitoring (Group 2)*

Span 1									
North Panel	Sensor	Sensor	Sensor	Sensor	South Panel	Sensor	Sensor	Sensor	Sensor
2	N-2-A	N-2-B	N-2-D		2	S-2-A	S-2-C	S-2-D	
Pier 1									
4	N-4-D	N-4-F			4	S-4-E	S-4-F		
Span 2									
7	N-7-D	N-7-D'	N-7-G	N-7-G'	7	S-7-E	S-7-E'	S-7-G	S-7-G'
8	N-8-D	N-8-D'	N-8-G	N-8-G'	8	S-8-E	S-8-E'	S-8-G	S-8-G'
9	N-9-D	N-9-D'	N-9-G	N-9-G'	9	S-9-E	S-9-E'	S-9-G	S-9-G'
Pier 2									
12	N-12-D	N-12-F			12	S-12-E	S-12-F		
Span 3									
15	N-15-D	N-15-D'	N-15-G	N-15-G'	15	S-15-E	S-15-E'	S-15-G	S-15-G'
16	N-16-D	N-16-D'	N-16-G	N-16-G'	16	S-16-E	S-16-E'	S-16-G	S-16-G'
17	N-17-D	N-17-D'	N-17-G	N-17-G'	17	S-17-E	S-17-E'	S-17-G	S-17-G'
Pier 3									
20					20	S-20-E	S-20-F		
Span 4									
22	N-22-B	N-22-D			22	S-22-C	S-22-D		
23	N-23-B	N-23-D			23	S-23-C	S-23-D		

* Yellow-highlighted sensors are declared non-operational.

TABLE 6: Sensors Used for Stress Monitoring at Joints between Panels (Group 3)

Span 1					
North Panel	Sensor	Sensor	South Panel	Sensor	Sensor
1	N-1-B		1	S-1-B	
2	N-2-C		2	S-2-B	
Pier 1					
4			4		
Span 2					
7	N-7-B		7	S-7-B	
8	N-8-E	N-8-B	8	S-8-D	S-8-B
9		N-9-E	9		S-9-D
Pier 2					
12			12		
Span 3					
15	N-15-B		15	S-15-B	
16	N-16-E	N-16-B	16	S-16-D	S-16-B
17		N-17-E	17		S-17-D
Pier 3					
20			20		
Span 4					
22	N-22-A		22	S-22-A	
23	N-23-C	N-23-A	23	S-23-B	S-23-A
24		N-24-D	24		S-24-D

TABLE 7: Sensors Used for Stress Monitoring Along Cast-in-Place Grout (Group 4)

Span 1			
North Panel	Sensor	South Panel	Sensor
1	N-1-C	1	S-1-A
Pier 1			
4	N-4-C	4	S-4-A
Span 2			
7	N-7-C	7	S-7-A
8	N-8-C	8	S-8-A
9	N-9-C	9	S-9-A
Pier 2			
12	N-12-C	12	S-12-A
Span 3			
15	N-15-C	15	S-15-A
16	N-16-C	16	S-16-A
17	N-17-C	17	S-17-A
Pier 3			
20	N-20-C	20	S-20-A
Span 4			
24	N-24-C	24	S-24-A

5.0 ASSESSMENT OF THE RAPID BRIDGE CONSTRUCTION TECHNIQUE

The typical life cycle of a bridge includes planning, programming, and budgeting, design, construction, operation and maintenance, repair and rehabilitation, demolition and disposal, and replacement. This indicates that (1) a bridge ages, deteriorates, and requires regular inspections and maintenance to assure its functional soundness; (2) a bridge has a finite “life”, even though it could be as long as 100 years and can be further extended with proper treatments; and (3) at certain times during maintenance/repair/replacement, the service provided by a bridge will be interrupted or completely stopped. Consequently, innovations in the area of highway infrastructure maintenance, rehabilitation, and replacement are key to the health and wellness of this valuable national asset.

Bridge construction is associated with the following consequences:

- Traffic disruption due to partial or complete lane closure,
- Increased user costs with longer travel distances, delays, severe traffic congestions and extra fuel consumption, and
- Negative environmental impacts such as construction site run off, dust falls, erosion, noise, equipment emissions and air pollution.

These negative consequences have a relationship to the bridge construction duration. In other words, the longer the construction duration is, the more significant the consequences are. The nation’s highways are very congested considering the demand that reached nearly three trillion vehicle miles in 2005 and their limited capacity (BTS 2007b). This congestion situation is further worsened by the large number of bridges demanding major work and long construction durations, particularly in conventional cast-in-place concrete bridges. Typically, traffic control accounts for approximately 20 to 40 percent of the construction costs and reducing bridge construction time in heavy traffic areas can yield significant savings (NCHRP 2003). Therefore, innovative/new construction technologies are being called for to greatly reduce construction project duration.

Examining the conventional cast-in-place concrete bridge construction has revealed that the main cause for its time intensiveness is the way in which bridges are constructed. Conventional bridge construction must follow the sequence of completing the foundation, the substructure, the superstructure components, the railings, and other accessories (FHWA 2004). Moreover, the construction of each cast-in-place concrete component has to go through reinforcement assembly and formwork setup, concrete placing, curing, and stripping formwork. Subsequent components will have to wait until concrete cures to reach a certain strength (7 day strength, for example).

On the other hand, precast concrete technology solves the time-intensive problem of the conventional cast-in-place concrete approach by moving the fabrication offsite, thus greatly reducing construction time and decreasing traffic and environmental impacts. The RBC method has emerged as a promising alternative to cast-in-place concrete bridge construction. With the increased awareness of the availability and benefits of prefabricated concrete bridge elements, their use will become more widespread (FHWA 2008b). It is now possible to prefabricate all

elements of a bridge and install or replace the bridge in times that were never before thought possible.

Rapid bridge construction technology has attracted numerous research efforts due to its great potential of saving bridge construction time and minimizing traffic disruption and environmental impacts. The past 20 years have witnessed many innovations in RBC technology and its successful applications in highway bridge construction, all of which are well documented in the literature. This section examines the RBC approach used on the Parkview Bridge project in detail and compares it to the same bridge constructed using conventional methods to determine: (1) the source for the time savings; (2) how to quantify time savings of RBC projects; and (3) how to quantify user cost travel time delays and combine it with construction cost to assist decision makers in adopting the RBC technology. It is believed that RBC technology can greatly enhance the infrastructure sustainability by reducing traffic disruption, minimizing environmental impacts, improving work-zone safety, and lowering the total life cycle cost.

5.1 Advantages and Disadvantages of RBC

Prefabricated bridges have significant advantages over conventional ones in several key aspects. The main advantage is the reduction of onsite time required to construct the bridge, which in turn lowers traffic disruption and improve work-zone safety. The offsite fabrication of bridge elements reduces environmental impacts and allows for better quality control that leads to a prolonged life span of a bridge and thus reduces its life cycle cost. Below is a summary of the main advantages of RBC:

1. **Minimization of traffic disruption:** Delays due to bridge construction cost the traveling public millions of dollars each year in both fuel cost and lost time (Matsumoto 2001). By using prefabricated bridge elements, lengthy construction processes such as the erection of formwork and curing can take place away from traffic. All components can be cast simultaneously rather than waiting for each individual element to cure before casting the next one on top of the previous element. Once all necessary components are completed, they can be shipped to the site where the entire bridge can be erected in days rather than months. Oftentimes, bridges in areas of high traffic density are replaced during night construction shifts or on weekends so that peak hour traffic is never affected (FHWA 2008b).
2. **Constructability:** By moving most of the fabrication offsite, projects taking place in areas with environmental or zoning restrictions can happen with much more ease. In fact, prefabrication is of the most use in projects over long spans of water, complex interchanges, and areas with limited available space. Projects completed with prefabricated elements also experience less delays due to weather conditions. Rain and cold weather are no longer a factor when placing and curing fresh concrete that must take place in a controlled environment, and installation can happen under any conditions that are safe for the construction crews (Georgia 2002).
3. **Higher Quality:** Typically, casting concrete in factories will result in a higher quality product when compared to on-site, cast-in-place construction. Environmental conditions such as humidity, temperature, and rain can be controlled or eliminated resulting in a more consistent and reliable product which can have a service life longer than a similar cast-in-place bridge (Hieber 2005). When prefabricated technologies are combined with high performance

concretes, bridges can be constructed with a useful life of over one hundred years. The reduced time constraint also results in higher quality workmanship. Quality assurance in the form of inspections and service load tests can be done in the plant rather than on-site, making it easier, quicker, and safer. Labor and inspection are made easier due to the casting of bridge elements at ground level allowing inspections to be easily performed at multiple stages during casting to ensure that the elements are progressing as expected (CPPCI 2002). A study on bridge durability found that a smaller percentage of prestressed concrete bridges were “structurally deficient” compared to cast-in-place bridges of similar age and span length (Dunker 1992).

4. Lower Life Cycle Costs: Bridges built using RBC have better durability and longer service lives than bridges built using cast-in-place concrete construction (FHWA 2005). Consequently, maintenance and major repair expenditures occur less frequently than conventionally-constructed bridges. Savings are further experienced with the use of prestressing with reduced raw materials consumption (smaller size elements can be used) (CPPCI 2002). The cost of formwork and its installation and removal is another area for huge savings.
5. Improved Safety (Work-Zone Safety): Many bridge construction projects occur in areas of high traffic, high elevations, or over water. Shortened construction periods mean that workers will spend significantly less time in dangerous areas by moving most of the processes out of harm’s way (Georgia 2002). Reduced construction time and less traffic disruption also indicate that drivers are less exposed to bridge construction and work-zone which, therefore, greatly reduces travel hazards.
6. Less Environmental Impacts: The use of prefabricated elements results in a much less invasive construction site. The most disruptive aspect of the process is the large equipment needed to place the various components (FHWA 2008b).

Despite the many advantages RBC technology has, the initial cost is the main hurdle to the wide adoption of this technology. RBC often incurs higher initial cost and higher shipping cost. Prefabricated bridge elements are usually custom made, and shipping these elements from offsite precast facilities to construction sites is more expensive than shipping conventional materials such as formwork and concrete. Also, equipment such as cranes that are needed for the installation of the larger elements such as bent caps will require extra load capacity, leading to technical challenges and higher costs. However, as this technology becomes more widely accepted and elements more standardized, the unit price of prefabricated elements is expected to decline, lowering the overall construction cost. Another challenge in applying RBC technology to bridge construction is the lack of contractor experience and expertise due to the fact that RBC technology is still relatively new to the construction industry. Therefore, justifying the use of RBC technology over the conventional approach becomes a key towards a successful implementation.

5.2 Time Study Methodology

An ideal way to quantify time savings and, consequently, user cost savings associated with RBC technology is to construct the same bridge twice at the same location and time point, using conventional cast-in-place concrete the first time and RBC the second time. The duration and

performance of building the same bridge with two different approaches would be closely monitored and compared, step by step and bridge element by bridge element. By doing so, not only can the overall time saving be quantified, but also the sources of time saving can be identified and computed. Obviously, this ideal way of assessing the RBC technology is practically infeasible, considering that only one method is used during construction, and cannot be implemented in reality. But this reveals that a comparison study is suitable to achieve the goal by using the historical project information of a bridge that is of similar size and shape, built in the same environment, and approximately within the same time frame.

The key to a comparison study is the establishment of a baseline for the use of the cast-in-place concrete approach. The productivity and performance of RBC technology can be compared to the established baseline to ultimately assess RBC's time saving benefits. To establish such a baseline, productivity should be determined based on a recently completed local bridge project that was constructed using conventional methods. Figure 4.1 below illustrates the flow chart of the design of a comparison study to quantify the time savings of the RBC technology.

- First, productivity information is acquired from a local, temporal bridge project constructed with the conventional cast-in-place concrete technology.
- Second, a work breakdown structure (WBS) analysis is conducted for the bridge to be constructed, resulting in two WBS structures, one for the use of the conventional cast-in-place concrete technology and the other for the RBC technology.
- The study process branches out from this point:
 - For the cast-in-place approach, activity durations are determined based upon the productivity information acquired from a local, temporal bridge project. A construction schedule is developed with project milestones and the critical path method (CPM) is applied to determine critical activities, the project duration, and early start, early finish, late start and late finish for each individual activity. Applying CPM resulted in a baseline for the comparison study.
 - For the RBC technology, field performance is closely monitored to determine the actual productivity and activity durations. An “as-built” schedule begins to develop when the project starts and completes when the project ends. Consequently, the “as-built” schedule is compared to the baseline schedule, step-by-step and bridge element by bridge element to quantify not only the overall time saving, but also to identify and assess time saving sources.
- The baseline CPM schedule of the conventional bridge method is compared to the actual performance of the RBC-based one to identify sources of time saving with quantified information.

5.3 Time Study Results and Discussions

Two onsite solar-powered cameras were set up in the field by MDOT on both sides (North and South) of the bridge to take still pictures every 15 minutes, and thus record construction activities in 15-minute intervals. As mentioned earlier, to establish a baseline for the comparison study, a conventional cast-in-place bridge is needed to provide productivity information. In this study, the researchers chose the Lovers Lane Bridge that spans I-94 in Portage, Michigan. The Lovers

Lane Bridge was constructed using conventional methods. It is located less than 5 miles from the Parkview Bridge and was completed in 2006. Table 8 below illustrates the specifications of these two bridges.

To start the comparison, a Work Breakdown Structure for the Parkview Bridge was created for analyzing RBC. Another WBS for the bridge was developed for analyzing the conventional construction method. The WBSs were developed using the current Parkview Bridge plans as well as the Lovers Lane Bridge productivity data. Table 9 details these WBSs side-by-side. After the activities were identified and organized, their durations were calculated for the conventional approach by referring to the productivity information extracted from the Lovers Lane Bridge. All these activities were put together into a schedule and the CPM technique was applied to determine the overall project duration, durations for individual bridge elements, and dates for milestones. Figure 5 illustrates the CPM schedule for the Parkview Bridge under the conventional approach with a total duration of 107 days. All critical activities are highlighted in Figure 5. In addition, this conventional bridge would have completed on September 15, 2008 if it were started on April 15, 2008, which was the actual start date for the construction of the Parkview Bridge. A tabular schedule report is provided in Table 10.

For the RBC approach, the duration for each individual activity was determined by checking the still pictures taken by the two onsite cameras and by visiting the construction job site on a regular basis. The actual start and end dates and duration for each activity were also extracted from the pictures and an as-built schedule was derived with a total project duration of 62 days, which is illustrated in Figure 6. Similar to Figure 5, all critical activities are highlighted. It also illustrates that the actual construction started on April 15, 2008 and should have finished by July 8, 2008 if the rework on deck panels did not take place. A tabular schedule report is provided in Table 11.

It is worth noting here that actual construction was delayed for a major “re-work” involving the complete prefabrication of the deck panels due to errors in the first set of panels, causing the actual opening to be pushed back to September 8th, 2008. This error suggests that there is risk associated with adopting a new technology. However, even with the mistakes and delays due to the unfamiliarity with the RBC technology, the project was still completed ahead of the conventional schedule. In our analysis of time savings, we elected to ignore the delays caused by the re-work and used the original July 8, 2008 completion date.

The overall time saving to the users is 45 days (107 – 62), about 42% of the project duration over the conventional bridge construction. In other words, adopting RBC can cut project duration by approximately half for a bridge at the scale of the Parkview Bridge. Examining the critical path activities in Figures 5 and 6 reveals that the main sources of time savings of RBC include the shorter on-site construction time required for each individual bridge element and the exclusion of the time needed for forming, placing reinforcement and concrete, and curing each element. Note that these activities are now shifted to off-site and sometimes to off-season (during winter) as some pre-cast facilities are able to produce bridge elements indoors. Also note that in this analysis, some pre-cast elements were not included in the time saving such as the I-beam girders

since they were used in both the conventional and RBC approaches. We only focused on those elements that are not typically constructed using the pre-cast approach such as abutments, piers, and bridge deck panels. Table 12 provides a comparison of durations to independently construct individual bridge elements using the conventional bridge construction method versus the RBC method.

The time saving realized by rapid bridge construction yields many benefits. Cost saving for transportation users is among the most visible and quantifiable ones. Obviously, the magnitude of the realized transportation user cost saving depends on the number of days shortened and the volume of affected traffic. Figure 7 (a) illustrates the available detour routes for the affected traffic. Figure 7 (b) shows a conceptual sketch of the intersection next to the bridge, with affected traffic volumes labeled as V1 through V6. It was observed in the field that by isolating the bridge, 50% of the affected traffic has node A as either origin or destination while the other 50% has node B as either origin or destination. The value of extra vehicle-miles travelled per day due to the construction of Parkview Bridge and the adoption of the detour outlined in Figure 7 can be calculated as:

$$\begin{aligned}
 & [(V_1 + V_2) * 50\% * (0.68 + 0.47 + 0.54 - 0.2 - 0.3)] \\
 & + [(V_1 + V_2) * 50\% * (0.68 + 0.47 + 0.54 + 0.2 - 0.3)] \\
 & + [(V_3) * 50\% * (0.47 + 0.54 - 0.2 - 0.68 - 0.3)] \\
 & + [(V_3) * 50\% * (0.47 + 0.54 + 0.2 - 0.68 - 0.3)] \\
 & + [(V_4) * 50\% * (0.2 + 0.54 + 0.47 - 0.68 - 0.3)] \\
 & + [(V_4) * 50\% * (0.54 + 0.47 - 0.68 - 0.3 - 0.2)] \\
 & + [(V_5 + V_6) * 50\% * (0.54 + 0.47 + 0.68 - 0.2 - 0.3)] \\
 & + [(V_5 + V_6) * 50\% * (0.2 + 0.54 + 0.47 + 0.68 - 0.3)] \\
 & = 9,032 \text{ vehicle-miles}
 \end{aligned}$$

Assuming an average fuel efficiency of 18 miles/gallon, the above 9,032 vehicle-miles is transformed into 502 gallons/day. During the construction period, the fuel cost was over \$4 per gallon, and consequently the extra cost was over \$2,000 per day, without considering the extra emission, air pollution, and the deterioration of the traffic condition at nearby intersections. Adopting RBC technology would have shortened the project duration by 45 days, and consequently the saving could be quantified as \$90,000, considering extra vehicle-miles only. The saving amount is about 3% of the bridge construction contract amount (approximately \$2.85 millions) and is quite decent compared to the industry profit rate of construction. It is worth pointing out that the high-quality design of the detour schema was also a reason for the relatively small amount of extra vehicle-miles.

A similar calculation was done to estimate the extra travel time occurred due to the construction and the designed detour schema. Field experiments revealed that it took on average an extra 10 minutes to complete the travel for traffic V₁, V₂, V₅, and V₆; 5 extra minutes to complete the travel for traffic V₃; and 8 extra minutes to complete the travel for traffic V₄. The estimates revealed that the extra travelling time was 1,300 vehicle-hours per day. Consequently, shortening the project duration by 45 days saved approximately 58,800 vehicle-hours of travel

time. Even with a low average hourly wage rate of \$15, the RBC technology realized a saving of \$882,000 from the travel time perspective, which is approximately 31% of the construction contract amount.

In conclusion, the RBC technique can significantly save bridge construction time and consequently realizes a huge saving on user travel time. This travel time saving is significant enough that it can justify the relatively higher initial cost of the RBC technique. Considered together with other advantages of RBC, such as high quality and low maintenance cost, the technique offers a more efficient and economic alternative to the conventional method. More assessment studies such as this one will need to be conducted to fully understand and realize the advantages of RBC techniques.

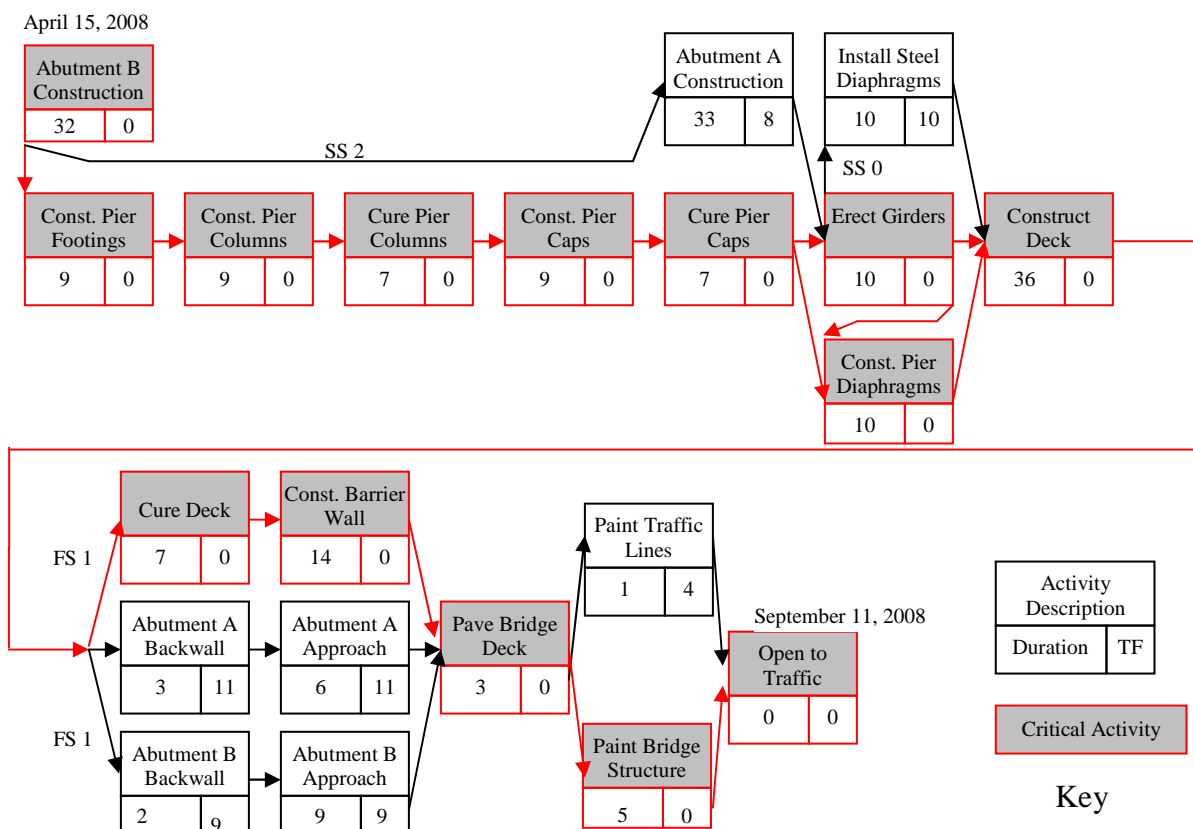


FIGURE 5: Conventional bridge construction schedule

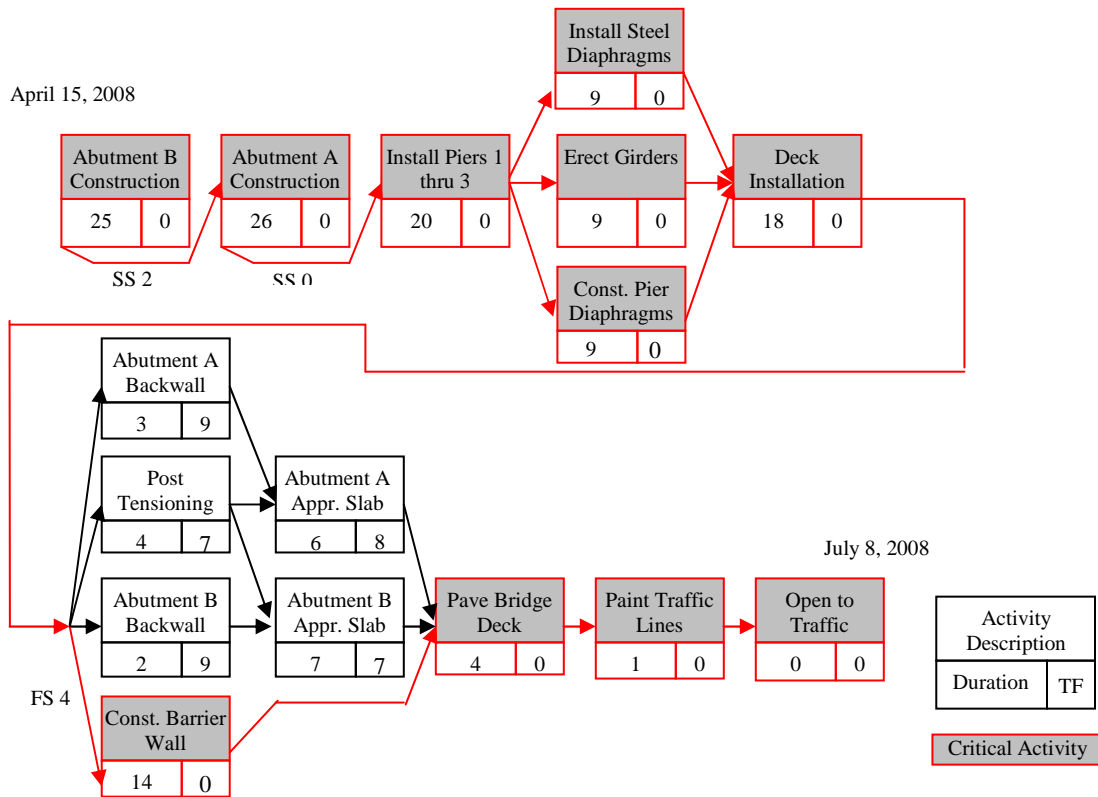


FIGURE 6: Rapid bridge construction schedule (without construction delays)

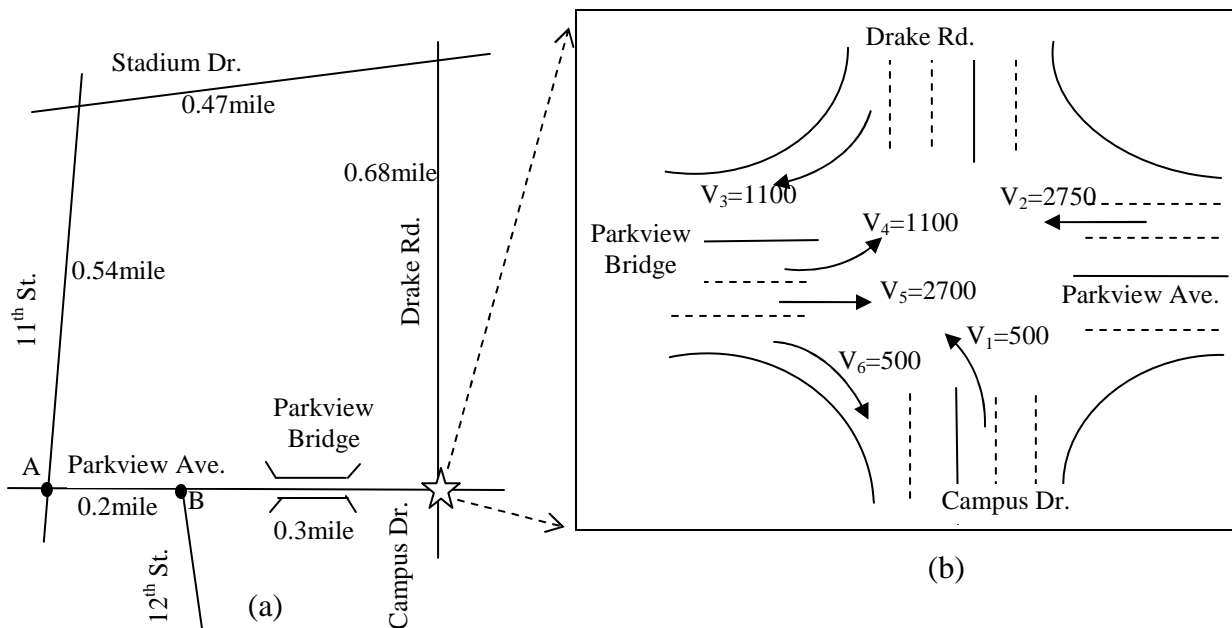


FIGURE 7: Detour and intersection

TABLE 8: Specifications of the Lovers Lane Bridge and the Parkview Bridge

Specifications	Lovers Lane Bridge	Parkview Bridge
Length (total of span lengths)	176.5 ft	249 ft
Width (outside to outside)	80.5 ft	55.5 ft
Number of Lanes	5	3
Number of Spans	2	4
Construction Method	Cast-in-place concrete	Precast, full-depth deck

TABLE 9: Parkview Bridge WBS: Conventional vs. Rapid Construction Methods

Conventional Method	Rapid Bridge Method
Mobilization	
<i>Preparation of for construction</i>	<i>Preparation of for construction</i>
Substructure	
<i>Excavation</i>	<i>Excavation</i>
<i>Piles (East, West Abutments)</i>	<i>Piles (East, West Abutments)</i>
<i>Delivery</i>	<i>Delivery</i>
<i>Drive</i>	<i>Drive</i>
<i>Spread Footings (East, Median, West)</i>	<i>CIP Spread Footings (East, Median, West)</i>
<i>Formwork</i>	<i>Formwork</i>
<i>Reinforcement</i>	<i>Reinforcement</i>
<i>Pouring</i>	<i>Pouring</i>
<i>Curing</i>	<i>Curing</i>
<i>Form Removal</i>	<i>Form Removal</i>
<i>Abutments (East, West)</i>	<i>Abutments (East, West)</i>
<i>Formwork</i>	Precast Abutment
<i>Reinforcement</i>	<i>Delivery</i>
<i>Pouring</i>	<i>Placement</i>
<i>Curing</i>	CIP Concrete Diaphragm
<i>Form Removal</i>	<i>Formwork</i>
	<i>Reinforcement</i>
	<i>Pouring</i>
	<i>Curing</i>
	<i>Form Removal</i>
	CIP Backwall
	<i>Formwork</i>
	<i>Reinforcement</i>
	<i>Pouring</i>
	<i>Curing</i>
	<i>Form Removal</i>
<i>Piers (East, Median, West)</i>	<i>Piers (East, Median, West)</i>
Columns (4 ea)	Precast Columns (4 ea)
<i>Formwork</i>	<i>Delivery</i>
<i>Reinforcement</i>	<i>Placement</i>
<i>Pouring</i>	<i>Grouting</i>
<i>Curing</i>	<i>Curing</i>
<i>Form Removal</i>	

Pier Cap	Precast Pier Cap
<i>Formwork</i>	<i>Delivery</i>
<i>Reinforcement</i>	<i>Placement</i>
<i>Pouring</i>	<i>Grouting</i>
<i>Curing</i>	<i>Curing</i>
<i>Form Removal</i>	
CIP Pier Diaphragm	CIP Pier Diaphragm
<i>Formwork</i>	<i>Formwork</i>
<i>Reinforcement</i>	<i>Reinforcement</i>
<i>Pouring</i>	<i>Pouring</i>
<i>Curing</i>	<i>Curing</i>
<i>Form Removal</i>	<i>Form Removal</i>
CIP Barrier Wall (East, West Only)	CIP Barrier Wall (East, West Only)
<i>Formwork</i>	<i>Formwork</i>
<i>Reinforcement</i>	<i>Reinforcement</i>
<i>Pouring</i>	<i>Pouring</i>
<i>Curing</i>	<i>Curing</i>
<i>Form Removal</i>	<i>Form Removal</i>
	<i>Slope Wall</i>
	<i>Formwork</i>
	<i>Reinforcement</i>
	<i>Pouring</i>
	<i>Curing</i>
	<i>Form Removal</i>
Superstructure	
<i>Precast Concrete I-Beams Span (1,2,3,4)</i>	<i>Precast Concrete I-Beams Span (1,2,3,4)</i>
<i>Delivery</i>	<i>Delivery</i>
<i>Placement</i>	<i>Placement</i>
<i>Steel Diaphragm</i>	<i>Steel Diaphragm</i>
<i>Delivery</i>	<i>Delivery</i>
<i>Placement</i>	<i>Placement</i>
<i>Deck (Span 1,2,3,4)</i>	<i>Deck (Span 1,2,3,4)</i>
<i>Formwork</i>	<i>Delivery</i>
<i>Reinforcement</i>	<i>Placement</i>
<i>Pouring</i>	<i>Match-casting/Grouting/Post-Tensioning</i>
<i>Curing</i>	<i>Curing</i>
<i>Form Removal</i>	
<i>Deck Barrier Walls</i>	<i>Deck Barrier Walls</i>
<i>Formwork</i>	<i>Formwork</i>
<i>Reinforcement</i>	<i>Reinforcement</i>
<i>Pouring</i>	<i>Pouring</i>
<i>Curing</i>	<i>Curing</i>
<i>Form Removal</i>	<i>Form Removal</i>
Earthwork	
<i>Backfill</i>	<i>Backfill</i>
<i>Landscaping</i>	<i>Landscaping</i>

TABLE 10: Tabular Schedule Report – Conventional Bridge Construction

Activity ID	Duration	Activity Description	Early Start	Early Finish	Late Start	Late Finish	Total Float
1	32	Abutment B Const.	15-Apr-08	21-May-08	15-Apr-08	21-May-08	0
2	9	Construct Pier Footings	17-Apr-08	26-May-08	17-Apr-08	26-May-08	0
3	9	Construct Pier Columns	28-Apr-08	7-May-08	28-Apr-08	7-May-08	0
4	7	Cure Pier Column	8-May-08	15-May-08	8-May-08	15-May-08	0
5	9	Construct Pier Caps	16-May-08	26-May-08	16-May-08	26-May-08	0
6	33	Abutment A Cons.	17-Apr-08	24-May-08	28-Apr-08	2-Jun-08	8
7	7	Cure Pier Cap	27-May-08	3-Jun-08	27-May-08	3-Jun-08	0
8	10	Erect Girders	4-Jun-08	14-Jun-08	4-Jun-08	14-Jun-08	0
9	10	Install Steel Diaphragms	4-Jun-08	14-Jun-08	15-Jun-08	25-Jun-08	10
10	10	Const. Pier Diaphragms	16-Jun-08	26-Jun-08	16-Jun-08	26-Jun-08	0
11	36	Construct Deck	27-Jun-08	8-Aug-08	27-Jun-08	8-Aug-08	0
12	7	Cure Concrete Deck	9-Aug-08	16-Aug-08	9-Aug-08	16-Aug-08	0
13	14	Const. Barrier Wall & Railing	18-Aug-08	2-Sep-08	18-Aug-08	2-Sep-08	0
14	3	Abutment A Backwall	11-Aug-08	13-Aug-08	23-Aug-08	26-Aug-08	11
15	6	Abutment A Approach Slab	14-Aug-08	20-Aug-08	27-Aug-08	2-Sep-08	11
16	2	Abutment B Backwall	11-Aug-08	12-Aug-08	21-Aug-08	22-Aug-08	9
17	9	Abutment B Approach Slab	13-Aug-08	22-Aug-08	23-Aug-08	2-Sep-08	9
18	3	Pave Bridge Deck	3-Sep-08	5-Sep-08	3-Sep-08	5-Sep-08	0
19	5	Paint Bridge Structure	6-Sep-08	11-Sep-08	6-Sep-08	11-Sep-08	0
20	1	Paint Traffic Lines	6-Sep-08	6-Sep-08	11-Sep-08	11-Sep-08	4
21	0	Open to Traffic	12-Sep-08	11-Sep-08	12-Sep-08	11-Sep-08	0
Project Duration (working days)*							107

TABLE 11: Tabular Schedule Report – Rapid Bridge Construction

Activity ID	Duration	Activity Description	Early Start	Early Finish	Late Start	Late Finish	Total Float
1	25	Abutment B Const.	15-Apr-08	13-May-08	15-Apr-08	13-May-08	0
2	26	Abutment A Const.	17-Apr-08	16-May-08	17-Apr-08	16-May-08	0
3	20	Install Piers 1 Thru 3	17-Apr-08	9-May-08	17-Apr-08	9-May-08	0
4	9	Const. Pier Diaphragms	10-May-08	20-May-08	10-May-08	20-May-08	0
5	9	Erect Girders	10-May-08	20-May-08	10-May-08	20-May-08	0
6	9	Install Steel Diaphragms	10-May-08	20-May-08	10-May-08	20-May-08	0
7	18	Deck Installation	21-May-08	10-Jun-08	21-May-08	10-Jun-08	0
8	2	Abutment B Backwall	11-Jun-08	12-Jun-08	21-Jun-08	23-Jun-08	9
9	4	Post Tensioning	11-Jun-08	14-Jun-08	19-Jun-08	23-Jun-08	7
10	3	Abutment A Backwall	11-Jun-08	13-Jun-08	21-Jun-08	24-Jun-08	9
11	7	Abutment B Approach Slab	16-Jun-08	23-Jun-08	24-Jun-08	1-Jul-08	7
12	6	Abutment A Approach Slab	16-Jun-08	21-Jun-08	25-Jun-08	1-Jul-08	8
13	14	Const. Barrier Wall & Railing	16-Jun-08	1-Jul-08	16-Jun-08	1-Jul-08	0
14	4	Pave Bridge Deck	2-Jul-08	7-Jul-08	2-Jul-08	7-Jul-08	0
15	1	Paint Traffic Lines	8-Jul-08	8-Jul-08	8-Jul-08	8-Jul-08	0
16	5	Paint Bridge Structure	2-Jul-08	8-Jul-08	2-Jul-08	8-Jul-08	0
17	0	Open to Traffic	9-Jul-08	8-Jul-08	9-Jul-08	8-Jul-08	0
Project Duration (working days)*							62

TABLE 12: Element-by-Element Comparison of Conventional vs. Rapid Construction

CONVENTIONAL CONSTRUCTION		RAPID CONSTRUCTION	
Activities	Duration	Duration	Activities
ABUTMENTS			
Abutment A (West)			
Form Abutment Wall	5	1	Install Precast Abutments
Install Abutment Wall Resteel	4	1	Grout Pile/Abutment Pockets
Pour Abutment Wall	1	1	Form & Pour Abutment Splice
Total Duration	10 Days	3 Days	Total Duration
Abutment B (East)			
Form Abutment Wall	5	1	Install Precast Abutments
Install Abutment Wall Resteel	4	1	Grout Pile/Abutment Pockets
Pour Abutment Wall	1	1	Form & Pour Abutment Splice
Total Duration	10 Days	3 Days	Total Duration
PIERS			
Pier 1 (West)			
Form Pier Collum & Install Reinforcement	2+1 = 3		
Pour Pier Column	3	1	Erect Columns
Form Pier Cap	2	1	Grout Columns
Install Cap Resteel	2	1	Erect Pier Cap
Pour Pier Cap	1	2	Grout Pier Cap
Total Duration	11 Days	5 Days	Total Duration
Pier 2 (Median)			
Form Pier Column & Install Reinforcement	2+1 = 3		
Pour Pier Column	3	1	Erect Columns
Form Pier Cap	2	1	Grout Columns
Install Cap Resteel	2	1	Erect Pier Cap
Pour Pier Cap	1	3	Grout Pier Cap
Total Duration	11 Days	6 Days	Total Duration
Pier 3 (East)			
Form Pier Column & Install Reinforcement	2+1 = 3		
Pour Pier Column	3	1	Erect Columns
Form Pier Cap	2	1	Grout Columns
Install Cap Resteel	2	1	Erect Pier Cap
Pour Pier Cap	1	1	Grout Pier Cap
Total Duration	11 Days	4 Days	Total Duration
DECK			
		1**	Install Haunch Forms
		1**	Install Shim Packs
		1	Erect Panels
		2	Install Deck Joint & Backer Rod
		2	Install PT Couplers
Forming Fascia	11	2	Grout Deck Joints
Form Bulkhead	2	2**	Install Coil Bolts Shear Developers
Install Deck Re-steel*	12	2**	Install Diaphragm Shear Developers
Pour Concrete Deck	3	1	Adjust Haunch Forms
Cure Concrete Deck	8	2	Pour Haunch and Shear Pockets
Total Duration	36 Days	13 Days	Total Duration

* Due to the relatively small size of the deck surface area, we assumed that the placing of reinforcement activity would occur after the deck has been formed (i.e. no overlap) to avoid crew (carpenters/ironworkers) congestion and/or interferences.

** Same-color activities take place concurrently, and hence their durations are only counted once in the total deck duration.

6.0 LOAD TESTING

Load testing is recommended by American Association of State Highway and Transportation Officials (AASHTO) as an “effective means of evaluating the structural performance of a bridge” (AASHTO 2000). The purpose of conducting load testing to existing bridges is to evaluate their structural performance, within the serviceability loading. Therefore, load testing is usually conducted in a nondestructive manner and is sometimes the synonym of nondestructive load testing. The principle is to compare the field response of the bridge under test loads with its theoretical performance as the theory indicates (NCHRP 1998). Nondestructive load testing can be further categorized into diagnostic testing and proof testing. Diagnostic testing methods provide the measurements necessary to analyze differential loading effects (i.e. moment, shear, axial force, deflection, etc.) present in various structural members due to applied loads (Phares 2005). Proof load testing aims at determining the maximum load configuration that forces the bridge to approach its elastic limit.

Tasks involved in a load testing typically include the determination of testing objectives, the design of load configuration, the selection and placement of instrumentation, the adoption of appropriate analysis techniques, and the analysis of results (Kleinhans 2007). Load testing is being carried out widely to evaluate and rate bridge performance on a case-by-case manner to test the impacts from new construction materials and technologies (Kleinhans 2007, Hou 2006). While a number of bridge load testing studies can be found in the literature, such studies on bridges using embedded sensors are almost nonexistent.

The load testing of the Parkview Bridge was carried out twice: one in September 2008 before the bridge was open to traffic and one in June 2009. During the first load testing, the sensors were not yet operational. During the second load testing, the sensor network was functional and was used in the load testing of the bridge. This section describes the design and implementation of the load testing in this study in the aspects of load testing objectives and approaches, testing scenarios, load configuration, and testing procedure.

6.1 Load Testing Objectives and Approaches

The overall goal of conducting load testing is to quantify its performance under varying conditions of design loads. Specific objectives include measuring surface deflections, deriving stresses from measured deflections via analytical models, and cross-validating analytical results and sensor readings. Figure 8 presents a flow chart that describes the approaches and tasks in carrying out the testing. The first task is to develop testing scenarios. The second task is to design load configuration to such that when these loads are applied to the locations specified in the first task, they would yield the maximum moments and deflections. The next step is to compute stresses using the girder-deck section properties and measured deflections. Surface deflections are measured by optical surveying using Trimble® Dini level with an accuracy of 0.0012 inch. These stresses are compared to stresses extracted from the sensors embedded in the bridge deck panels for validation and further analysis.

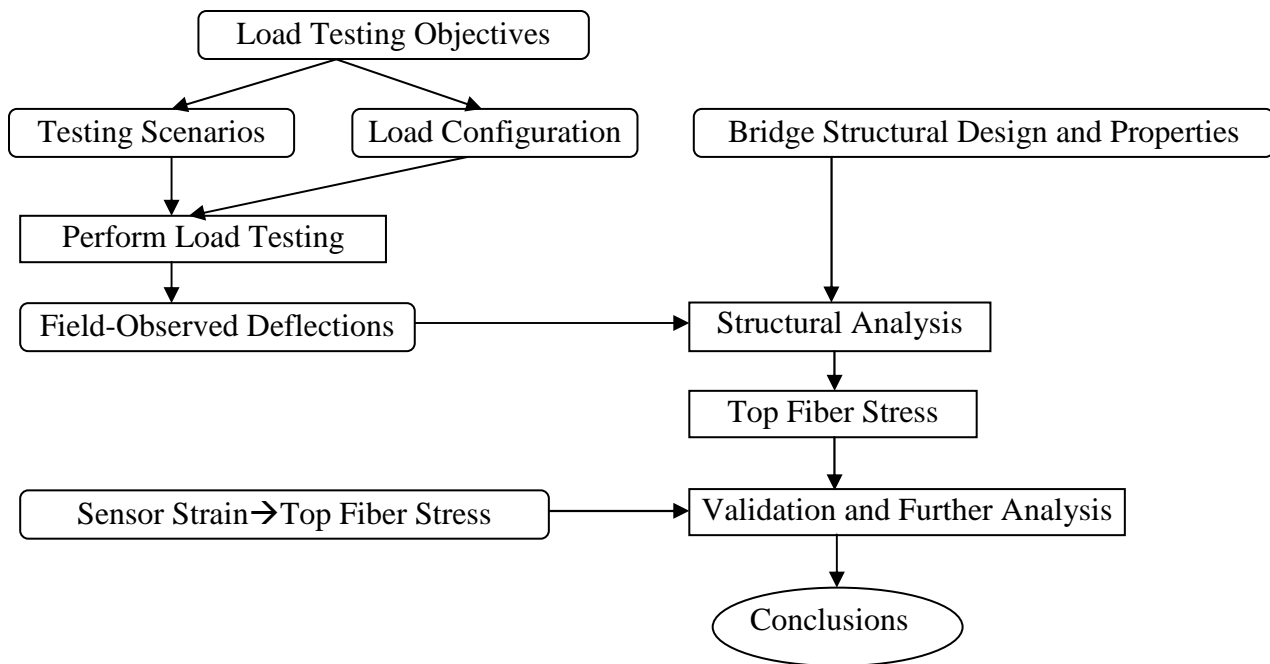


FIGURE 8: Flow chart for the bridge load testing process

6.2 Load Testing Scenarios

A total of ten load scenarios, including four single-directional and six bi-directional, were designed and implemented in this study. Figure 9 illustrates the mid-span, where the testing loads were placed. Table 13 lists the testing scenarios with their load locations. During the load testing, surface elevations at these mid-span locations and also those points above the bridge piers (represented by triangles) were measured before the load were in place to provide a surface baseline. When the loads were in place, surface elevations at these locations were measured again to determine surface deflections due to specific loads.

6.3 Load Configuration

Two types of trucks were used to provide testing loads. Figure 10 illustrates the configuration for the trucks used for the single-directional and the bi-directional testing. These truck configurations were obtained from the pool of legal trucks in Michigan. The type I truck illustrated in Figure 10 was chosen to be the closest to the HS20 design truck used by the designer of the bridge. Table 14 provides the actual axle weights for all three trucks (one type I truck and two type II trucks) used in this study.

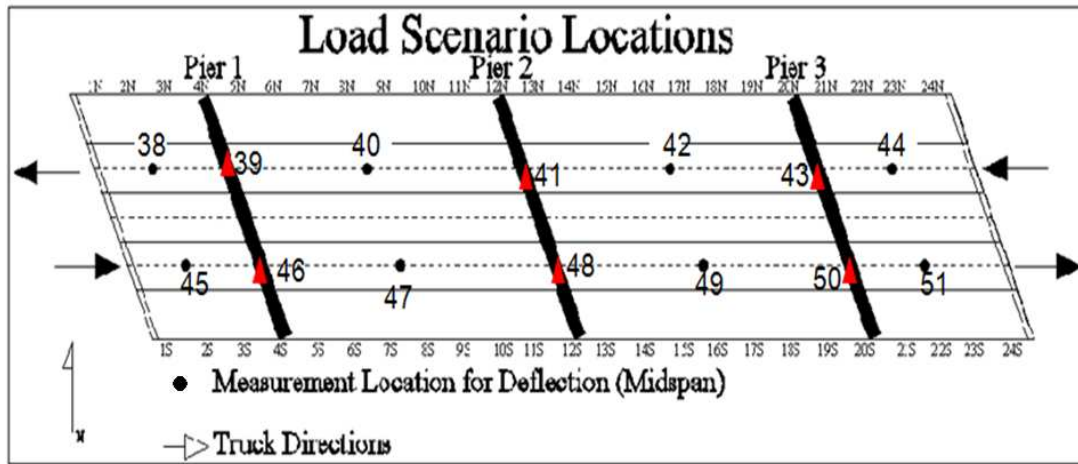


FIGURE 9: Load testing locations



Type I truck for single-directional testing



Type II truck for bi-directional testing

FIGURE 10: General configurations for trucks.

TABLE 13: Testing Scenarios

Testing Scenarios	Truck Type 1 Location (Single Direction – 1 truck)	Truck Type 2 Location (Bi-Directional – 2 trucks)
1	47	-
2	42	-
3	49	-
4	40	-
5	-	45, 44
6	-	47, 42
7	-	49, 40
8	-	51, 38
9	-	47, 40
10	-	45, 38

TABLE 14: Actual Loaded Truck Weights (Pounds)

Axle #	Single Directional Truck Type 1 Weights	Bi-directional Truck Type 2 Weights	
Front Axle	9,640	17,850	18,350
#2 Axle	35,540	18,050	18,600
#3 Axle		17,800	18,250
#4 Axle	34,580	-	-
#5 Axle		-	-
Gross Weight	79,760	53,700	55,200

6.4 Load Testing Procedure

The steps below were followed in this study to complete bridge load testing (see Figure 9).

- Step 1: Load trucks according to load specifications and configurations and utilize truck weigh stations to determine actual axle weight.
- Step 2: Based upon actual axle weight, mark a point on each truck in such a way that when this point is aligned with mid span locations, the truck load causes the maximum moment.
- Step 3: While loading of the trucks take place prior to testing; the survey crew set up and determine mid spans along with center line of pier locations per the plan.
- Step 4: Measure surface elevations for all the marked points to establish a baseline for Testing Scenario 1.
- Step 5: Move truck of type I to point 47 (scenario 1). After the truck is in place, measure surface elevations for those points to determine bridge deflection due to the truck load.
- Step 6: For load tests using the sensor network (load test 2), record the time the truck is in position and ensure that the truck stays in position for a minimum of 10 minutes to allow the sensors to register their readings (sensors collect data on 10-minute increments).
- Step 6: Move the truck off bridge.
- Step 7: Repeat Steps 4 to 6 for the remaining testing scenarios.

6.5 Top Fiber Stresses from Deflection Measurements

After validating field observations, moments were derived from surface deflections and used to compute the top fiber stresses utilizing the two PCI equations below and using the simply supported moments at mid spans (i.e. assuming zero moments at the piers for conservative results at mid spans) (PCI 2003). The moments at the piers were then computed from the mid span moments using distribution factors obtained from simulated, unit-force loadings that mimic the truck loads from the 10 scenarios.

$$M_{LL} = D (48 EI_c / 5L^2) \quad \text{and} \quad \sigma_{LL} = M_{LL} / I_c$$

- where M_{LL} – Live load moment (lb-in);
 D – Deflection (inches);
 E – Section modulus of elasticity (4,595,487 psi);
 I – Moment of inertia of composite section (438,913 in⁴);
 L – Span length (inches);
 y – Distance from the top fiber to the neutral axis (18 inches); and
 σ_{LL} – Stress (psi).

Table 15 summarizes the dead load stresses at the various points used for the load testing. The values were extracted from the design calculations provided by the Parkview Bridge designer (Parsons Transportation Group 2007).

TABLE 15: Deck Dead Load Stresses from Design Calculation (psi)

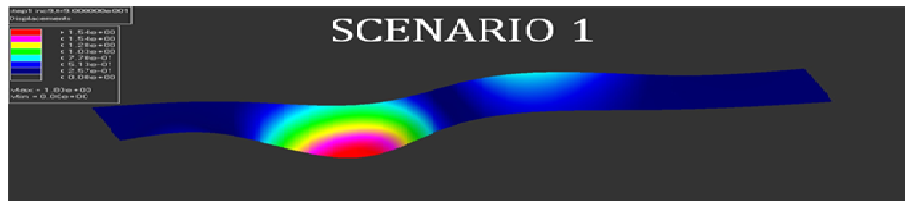
Top Fiber Dead Load Stresses – South								
West Abut	Midspan (45)	Pier 1 (46)	Midspan (47)	Pier 2 (48)	Midspan (49)	Pier 3 (50)	Midspan (51)	East Abut
0	-436	-466	-773	-430	-760	-379	-428	0
Top Fiber Dead Load Stresses – North								
East Abut	Midspan (44)	Pier 3 (43)	Midspan (42)	Pier 2 (41)	Midspan (40)	Pier 1 (39)	Midspan (38)	West Abut
0	-428	-379	-760	-430	-773	-466	-436	0

The average 28-day compression strength (f'_c) was recorded as approximately 8,000 psi. Therefore, maximum allowable stresses in the concrete are:

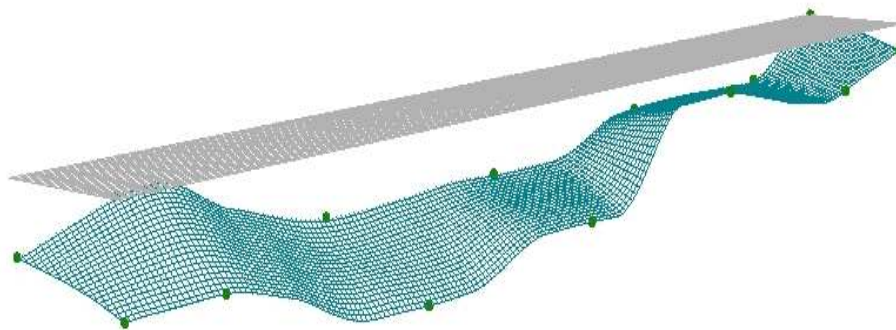
$$\begin{aligned} \text{Compression } (f_c): \quad & f_c \leq 0.45 f'_c \Rightarrow -3,600 \text{ psi} \\ \text{Tension } (f_t): \quad & f_t \leq 6\sqrt{f'_c} \Rightarrow 537 \text{ psi} \end{aligned}$$

6.6 Field Measurements Validation

Three-dimensional surface plots of deflection measurements were developed and compared with the finite element (FE) simulation results to validate the behavior and field measurements. Figure 11 illustrates an example of the comparison for scenario 1 in load test 1. The field observations match the theoretically simulated results, providing confidence in the measurements from scenario 1 observations. Similar comparisons were conducted to validate results in all 10 testing scenarios. A complete set of deflected shapes for all scenarios in both load tests are provided in Appendix C. Note that scenarios 2, 6, and 9 from load test 1 were declared erroneous due to the apparently inconsistent behavior of the bridge under the applied loads. This was further verified when load test 2 was completed, as discussed in section 6.9.



(a) Simulated deflected shape



(b) Actual deflected shape

FIGURE 11: Validating scenario 1 results from load test 1 (drawn not to scale)

6.7 Load Test 1 - Before Opening

This section presents the results of the load testing that was completed on September 8, 2008 and involved deflection measurements.

Table 16 displays the measured deflections for load test 1 (note that negative values indicate downward movement). The stresses resulting from these deflection measurements are presented in Tables 17 and 18 (note that negative values indicate compression). Also, note that scenarios 2, 6, and 9 are declared erroneous from the validation process based on deflected shapes and bridge deck behavior. The columns representing these scenarios are highlighted in yellow in Tables 16 through 20.

Combining the dead load stresses given in Table 15 with the live load stresses given in Tables 17 and 18 results in total stresses presented in Tables 19 and 20 for all scenarios using the deflection measurements and sensor readings methods. It is clear from these tables that the total stresses are within the allowable limits for all testing scenarios for both the south and north panels.

TABLE 16: Load Test 1 Summary of Deflections

Location	Scenario Change in Elevation (inches)									
	1	2	3	4	5	6	7	8	9	10
38	-0.02	-0.06	-0.03	-0.05	-0.02	0.00	0.01	0.01	0.01	0.00
39	-0.01	0.00	-0.04	-0.01	-0.01	-0.02	0.05	-0.01	-0.01	-0.01
40	-0.03	0.19	-0.03	-0.07	0.00	0.01	-0.32	0.01	0.04	0.02
41	-0.03	0.34	-0.03	-0.04	0.00	-0.02	-0.03	0.01	-0.32	0.01
42	-0.02	0.43	-0.03	-0.03	0.00	0.47	-0.01	0.03	-0.46	0.01
43	-0.02	0.06	-0.02	-0.03	-0.01	-0.68	-0.02	0.01	-0.61	-0.01
44	0.00	0.07	-0.02	-0.04	-0.02	-0.73	-0.03	-0.02	-0.67	-0.01
45	-0.03	0.01	0.04	-0.04	-0.02	0.00	0.03	-0.01	0.01	0.02
46	-0.03	0.10	0.14	-0.06	-0.09	0.01	-0.01	0.00	-0.01	0.01
47	-0.05	0.28	0.30	-0.03	0.01	-0.03	-0.01	-0.01	-0.01	0.03
48	-0.04	0.42	0.42	-0.03	0.01	-0.45	0.00	0.01	-0.41	0.00
49	-0.01	0.59	-0.05	-0.04	0.01	-0.02	-0.39	0.02	-0.56	-0.01
50	-0.02	0.78	-0.03	-0.02	-0.01	-0.01	-0.03	-0.02	-0.72	0.01
51	-0.01	0.89	-0.04	-0.02	0.02	0.01	0.00	0.03	-0.84	0.02

TABLE 17: Live Load Stresses Based on Deflections - South Side Panels (psi)

Scenarios	Midspan (45)	Pier 1 (46)	Midspan (47)	Pier 2 (48)	Midspan (49)	Pier 3 (50)	Midspan (51)
Scenario 1	-117	-100	-40	-15	-8	-8	-28
Scenario 2	39	33	224	81	471	454	2460
Scenario 3	155	133	240	87	-40	-38	-111
Scenario 4	-155	-133	-24	-9	-32	-31	-55
Scenario 5	-78	-66	8	3	8	-8	55
Scenario 6	0	0	-24	-9	-16	-15	28
Scenario 7	117	-100	-8	3	-312	-300	0
Scenario 8	-39	33	-8	3	16	-15	83
Scenario 9	39	-33	-8	-3	-447	-431	-2322
Scenario 10	78	66	24	9	-8	8	55

TABLE 18: Live Load Stresses Based on Deflections - North Side Panels (psi)

Scenarios	Midspan (44)	Pier 3 (43)	Midspan (42)	Pier 2 (41)	Midspan (40)	Pier 3 (39)	Midspan (38)
Scenario 1	0	0	-16	-6	-24	-23	-78
Scenario 2	194	165	0	0	152	146	-233
Scenario 3	-55	-47	-24	-9	-24	-23	-117
Scenario 4	-111	-94	-24	-9	-56	-54	-194
Scenario 5	-55	-47	0	0	0	0	-78
Scenario 6	-2018	-1724	375	-136	8	-8	0
Scenario 7	-83	-71	-8	-3	-256	246	39
Scenario 8	-55	47	24	9	8	-8	39
Scenario 9	-1852	-1582	-367	-134	32	-31	39
Scenario 10	78	66	24	9	-8	8	55

TABLE 19: Total Stresses Based on Deflections - South Side Panels (psi)

Scenarios	Midspan (45)	Pier 1 (46)	Midspan (47)	Pier 2 (48)	Midspan (49)	Pier 3 (50)	Midspan (51)
Scenario 1	-553	-566	-812	-444	-768	-386	-455
Scenario 2	-397	-433	-549	-349	-289	76	2033
Scenario 3	-281	-333	-533	-343	-800	-417	-538
Scenario 4	-592	-599	-796	-439	-792	-409	-483
Scenario 5	-514	-533	-765	-427	-752	-386	-373
Scenario 6	-436	-466	-796	-439	-776	-394	-400
Scenario 7	-320	-566	-780	-427	-1072	-679	-428
Scenario 8	-475	-433	-780	-427	-744	-394	-345
Scenario 9	-397	-499	-780	-433	-1208	-810	-2750
Scenario 10	-359	-400	-749	-421	-768	-371	-373

TABLE 20: Total Stresses Based Deflections - North Side Panels (psi)

Scenarios	Midspan (44)	Pier 3 (43)	Midspan (42)	Pier 2 (41)	Midspan (40)	Pier 1 (39)	Midspan (38)
Scenario 1	-428	-379	-776	-436	-796	-489	-514
Scenario 2	-234	-213	-760	-430	-621	-320	-669
Scenario 3	-483	-426	-784	-439	-796	-489	-553
Scenario 4	-538	-473	-784	-439	-828	-520	-630
Scenario 5	-483	-426	-760	-430	-773	-466	-514
Scenario 6	-2446	-2103	-385	-566	-765	-474	-436
Scenario 7	-511	-449	-768	-433	-1028	-220	-397
Scenario 8	-483	-331	-736	-421	-765	-474	-397
Scenario 9	-2280	-1961	-1128	-563	-741	-497	-397
Scenario 10	-350	-312	-736	-421	-780	-459	-381

6.8 Load Test 2 – After Opening

This section presents the results of the load testing that was completed on June 2, 2009, which involved two different methods: deflection measurements and sensor readings.

6.8.1 Top Fiber Live Load Stresses from Deflection Measurements

Table 21 displays the measured deflections for load test 2. The stresses resulting from these deflection measurements are presented in Tables 22 and 23 (note that negative values indicate compression).

TABLE 21: Load Test 2 Summary of Deflections

Location	Scenarios Change in Elevation (inches)									
	1	2	3	4	5	6	7	8	9	10
38	0.01	0.05	-0.05	0.04	0.01	0.00	0.01	-0.06	0.00	-0.05
39	0.01	-0.04	-0.02	0.02	0.02	-0.01	-0.02	0.00	0.00	-0.01
40	0.00	-0.05	-0.02	-0.04	0.00	-0.01	-0.06	0.01	-0.07	0.02
41	0.02	-0.02	-0.04	-0.03	0.00	0.00	-0.02	0.00	0.00	-0.01
42	0.00	-0.09	-0.02	0.04	0.01	-0.07	-0.01	0.02	0.02	0.00
43	0.00	-0.02	-0.03	0.01	0.04	-0.01	0.00	0.01	0.01	-0.01
44	-0.02	-0.01	-0.03	0.00	-0.03	0.00	0.01	0.01	0.00	0.01
45	0.01	-0.05	-0.04	0.02	0.02	0.00	0.00	-0.02	0.01	-0.02
46	0.10	-0.02	-0.04	0.04	0.01	0.02	-0.01	-0.01	0.02	0.21
47	-0.04	-0.04	-0.02	0.01	-0.01	-0.07	0.00	0.02	-0.06	0.01
48	0.02	-0.01	-0.05	0.00	-0.02	0.00	0.02	0.01	-0.02	0.00
49	0.01	-0.01	-0.07	0.01	-0.01	0.01	-0.04	0.03	-0.01	0.00
50	0.00	-0.01	-0.03	-0.01	-0.02	-0.02	0.01	0.01	0.00	0.00
51	-0.02	-0.01	0.00	-0.02	0.00	0.01	0.00	-0.01	-0.01	0.01

TABLE 22: Live Load Stresses from Deflections - South Side Panels (psi)

Scenarios	Midspan (45)	Pier 1 (46)	Midspan (47)	Pier 2 (48)	Midspan (49)	Pier 3 (50)	Midspan (51)
Scenario 1	47	40	-34	12	10	-9	-50
Scenario 2	-186	-159	-29	-10	-11	-10	-17
Scenario 3	-140	-119	-19	-7	-57	-55	-7
Scenario 4	93	80	6	2	6	-6	-63
Scenario 5	70	60	-7	-2	-6	-6	-10
Scenario 6	0	0	-58	21	5	-5	33
Scenario 7	0	0	0	0	-35	34	-3
Scenario 8	-93	-80	14	5	20	19	-30
Scenario 9	47	40	-51	-19	-8	-7	-23
Scenario 10	-96	82	9	-3	-2	2	36

TABLE 23: Live Load Stresses from Deflections - North Side Panels (psi)

Scenarios	Midspan (38)	Pier 1 (39)	Midspan (40)	Pier 2 (41)	Midspan (42)	Pier 3 (43)	Midspan (44)
Scenario 1	47	0	0	0	0	-57	-66
Scenario 2	186	-37	-38	-25	-68	-23	-27
Scenario 3	-186	-18	-19	-5	-12	-60	-70
Scenario 4	140	27	-28	-13	35	9	10
Scenario 5	47	4	-4	-2	5	81	-95
Scenario 6	0	-9	-10	21	-58	-9	10
Scenario 7	47	-5	-5	-4	-12	31	36
Scenario 8	-233	6	7	-7	19	23	27
Scenario 9	0	57	-59	4	10	9	-10
Scenario 10	-143	-15	15	-1	-3	-20	23

6.8.2 Top Fiber Live Load Stresses from Sensor Readings

During the load testing, top fiber strains were recorded by the embedded sensors in the bridge deck panels and downloaded to the laboratory computer for analysis. Even though the sensors are installed throughout the entire bridge deck, only those sensors located along the longitudinal load path were used to extract live load stresses and to compare them to the stresses derived from deflections. Tables 24 and 25 present the stresses from these sensors for the south side and the north side panels, respectively (note that negative values indicate compression).

6.8.3 Top Fiber Total Stresses – Deflection and Sensor Readings

Combining the dead load stresses given in Table 15 with the live load stresses given in Tables 22 through 25 results in total stresses presented in Tables 26 through 29 for all scenarios using the deflection measurements and sensor readings methods. It is clear from these tables that the total stresses are within the allowable limits for all testing scenarios for both the south and north panels.

TABLE 24: Live Load Stresses from Sensors - South Side Panels (psi)

Scenarios	Midspan (45)	Pier 1 (46)	Midspan (47)	Pier 2 (48)	Midspan (49)	Pier 3 (50)	Midspan (51)
Scenario 1	1.48	10.60	-11.68	6.52	5.38	-6.82	-0.33
Scenario 2	0.80	-1.50	2.52	1.00	9.57	-14.05	0.45
Scenario 3	1.55	0.65	2.48	11.77	-24.14	8.97	2.80
Scenario 4	3.00	11.70	-2.43	11.95	2.75	-0.65	-0.20
Scenario 5	-2.80	-2.05	0.28	-0.20	-0.27	-0.55	-0.15
Scenario 6	-0.40	6.30	-13.50	22.10	-3.65	11.30	-0.15
Scenario 7	0.93	-0.28	-0.69	11.30	-30.68	4.72	1.18
Scenario 8	-5.95	0.00	0.85	-0.55	0.93	3.35	2.65
Scenario 9	3.50	-2.00	15.63	-21.35	-5.12	3.70	-1.60
Scenario 10	-8.55	-2.40	0.20	0.25	1.38	-0.55	0.05

TABLE 25: Live Load Stresses from Sensors - North Side Panels (psi)

Scenarios	Midspan (38)	Pier 1 (39)	Midspan (40)	Pier 2 (41)	Midspan (42)	Pier 3 (43)	Midspan (44)
Scenario 1	1.60	8.85	-8.88	4.55	5.47	-0.87	-0.10
Scenario 2	1.95	-1.95	2.32	1.45	14.63	-19.70	0.40
Scenario 3	1.95	0.70	3.82	10.63	-11.06	4.93	4.02
Scenario 4	3.95	18.75	-26.33	17.75	3.53	0.25	0.50
Scenario 5	-2.75	-1.30	-0.10	-0.65	0.65	0.10	0.15
Scenario 6	-0.15	4.45	-6.53	21.90	-25.93	16.60	0.20
Scenario 7	1.55	5.45	-10.87	11.82	-3.51	0.02	1.70
Scenario 8	-6.05	0.35	-0.60	-0.95	-0.92	-2.65	2.55
Scenario 9	4.45	8.65	10.67	-21.30	-10.75	3.45	-0.95
Scenario 10	-6.90	3.10	0.17	-1.25	-1.22	-1.95	0.20

TABLE 26: Total Stresses Based on Deflection Measurements - South (psi)

Scenarios	Midspan (45)	Pier 1 (46)	Midspan (47)	Pier 2 (48)	Midspan (49)	Pier 3 (50)	Midspan (51)
Scenario 1	-390	-426	-806	-418	-751	-388	-478
Scenario 2	-623	-626	-801	-440	-771	-389	-444
Scenario 3	-576	-586	-792	-437	-817	-433	-434
Scenario 4	-343	-387	-767	-428	-755	-384	-491
Scenario 5	-366	-407	-779	-432	-766	-384	-438
Scenario 6	-436	-466	-830	-409	-755	-383	-395
Scenario 7	-436	-466	-773	-430	-796	-344	-431
Scenario 8	-529	-546	-758	-425	-740	-359	-458
Scenario 9	-390	-426	-824	-448	-768	-386	-451
Scenario 10	-532	-385	-764	-433	-762	-377	-391

TABLE 27: Total Stresses Based on Deflection Measurements - North (psi)

Scenarios	Midspan (38)	Pier 1 (39)	Midspan (40)	Pier 2 (41)	Midspan (42)	Pier 3 (43)	Midspan (44)
Scenario 1	-390	-466	-773	-430	-760	-435	-494
Scenario 2	-250	-503	-811	-455	-828	-401	-454
Scenario 3	-623	-485	-792	-434	-773	-438	-498
Scenario 4	-296	-439	-801	-442	-726	-370	-418
Scenario 5	-390	-463	-776	-432	-755	-298	-522
Scenario 6	-436	-475	-782	-409	-819	-387	-418
Scenario 7	-390	-471	-777	-434	-772	-347	-391
Scenario 8	-669	-460	-766	-437	-741	-356	-401
Scenario 9	-436	-409	-832	-426	-750	-370	-438
Scenario 10	-579	-481	-757	-431	-763	-398	-405

TABLE 28: Total Stresses Based on Sensor Readings – South (psi)

Scenarios	Midspan (45)	Pier 1 (46)	Midspan (47)	Pier 2 (48)	Midspan (49)	Pier 3 (50)	Midspan (51)
Scenario 1	-435	-455	-785	-423	-755	-386	-428
Scenario 2	-435	-468	-770	-429	-750	-393	-428
Scenario 3	-434	-465	-771	-418	-784	-370	-425
Scenario 4	-433	-454	-775	-418	-757	-380	-428
Scenario 5	-439	-468	-773	-430	-760	-380	-428
Scenario 6	-436	-460	-787	-408	-764	-368	-428
Scenario 7	-435	-466	-774	-419	-791	-374	-427
Scenario 8	-442	-466	-772	-431	-759	-376	-425
Scenario 9	-433	-468	-757	-451	-765	-375	-430
Scenario 10	-445	-468	-773	-430	-759	-380	-428

TABLE 29: Total Stresses Based on Sensor Readings – North (psi)

Scenarios	Midspan 38	Pier 1 39	Midspan 40	Pier 2 41	Midspan 42	Pier 3 43	Midspan 44
Scenario 1	-426	-370	-769	-425	-768	-467	-436
Scenario 2	-426	-381	-758	-429	-758	-486	-436
Scenario 3	-426	-378	-756	-419	-784	-461	-432
Scenario 4	-424	-360	-786	-412	-769	-466	-436
Scenario 5	-431	-380	-760	-431	-772	-466	-436
Scenario 6	-428	-375	-767	-408	-799	-449	-436
Scenario 7	-426	-374	-771	-418	-777	-466	-434
Scenario 8	-434	-379	-761	-431	-774	-469	-433
Scenario 9	-424	-370	-749	-451	-784	-463	-437
Scenario 10	-435	-376	-760	-431	-774	-468	-436

6.9 Discussion of the Results

Overall the load tests were effective in providing information about the bridge's structural stability. None of the maximum allowable deflections were exceeded on scenarios where data collected was determined to be valid. The majority of the scenarios were well under the maximum allowable limits.

In load test 1, scenarios 2, 6, and 9 had questionable results that were determined to be invalid. The data recorded in these scenarios of load test 1 may have had possible errors due to the following:

- Deflection measurements were very small in most cases where data collected may not have been accurate enough to provide feasible results.
- The first load test used one surveying instrument that was continuously being relocated to access the various points on the deck. The continuous relocation of the instrument may have

caused erroneous readings (human errors in setup). This was corrected in load test 2 by using 3 surveying instruments set once in permanent locations throughout the testing period.

In the load test 2, the stress values extracted from the sensor network were compared to those derived from the measured deflections at every location and every scenario. An example comparison for the south deck panels under scenario 1 yielded the following observations:

- Live load stresses at the deck top fiber are consistently small (both compression and tension are less than 50 psi for scenario 1).
- The stress types (compression and tension) in scenario 1 match. In other words, for a given location, the deflection and the sensor results are consistent from the perspective of whether the top fiber stress is compression or tension.
- At a given point location under a specific testing scenario, the stresses from the sensor observations are consistently smaller than those from deflection measurements.
- The stress distribution reveals compression on the top fiber (positive moment) at the mid-span location where the truck load was located in testing scenario 1 and tension on the top fiber (negative moment) at the neighboring pier location. The stresses of the mid points of nearby spans and pier locations are consistent with the loading configuration.

These comparisons were conducted for all 10 scenarios. It was observed from both sets of results that top fiber stresses due to live load are relatively small when compared to the stresses caused by dead loads and temperature variation. However, the difference between the two sets is quite significant, considering the small stress values. Stress values based on deflection measurements are consistently larger than those from sensor readings. Also, the stress types (tension/compression) from the deflection measurements do not always match the sensor readings. In other words, some locations may have compression stresses based on deflection measurements when the sensors are reading tension stresses. These differences may be explained as follows:

- The conservative assumptions used for computing stresses from deflections, namely using simply supported span moment when the bridge is continuously supported over four spans, result in large computed stresses.
- The bridge has a 2-inch flexible asphalt overlay on top of the concrete deck panels, possibly resulting in larger surface deflections than what the concrete deck is actually experiencing.
- Even though the surveying equipment has an accuracy of 0.0012 inch, the human error at such small measurements may not be easily eliminated. Any measured deflections less than 0.1 inch may be considered negligible and inaccurate due to the difficulty of eliminating human errors in reading the targets or holding the rod vertically at such small measurements.
- Sensors are not exactly at the top fiber (18 inches from the neutral axis of the composite section). Rather, they are 2.5 inches below the surface (cover requirements) or 15.5 inches from the neutral axis, resulting in proportionally less stress than would exist at the top fiber.

Advanced deflection measuring instruments and techniques may eliminate some of the human error but at a premium cost. In our case, however, since the sensors already existed for the purpose of monitoring the health of the bridge, they provided a low-cost, accurate, and quick alternative to the deflection measurement load testing method.

7.0 ONE-YEAR HEALTH MONITORING

This section presents the one-year data that has been collected by the sensor-based health monitoring system that was developed and deployed for the Parkview Bridge in Kalamazoo, Michigan. The deployment of the structural health monitoring system enabled the remote collection of continuous strain and temperature data to be collected at ten-minute intervals. The two data loggers are contacted weekly through the modems and telephone lines were dedicated to download and archive the sensor data for future analysis. The SHM system started to function in December 2008. Data archiving for a time period of three years is currently underway to develop a solid baseline for future continuous monitoring of this bridge's health condition. Examples of data analysis are presented in this section to illustrate how such data is interpreted.

7.1 SHM Initial Configuration Setup

Once the health monitoring system was operational, the data loggers used for controlling the on-site monitoring, and collecting and storing the data from the sensors were programmed using Canary Systems Multi Logger Software, version 4.1. The software provides a flexible user interface that offers many useful functions for proper configuration, collection, and monitoring of the performance of the bridge. After testing and validating the proper configuration and operation of all sensors, the data logger's storage capacity needed to be determined. The initial estimate for a downloading schedule was two weeks. After further analysis and testing, the loggers were found to have a capacity of one week's worth of data from all sensors. The downloading schedule was then adjusted to weekly.

After the data was downloaded from the loggers to the remote laboratory computer workstation, the values of strain and temperature had to be filtered and sorted to check for erroneous readings. These readings must be positively identified as incompatible rather than mistakenly considered as alarming or indicating abnormal behavior of the bridge. To confirm the readings were invalid, they were manually checked by comparing redundant sensor readings within the same vicinity and over the same time period. If proven invalid and unusable, they are removed from the data file since they would affect the integrity of the data and cause errors in interpretations. This validation process is often referred to as data normalization (Phares 2005).

Once the validation and normalization processes are complete, the data is sorted by month due to the large volume of sensors and the number of readings is recorded daily. This provided accessibility to all data for each month and each sensor. In each of these files, all sensors followed a strict labeling system. Each sensor was represented by an array that included a label that identified its location, strain, temperature, date, and time for each ten-minute reading. Temperature readings between gages were easily validated since they remained consistent within surrounding locations. The sensors readings are limited to a range of $\pm 3,000$ micro-strain ($\pm 15,000$ psi) for strain and a range of -20 degrees Celsius to +80 degrees Celsius for temperature. If readings become close to these limits, results may not be as accurate.

After data was clearly organized and sorted, strain readings were converted to stress values. The temperature are also stored along with the stresses. Note that the sensors read temperatures in degrees Celsius. To get an accurate representation of the mechanical properties of the concrete

used for the individual deck panels, samples (cylinders) were collected during casting. These samples were left on site so environmental curing conditions would remain the same between the panels and corresponding samples. Each sample was labeled by panel number and date to determine age and location. The average 28-day compression strength ($f'c$) was recorded as approximately 8,000 psi. The Modulus of Elasticity (E) was then calculated using the American Concrete Institute's equation:

$$E = 57,000\sqrt{f'c} \approx 5000 \text{ ksi}$$

This value was then used to convert strain readings into stress values using:

$$\text{Modulus of Elasticity } (E) = \frac{\text{Stress } (\sigma)}{\text{Strain } (\epsilon)}$$

Also, as was mentioned earlier in Section 6, the maximum allowable stresses in the concrete are:

$$\begin{aligned} \text{Compression: } f_c &\leq 0.45 f'c &\Rightarrow & -3,600 \text{ psi} \\ \text{Tension: } f_t &\leq 6\sqrt{f'c} &\Rightarrow & 537 \text{ psi} \end{aligned}$$

After strain values are converted to stresses, allowable design values provided by the designer are compared to actual measured values. Bridge condition and performance are the primary concern. Weekly recorded values are sorted and filtered to make sure allowable stresses are not exceeded and to ensure that no sudden changes in pattern are observed. This process is performed after the data are normalized and ready to be interpreted for further examination.

7.2 SHM Sensor Data Collection and Representation

Four main categories for investigating the bridge deck's behavior and performance were developed:

- Longitudinal stress monitoring due to loading (Group 1 sensors)
- Transverse stress monitoring due to loading (Group 2 sensors)
- Stress monitoring along panel edges (Group 3 sensors)
- Stress monitoring along cast-in-place grout (Group 4 sensors)

The data was further separated into North and South to easily identify the panels of the bridge deck. Graphical representations were found to be an effective and efficient way to observe behavior over time. The behavior for each category was observed over a year. The total duration of monitoring in this report spans from December 2008 through December 2009.

The goal is to determine signature behavioral characteristics over time. These behavioral characteristics will eventually provide an envelope (baseline) that can be used to determine if behavior is normal or critical. Once values exceed these envelopes, they would trigger an alarm

for further investigation. Selected charts are presented in this section. The full year charts are provided in Appendix D and organized by panel type (N or S), sensor group (1 through 4), and month (December 2008 through December 2009). Raw data are also provided in Appendix D as monthly spreadsheets.

7.2.1 Longitudinal Load Stress Monitoring (Group 1)

Figure 12 shows the longitudinal stress monitoring for the North panels of Span 2 (Group 1) in January 2009. Note that a negative stress value represents compression. Also, note that the bridge deck is designed to be in compression at all times and that the maximum compression allowed is -3600 psi and the maximum allowable tension is +537 psi. The coinciding temperatures recorded are illustrated in Figure 13. Based on the limited information (one month in the first year), it is observed from Figures 13 that the difference in magnitudes between sensors as well as the slope of the lines over similar time periods are fairly similar (almost identical) with respect to temperature, suggesting a uniform behavior. The trend patterns for each sensor in Figure 12 demonstrate a uniform behavior as well.

Since all deck panels are fully restrained between supports, examining Figures 12 and 13 reveals that as temperature decreases, tension increases, reducing the total compression in the deck panels. It also reveals that as temperature increases, compression increases. This is clearly amplified in Figures 12 and 13 in the period from Tuesday 1/13/09 to Saturday 1/17/09 where the temperature has decreased by 17 degrees Celsius, resulting in a decrease in compressive stress of about 500 psi. The fluctuations between different locations are very minimal, indicating how little effect daily traffic has over the given time period and suggesting that temperature variation is the controlling factor in stress variation. This relationship between stresses and temperatures is key in this analysis. Any change in observed patterns over time may suggest that cracks are beginning to develop in the deck or that the deck is not acting as a fully composite unit (loss of bonding between joints).

When significant variations are noticed between stress lines of different sensors in similar locations over the same time period, further analysis should be performed to distinguish between abnormal and normal behavior. Examining Figure 12 reveals a steep change in stress over a single day from 1/17/09 to 1/18/09. Figures 14 and 15 isolate this day and display the data on an hourly scale. The trend is clearly similar for the sensors under consideration: temperature increased causing compressive stresses to increase. The slopes of the lines over the given time period in similar locations are very close and consistent. The difference in locations caused a slight difference in temperature but the behavior is the same. When changes in consistency are noticed, a further investigation must be performed. Over the month of January, similar analyses were performed for all locations under this group and no concerns for safety or maintenance were noticed, which is expected since the bridge is new.

A similar look was provided for the piers as well. Figures 16 and 17 shows stress and temperature monitored for the month of January at pier locations. No differences in behavior were noticed between the spans and piers. Similar results were found with the transverse gages. All charts under this category can be found in Appendix D.

7.2.2 Transverse Load Stress Monitoring (Group 2)

Stress monitoring in the transverse direction was performed in the same manner as the longitudinal direction. Figure 18 provides the stresses recorded for January in the transverse direction under the loading category. The coinciding recorded temperature values are shown in Figure 19. The only noticeable observation was that the sensors in the transverse direction recorded lower stress values compared to those orientated longitudinally in a similar location. Consistently, the compressive stresses were higher in the longitudinal direction. The North showed greater difference in magnitude while the South was similar. If this behavior changed, that would indicate a change in load distribution that may be caused by the deck not behaving as a composite where joint failure or cracking may have occurred. This would signal a further investigation. All charts under this category can be found in Appendix D.

7.2.3 Stress Monitoring at Joints between Panels (Group 3)

The stresses at the joints between panels are very important to monitor due to the unique nature of the Parkview Bridge design. To transfer stresses efficiently, the bond between panels must be maintained so that the deck behaves as a uniform composite member. Once again temperature had the greatest impact on stress fluctuation. The stresses are within allowable limits causing no concern for performance at this time. This investigation focused on the behavior of stress readings between adjacent panel edges. Figures 20 and 21 show the recorded values for the month of January. The stresses at the joint between North panels 7 and 8 (N-7-B and N-8-E sensors) were compared to each other. These sensors should provide similar stress patterns to demonstrate that bonding remains intact between the two different panels. If stress patterns were to change, then a closer look would be needed to determine causes for the change in pattern. If changes were to occur, the prediction would be that bonding had failed or cracks had developed to weaken the bond between the two panels. This analysis was performed on all sensors in this category (Group 3) and no concerns for performance or maintenance were noticed. All charts under this category can be found in Appendix D.

7.2.4 Stress Monitoring Along Cast-in-Place Grout (Group 4)

A similar approach was taken when analyzing the grout section joining the North and South panels. The sensors compared were located in similar locations along the grout joint in pairs but on opposite sides: one on the North and the other on the South. For example, a closer comparison would be made between N_8_C and S_8_A. Looking at the results in Figures 22 and 23, N_8_C and S_8_A demonstrate that the grout joint remains bonded providing similar trends in behavior over time. Once again, the magnitudes may differ, but the important characteristic is that the slope and trend over a given time remain close when comparing the two. Abnormal behavior would be interpreted if the two comparable sensors begin to display dissimilar patterns and slopes. This process was carried out for the length of the bridge to verify that the two sides of panels North and South remain bonded. The complete graphical output for this category can be found in Appendix D.

7.3 Discussion of Results

Typically, the strain (and stress) readings from sensor network are caused by four types of loading:

1. Dead Load (weight of the bridge)
2. Post tensioning
3. Live Load (traffic loading)
4. Environmental Loads (Temperature)

The one-year monitoring of the bridge deck using the four categories of sensors suggests that traffic loads seem to have the least effect on stresses in the deck while temperature appears to have the most impact on stress levels and variations. The extreme changes in temperature were found to generate the highest fluctuations in stress throughout the bridge deck. However, the stress values measured by all sensors are still within design limits.

Tables 30 and 31 and Figures 24 through 27 illustrate the monthly maximum and minimum stress levels experienced at critical points (mid spans and piers) in longitudinal and transverse directions during the one-year monitoring. While there is no observed abnormal bridge deck behavior, there are a few instances that have experienced small tensile stresses in the transverse direction. Note that in these tables we are reporting the absolute maximum and minimum stresses experienced during a given month and that some of these readings may not necessarily be correct when the temperatures approach the lower sensor limit (-20° C).

Once a three-year data set has been collected and the bridge deck behavior analyzed, stress envelopes can be developed to provide a baseline for normal maximum and minimum stress values. We feel that three years of stress data collection and analysis in the early stages of the bridge life-cycle are necessary to experience all stress scenarios from traffic, environmental, and bridge weight (creep) loads to enable the development of a representative set of stress envelopes (baseline). If stresses fall outside these envelopes, this would trigger further investigation to determine the cause(s) for the deviation and to recommend the course(s) of action.

TABLE 30: Maximum and Minimum Stresses - North (psi)

	Month	NORTH													
		Longitudinal							Transverse						
		S1	P1	S2	P2	S3	P3	S4	S1	P1	S2	P2	S3	S4	
Dec-08	Max	-1736	-1602	-1717	-1485	-1780	-1511	-1697	-1242	-1055	-1113	-1154	-1557	-768	
	Tem	2.32	2.66	3.08	3.08	3.26	3.12	2.75	2.27	2.66	3.35	3.44	3.26	3.08	
	Min	-1500	-1342	-806	-1198	-736	-1155	-1449	-949	-863	-521	-853	-422	-409	
	Tem	-8.66	-8.76	-8.76	-9.7	-9.15	-10.27	-10.15	-7.64	-6.35	-9.9	8.66	-10.09	-10.27	
Jan-09	Max	-1638	-1516	-1594	-1369	-1659	-1377	-1586	-1162	-961	-997	-1067	-1394	-670	
	Tem	-0.34	-0.8	-0.09	-0.3	0	-0.1	-0.09	-0.57	-1.04	-0.08	-0.17	0.05	-0.5	
	Min	-1155	-957	-539	-820	-424	-735	-1090	-694	-609	-224	-596	-128	-66	
	Tem	-19.1	-19.6	-18.5	-20.2	-19.5	-20.8	-20.8	-16.8	-18.9	-20.7	-17	-20.74	-21	
Feb-09	Max	-1843	-1780	-1927	-1690	-2037	-1726	-1825	-1325	-1105	-1150	-1240	-1567	-870	
	Tem	12.2	11.37	13.78	13.17	14.17	13.72	13.45	12.08	10.55	13.63	13.69	13.72	13.63	
	Min	-1310	-1211	-706	-1013	-643	-974	-1278	-833	-749	-367	-746	-262	-254	
	Tem	-16.1	-13.3	-14.28	-12.52	-13.86	-13	-14.18	-10	-9.38	-13.86	-9.7	-13.86	-13.54	
Mar-09	Max	-2005	-1944	-2109	-1865	-2210	-1934	-1918	-1459	-1266	-1277	-1359	-1691	-1006	
	Tem	19.3	18.28	20.69	20.04	20.9	20.66	20.28	20.79	18	21.2	21	20.69	21.31	
	Min	-1325	-1200	-713	-1029	-654	-1010	-1322	-744	-775	-356.6	-684	-180	-264	
	Tem	-13.01	-11.23	-11.65	-11.84	-12.13	-12.24	-11.45	-13.05	-10.18	-13.15	-12.14	-13.15	-12.74	
Apr-09	Max	-2224	-2155	-2365	-2129	-2468	-2205	-2129	-1618	-1346	-1430	-1496	-1845	-1176	
	Tem	26.8	25	28.1	27.03	28.19	27.98	27.74	28.71	24.52	28.83	28.22	27.86	29.2	
	Min	-1664	-1518	-939	-1382	-985	-1416	-1604	-997	-962	-669	-930	-511	-549	
	Tem	-0.53	0.08	-0.35	-0.44	-0.52	-0.61	-0.43	-0.71	0.51	-0.956	-0.61	-1.01	-0.78	
May-09	Max	-2399	-2237	-2545	-2331	-2666	-2410	-2282	-1742	-1604	-1553	-1521	-1969	-1292	
	Tem	32.83	32	33.14	32.69	33.1	33.05	32.42	34.5	33.75	32.83	32.56	32.56	34.1	
	Min	-1867	-1740	-1116	-1611	-1226	-1639	-1761	-1155	-1080	-824	-1158	-654	-709	
	Tem	9.59	10.03	9.41	8.97	8.92	8.1	8.11	9.68	8.66	7.93	11.02	7.58	7.49	

TABLE 30 (Continued): Maximum and Minimum Stresses - North (psi)

Month		NORTH													
		Longitudinal							Transverse						
		S1	P1	S2	P2	S3	P3	S4	S1	P1	S2	P2	S3	S4	
Jun-09	Max	-2572	-2523	-2769	-2567	-2908	-2627	-2456	-1828	-1667	-1660	-1697	-2067	-1402	
	Tem	39.59	39.54	39.88	39.84	39.88	40.21	39.45	40.21	39.38	38.02	39.23	37.62	40.54	
	Min	-2090	-1939	-1276	-1856	-1473	-1882	-2003	-1296	-1292	-994	-1246	-802	-906	
	Tem	13.54	14.65	14.37	14.28	14.01	13.64	14.37	13.55	15.12	13.09	14.09	13.09	13.64	
Jul-09	Max	-2570	-2449	-2663	-2459	-2798	-2518	-2433	-1819	-1630	-1686	-1683	-2078	-1383.2	
	Tem	33.24	32.9	33.02	32.95	32.83	33.02	33.24	34.64	33.8	32.7	33.91	32.29	34.79	
	Min	-2190	-2118	-1324	-1939	-1655	-1978	-2094	-1345	-1316	-1039	-1301	-942	-936	
	Tem	14.47	15.4	14.11	14.28	14.1	13.91	14.25	14.1	15.49	13.17	13.63	13.09	13.63	
Aug-09	Max	-2624	-2524	-2750	-2542	-2882	-2592	-2492	-1872	-1634	-1715	-1742	-2107	-1446	
	Tem	34.93	34.22	35.37	34.79	35.37	35.22	34.83	36.44	35.37	34.77	35.96	35.03	36.1	
	Min	-2277	-2071	-1375	-2002	-1724	-2033	-2160	-1380	-1381	-1073	-1347	-980	-985	
	Tem	12.9	13.73	13.18	13	12.92	12.63	13	12.81	14.09	12.09	12.63	11.98	12.36	
Sep-09	Max	-2579	-2435	-2654	-2442	-2790	-2510	-2447	-1800	-1614	-1686	-1687	-2081	-1390	
	Tem	29.45	28.96	29.7	29.6	30.08	30.18	29.95	30.59	29.7	29.2	30.54	29.45	31.23	
	Min	-2249	-2025	-1332	-1957	-1683	-1988	-2143	-1330	-1327	-1044	-1319	-947	-941	
	Tem	8.01	8.89	7.75	8.28	8.09	7.93	8.29	7.93	8.8	7.49	7.84	7.4	7.49	
Oct-09	Max	-2424	-2218	-2406	-2199	-2525	-2245	-2289	-1647	-1451	-1550	-1555	-1952	-1242	
	Tem	18.26	17.5	18.87	18.38	18.97	18.78	18.71	18.78	17.31	18.65	18.57	18.77	18.97	
	Min	-2167	-1898	-1244	-1834	-1565	-1835	-2043	-1252	-1210	-970	-1225	-872	-859	
	Tem	2.58	2.75	2.49	2.4	2.49	2.23	2.75	2.4	2.84	1.99	2.15	2.15	2.66	
Nov-09	Max	-2364	-2170	-2342	-2136	-2467	-2185	-2244	-1603	-1405	-1457	-1523	-1899	-1203	
	Tem	16.63	16.16	17.7	16.93	18.09	17.79	17.7	17.21	16.06	17.21	17.4	17.85	17.7	
	Min	-2083	-1801	-1184	-1722	-1448	-1708	-1954	-1170	-1132	-885	-1146	-769	-766	
	Tem	-1.12	-0.95	-1.39	-1.72	-1.65	-2.09	-1.91	-1.65	-0.61	-2.08	-1.83	-2	-1.83	

TABLE 31: Maximum and Minimum Stresses – South (psi)

	Month	South													
		Longitudinal							Transverse						
		S1	P1	S2	P2	S3	P3	S4	S1	P1	S2	P2	S3	P3	S4
Dec-08	Max	-1627	-1703	-1012	-1616	-1582	-1778	-1799	-869	-1005	-1112	-914	-1571	-1119	-938
	Tem	12.08	11.1	12.18	12.73	12.27	13.08	13	12.63	10.3	13.08	13	13.22	13.18	13
	Min	-1195	-1061	-147	-925	-617	-1058	-1318	-269	-619	-176	-378	-20	-374	-306
	Tem	-13.45	-13.45	-14.28	-14.3	-14.5	-14.79	-14.7	-14.66	-13.39	-14.81	-15.02	-14.81	-15.04	-15.02
Jan-09	Max	-1416	-1406	-807	-1288	-1302	-1458	-1578	-624	-815	-924	-706	-1379	-907	-706
	Tem	-0.17	-0.6	-0.6	-0.27	-0.5	-0.11	-0.09	-0.5	-1.2	-0.08	-0.43	0.1	-0.26	0.09
	Min	-992	-834	22	-693	-405	-849	-1109	-66	-457	26	-179	202	-185	-102
	Tem	-19.28	-19.1	-19.76	-19.9	-19.76	-20.25	-20.5	-20.58	-18.93	-20.35	-20.74	-20.74	-20.86	-20.76
Feb-09	Max	-1614	-1739	-975	-1664	-1540	-1827	-1813	-808	-968	-1088	-878	-1545	-1100	-919.5
	Tem	13	12.2	11.3	13.91	12.27	14	14	12.09	10.39	13.9	12.92	14.14	13.12	13.91
	Min	-1107	-1024	-153	-865	-651	-1040	-1275	-227	-613	-126	-353	73	-355	-277
	Tem	-13.5	-11.84	-12.54	-12.85	-12.44	-12.94	-12.74	-13.87	-11.35	-13.66	-13.15	-13.76	-13.05	-13.66
Mar-09	Max	-1771	-1907	-1129	-1834	-1766	-2011	-1928	-969	-1113	-1209	-999	-1657	-1221	-1057
	Tem	20.38	19.37	19.27	20.77	19.86	20.96	20.67	20.38	18.48	21.1	21.2	20.79	21.2	20.69
	Min	-1110	-1049	-18.8	-905	-708	-1071	-1299	-231	-647	-123	-381	48	-396	-296
	Tem	-13.25	-11.35	-11.84	-12.14	-11.55	-12.24	-11.74	-13.56	-10.57	-12.84	-12.42	-12.94	-12.14	-12.54
Apr-09	Max	-1980	-2131	-1246	-2097	-1957	-2291	-2136	-1109	-1197	-1372	-1121	-1774	-1340	-1250
	Tem	27.93	26.33	25.2	27.86	26.33	28.21	28.04	27.2	24.63	28.67	28.05	27.82	28.22	28.22
	Min	-1427	-1401	-441	-1290	-1047	-1469	-1595	-544	-824	-440	-638	-219	-869	-578
	Tem	-0.73	-0.01	-0.35	-0.35	-0.35	-0.62	-0.69	-0.94	0.34	-0.87	-0.69	-0.82	-0.61	-1.04
May-09	Max	-2059	-2220	-1338	-2170	-2088	-2345	-2202	-1237	-1350	-1487	-1230	-1889	-1431	-1364
	Tem	29.57	29	27.15	28.86	28.1	28.72	28.53	33.31	32.62	33.8	33.64	32.22	33.38	33.1
	Min	-1614	-1657	-635	-1529	-1282	-1723	-1774	-726	-1030	-611	-802	-386	-804	-771
	Tem	9.5	10.39	9.17	8.89	9.15	8.28	8.1	8.88	9.86	7.84	8.27	7.836	8.18	7.49

TABLE 31 (Continued): Maximum and Minimum Stresses – South (psi)

Month		South													
		Longitudinal							Transverse						
		S1	P1	S2	P2	S3	P3	S4	S1	P1	S2	P2	S3	P3	S4
Jun-09	Max	-2329	-2574	-1640	-2558	-2455	-2741	-2506	-1396	-1519	-1612	-1362	-1810	-1573	-1503
	Tem	41.06	41.41	39.71	40.87	39.88	40.89	40.05	40.38	40.38	40.72	40.74	39.08	40.89	40.38
	Min	-1812	-1855	-891	-1751	-1504	-1963	-2019	-883	-1148	-774	-974	-540	-974	-955
	Tem	13.27	14.7	14.31	14.25	14	13.85	14.28	13.09	14.65	13.27	13.82	13.09	13.73	13.36
Jul-09	Max	-2312	-2459	-1554	-2409	-2386	-2608	-2466	-1315	-1477	-1587	-1313	-1820	-1545	-1464
	Tem	34.36	34.5	33.1	33.66	33.1	33.38	33.8	33.84	34.35	33.87	34.08	32.02	33.83	33.38
	Min	-1930	-1940	-958	-1823	-1596	-2045	-2091	-935	-1200	-860	-1020	-600	-1027	-988
	Tem	14.11	15.35	14.23	14	14.19	14.1	14	14	15.49	13.45	13.82	13.44	14	13.45
Aug-09	Max	-2363	-2528	-1605	-2497	-2416	-2687	-2515	-1378	-1504	-1626	-1353	-2022	-1590	-1519
	Tem	36.09	35.81	34.5	35.51	34.64	35.22	35.07	35.55	35.22	35.37	35.92	34.07	35.51	35.07
	Min	-2000	-2000	-1004	-1892	-1678	-2108	-2171	-969	-1255	-904	-1085	-675	-1100	-1073
	Tem	12.72	13.64	13.09	12.81	12.82	12.63	12.72	12.45	13.64	12.18	12.63	12.08	12.63	12
Sep-09	Max	-2315	-2438	-1523	-2282	-2339	-2600	-2491	-1321	-1466	-1597	-1320	-1826	-1566	-1478
	Tem	30.57	30.46	29.47	30.08	30.21	30.53	30.55	30.72	30.45	30.59	31.06	29.83	31.4	30.51
	Min	-1980	-1953	-957	-1935	-1620	-2067	-2150	-925	-1213	-884	-1058	-644	-1078	-1022
	Tem	7.93	8.88	7.83	8.1	7.67	8.02	8.1	7.66	8.45	7.48	7.94	7.14	8.01	6.97
Oct-09	Max	-2131	-2186	-1325	-2130	-2029	-2318	-2306	-1156	-1297	-1460	-1183	-1901	-1439	-1325
	Tem	18.58	18.09	17.5	18.73	17.97	18.94	18.97	18.39	17.08	19.07	18.42	18.78	18.68	18.76
	Min	-1884	-1812	-881	-1867	-1516	-1930	-2048	-842	-1119	-814	-962	-588	-985	-958
	Tem	2.24	2.75	2.58	2.23	2.58	2.32	2.75	2.15	2.66	2.32	2.15	2.23	2.41	2.34
Nov-09	Max	-2066	-2111	-1321	-2066	-2006	-2249	-2242	-1149	-1283	-1415	-1168	-1867	-1443	-1283
	Tem	16.87	16.44	17.11	17.21	17.21	17.7	17.63	17.99	16.63	17.89	17.79	17.98	18.28	18.08
	Min	-1794	-1699	-810	-1784	-1392	-1801	-1946	-743	-1073	-732	-880	-537	-904	-855
	Tem	-1.48	-1.12	-1.22	-1.79	-1.48	-2.08	-1.96	-1.84	-0.61	-1.83	-1.92	-1.91	-2.09	-2

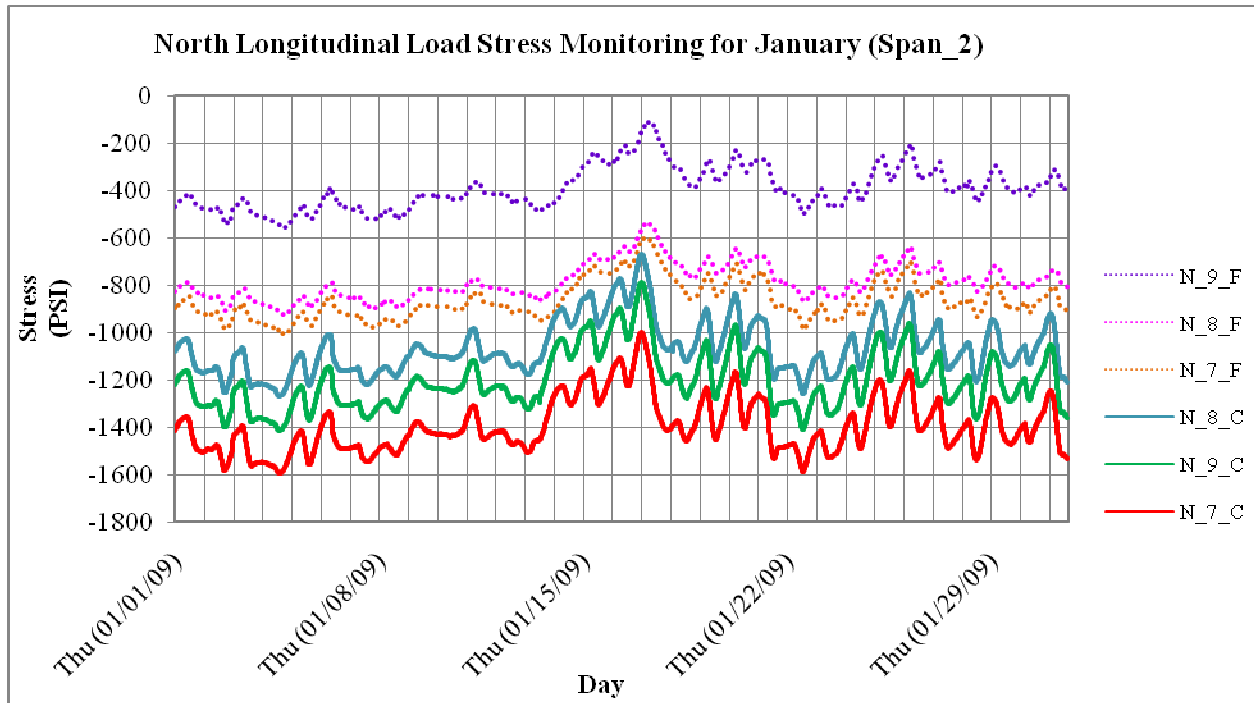


FIGURE 12: North longitudinal load stresses for span two (January)

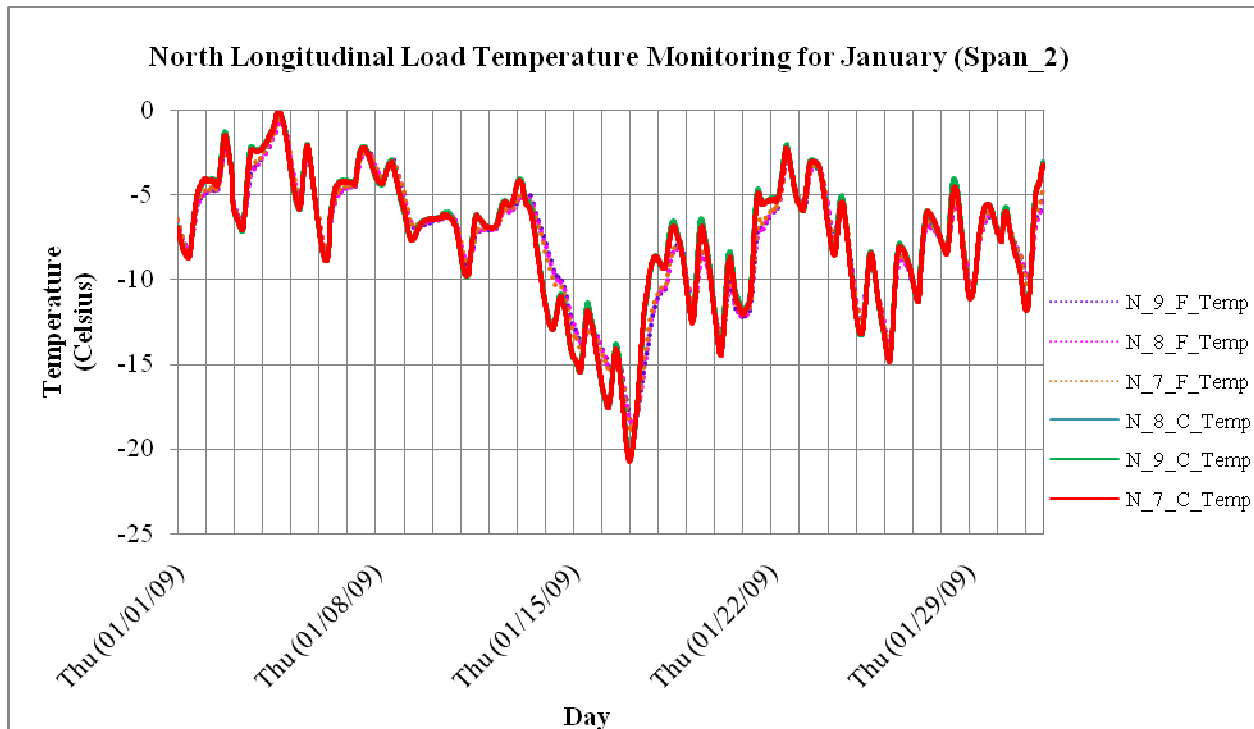


FIGURE 13: North longitudinal load temperature for span two (January)

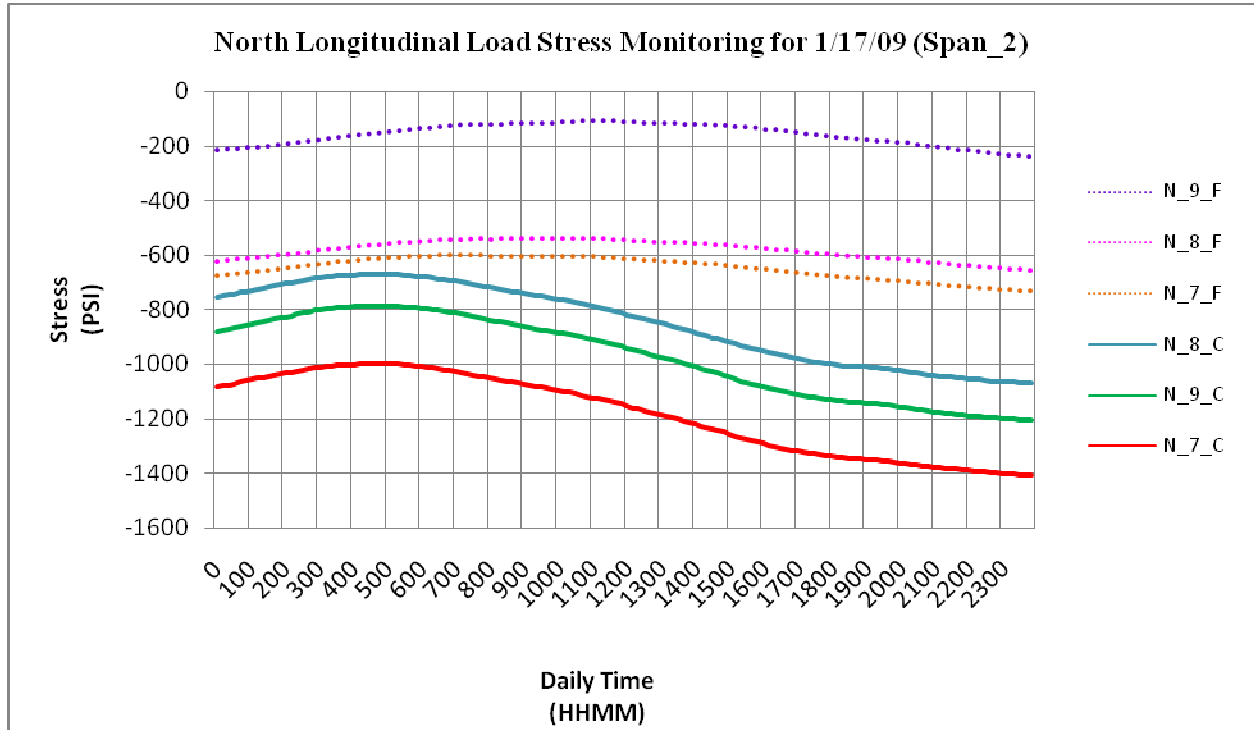


FIGURE 14: North longitudinal load stresses for span two (1/17/09)

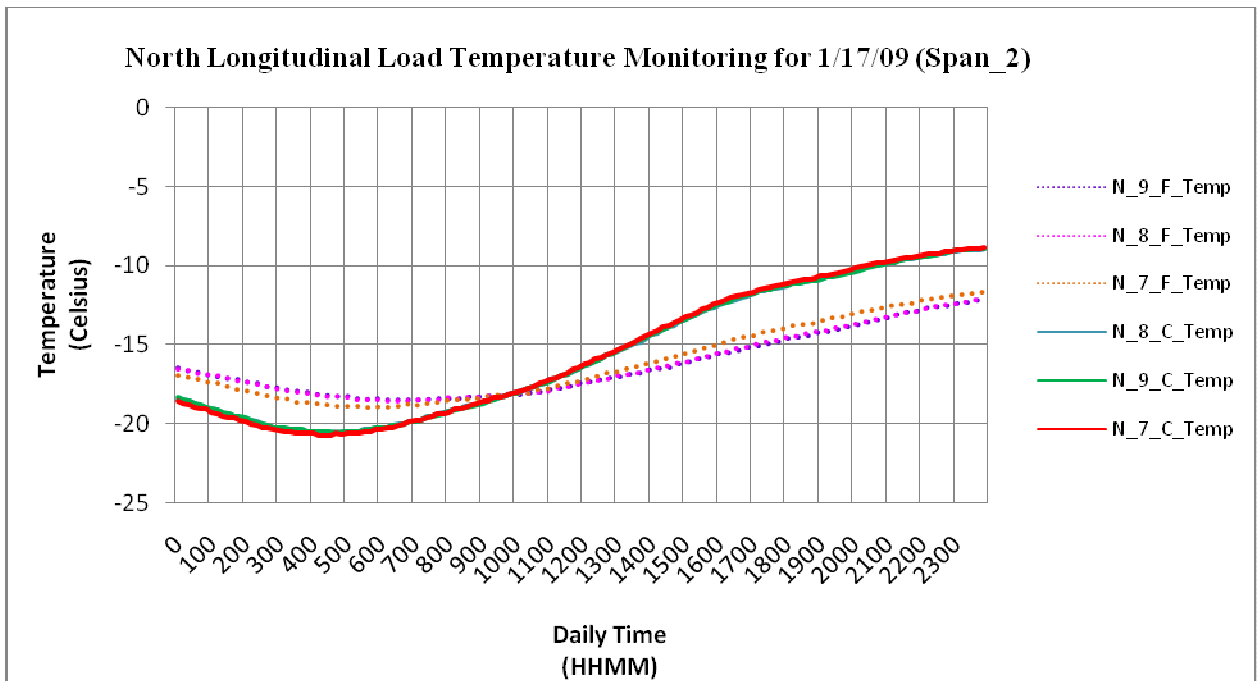


FIGURE 15: North longitudinal load temperature for span two (1/17/09)

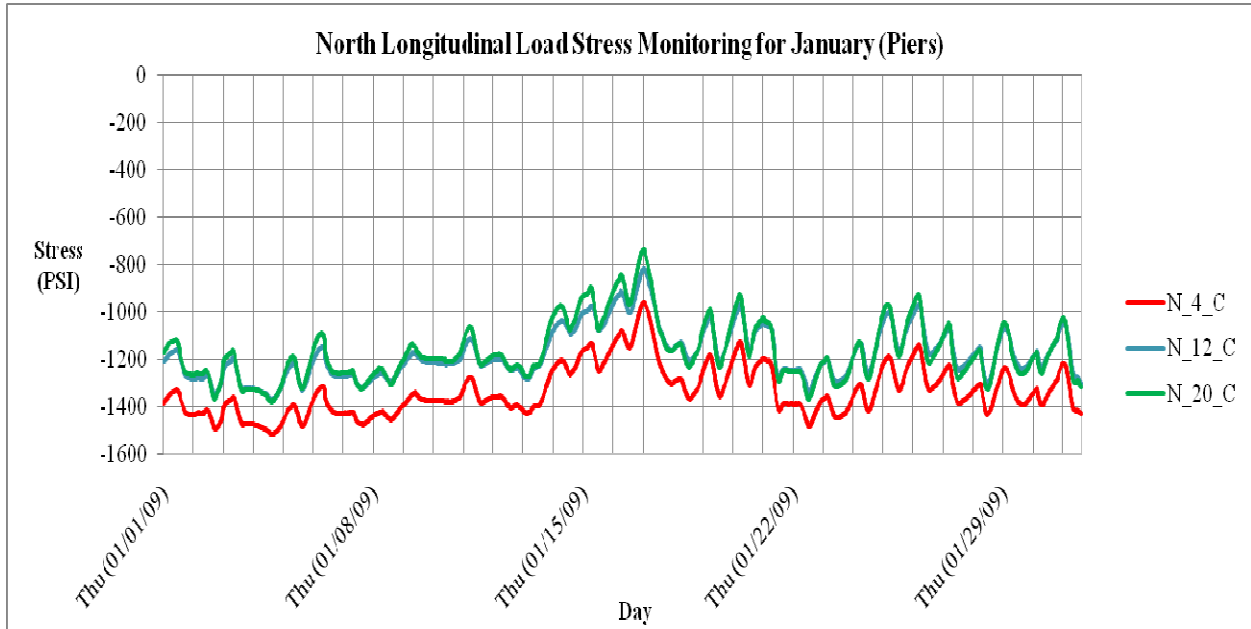


FIGURE 16: North longitudinal load stresses at piers 1, 2 and 3 (January)

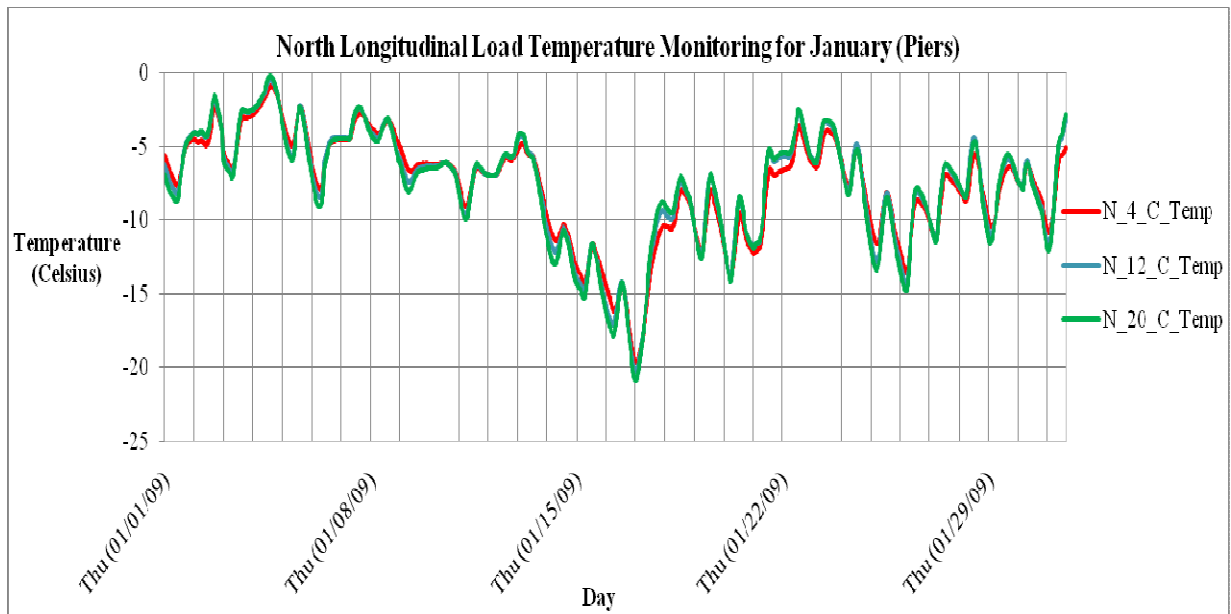


FIGURE 17: North longitudinal load temperature at piers 1, 2, and 3 (January)

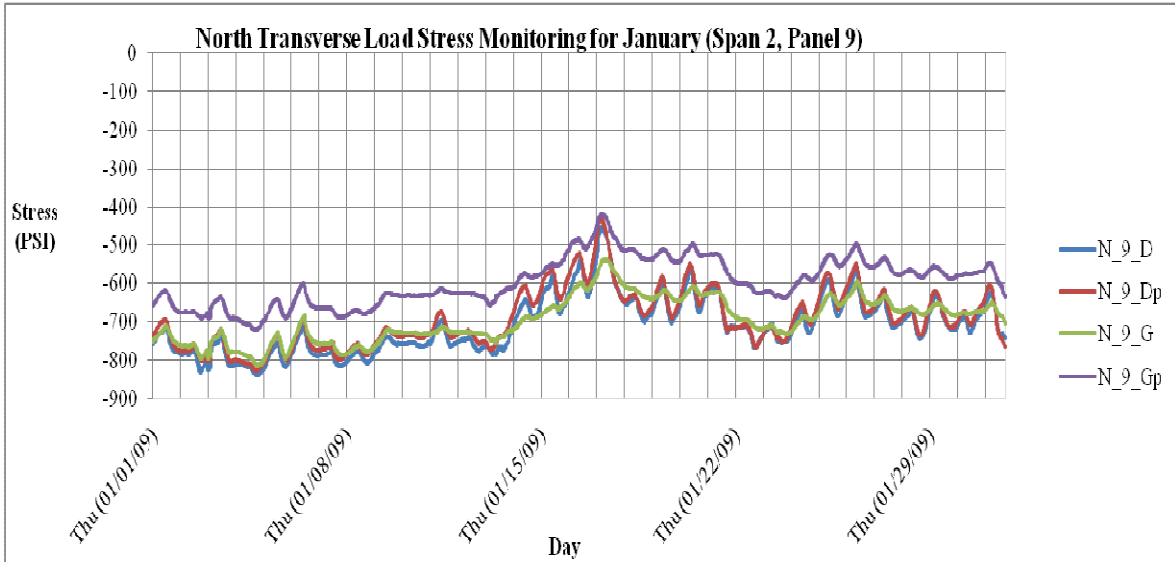


FIGURE 18: North transverse load stresses for span two (January)

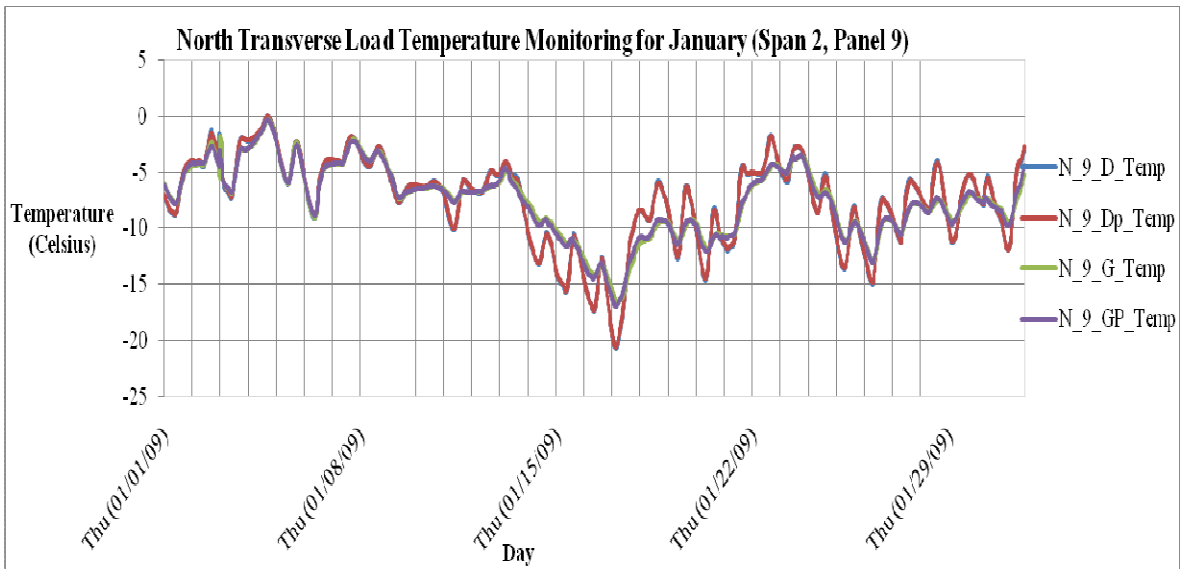


FIGURE 19: North transverse load temperature for span two (January)

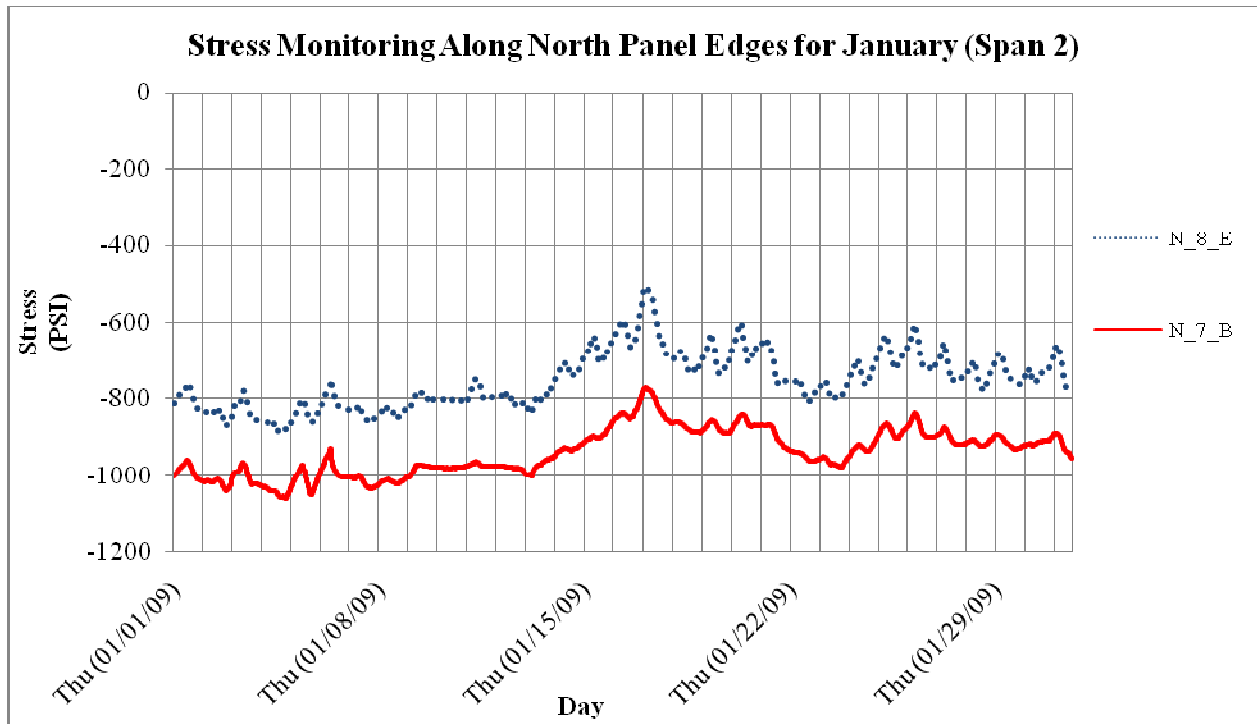


FIGURE 20: Stresses along north panel edge for span two (January)

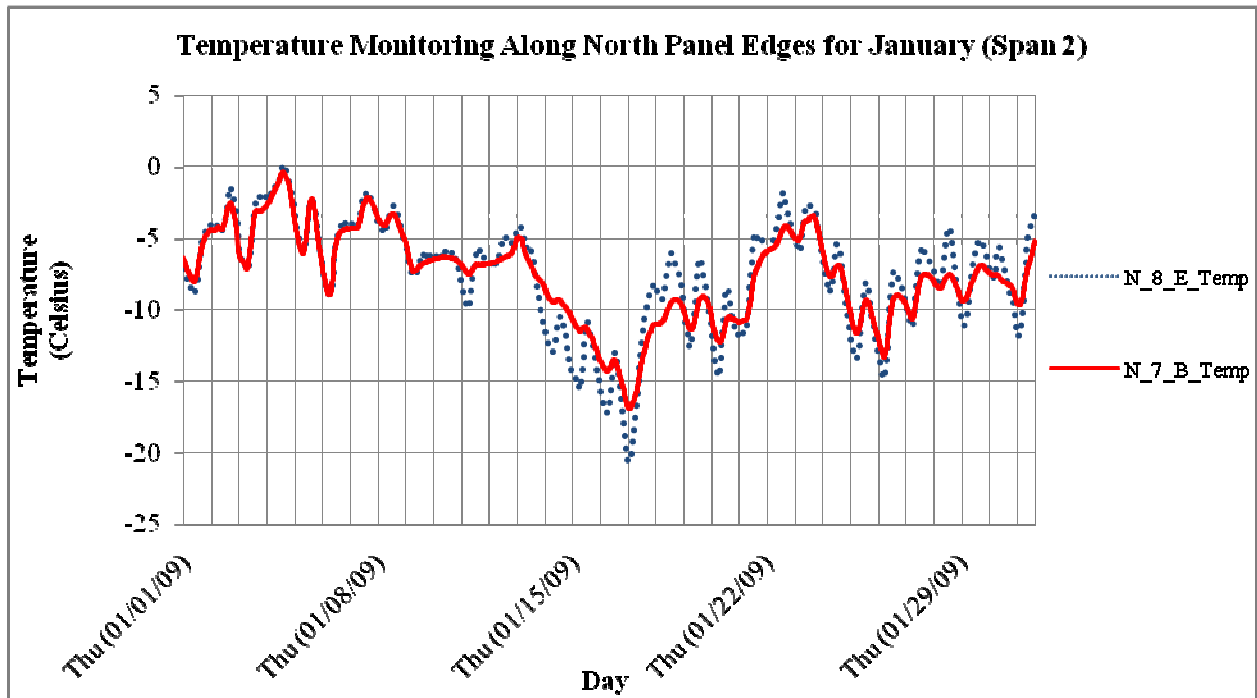


FIGURE 21: Temperature along north panel edge for span two (January)

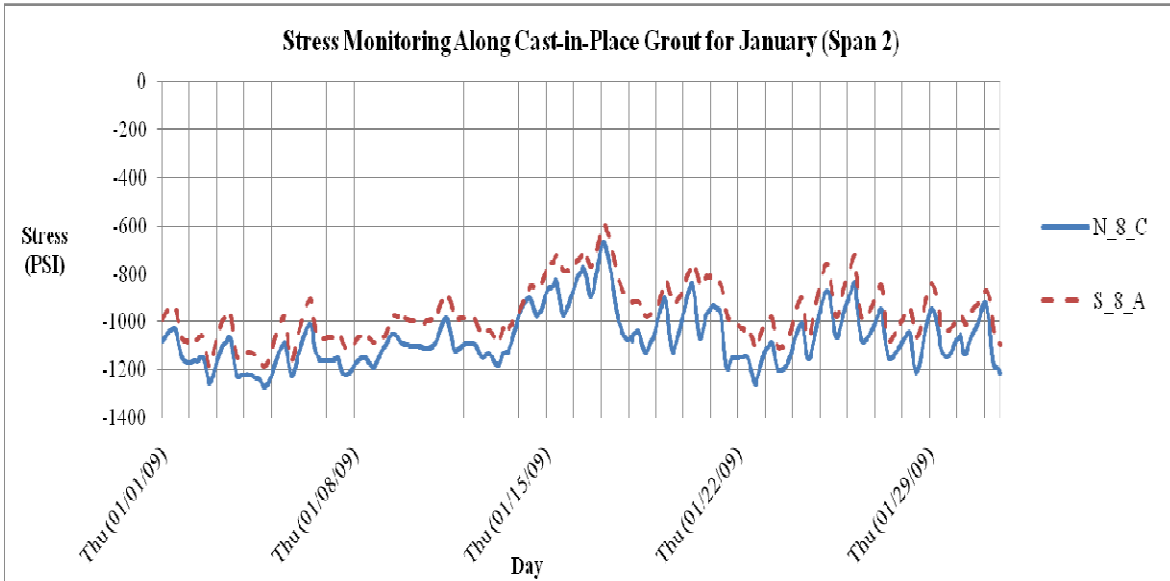


FIGURE 22: Stresses along cast-in-place grout for span two (January)

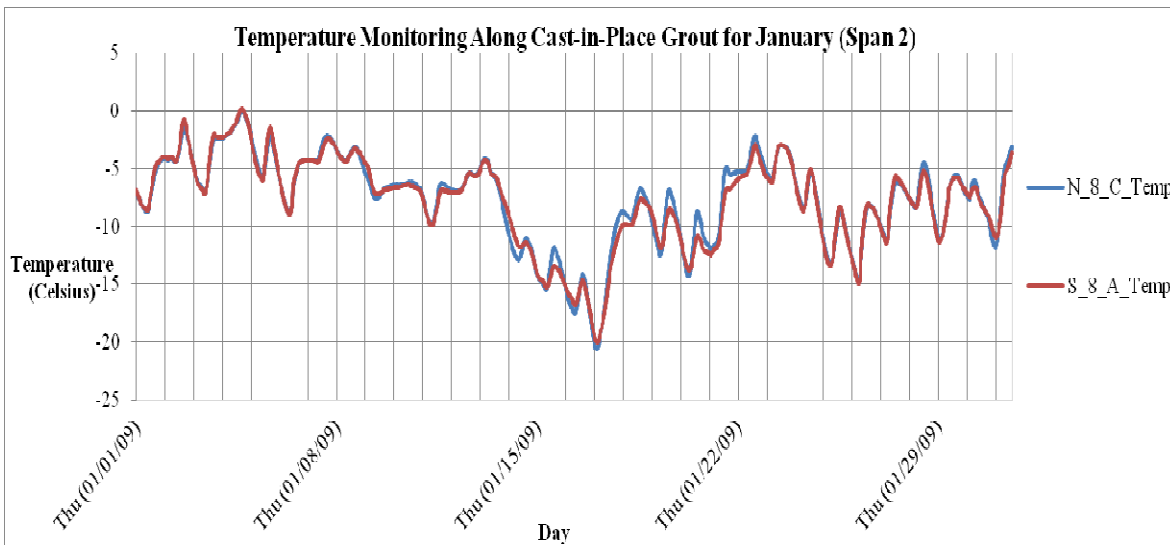
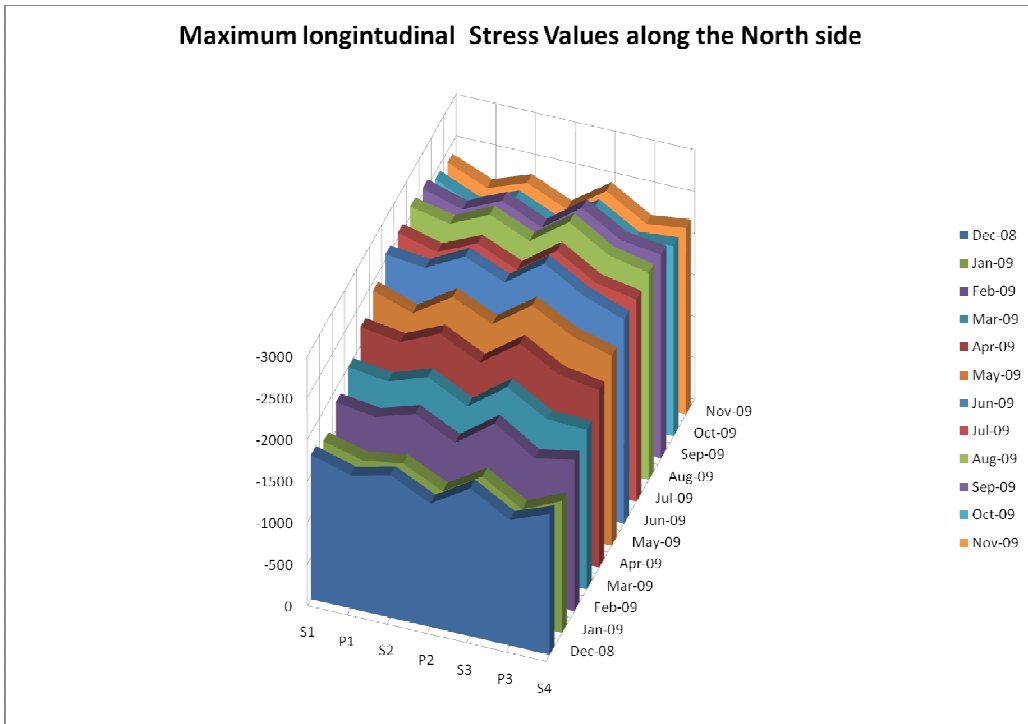
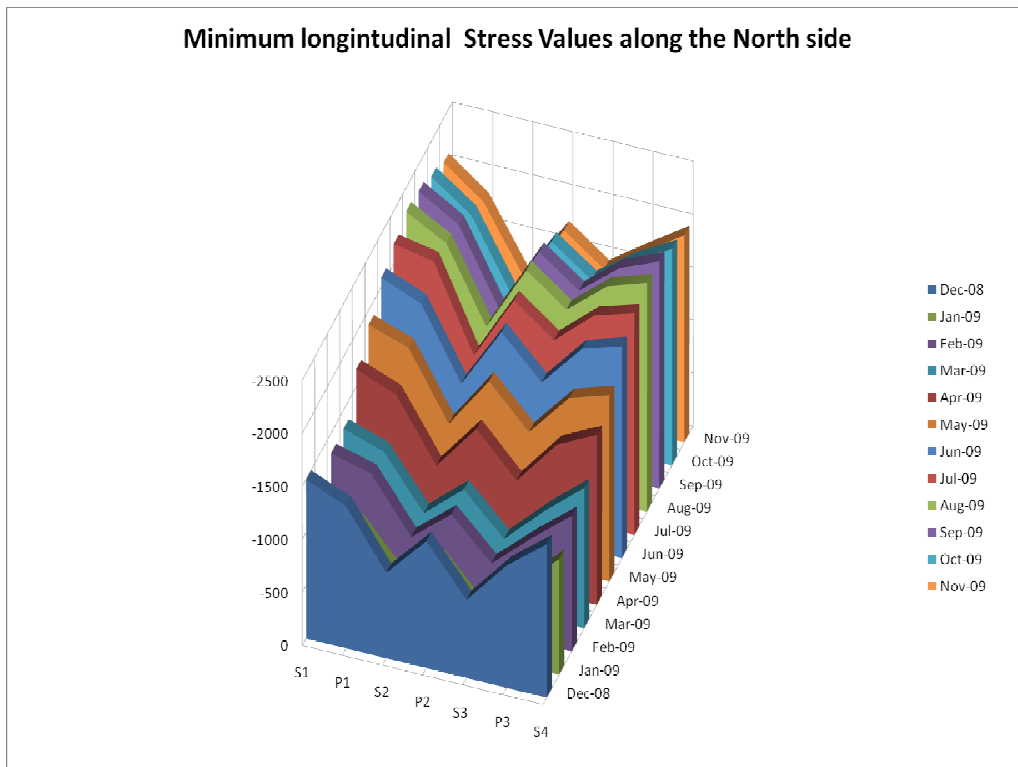


FIGURE 23: Temperature along cast-in-place grout for span two (January)

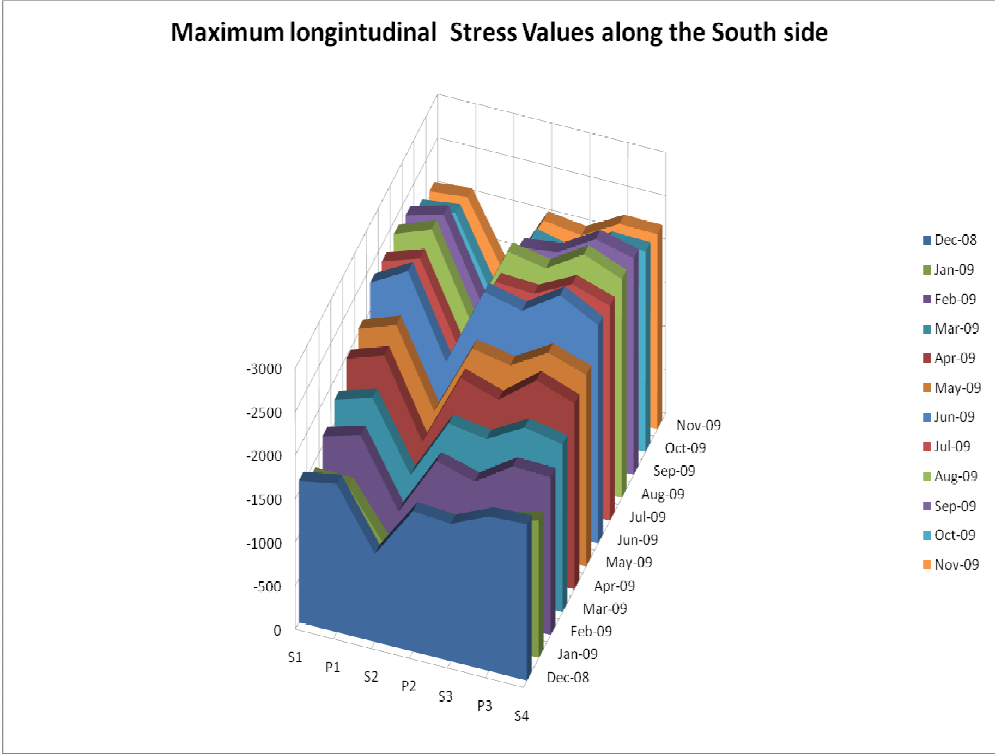


(a) Maximum

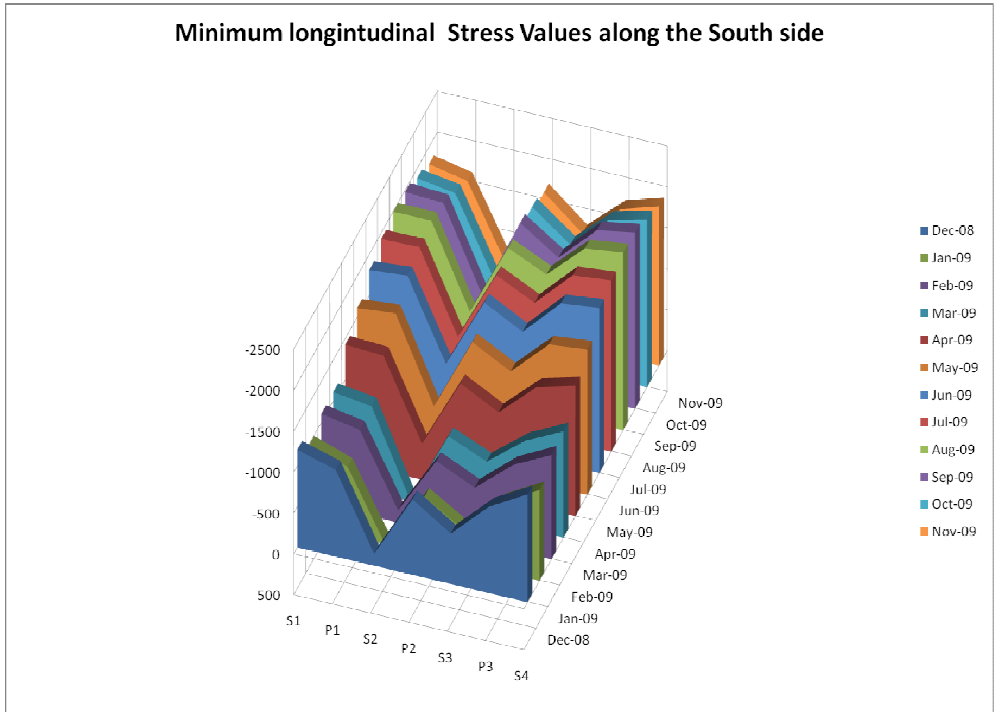


(b) Minimum

FIGURE 24: Maximum and Minimum Longitudinal Stresses – North Panels

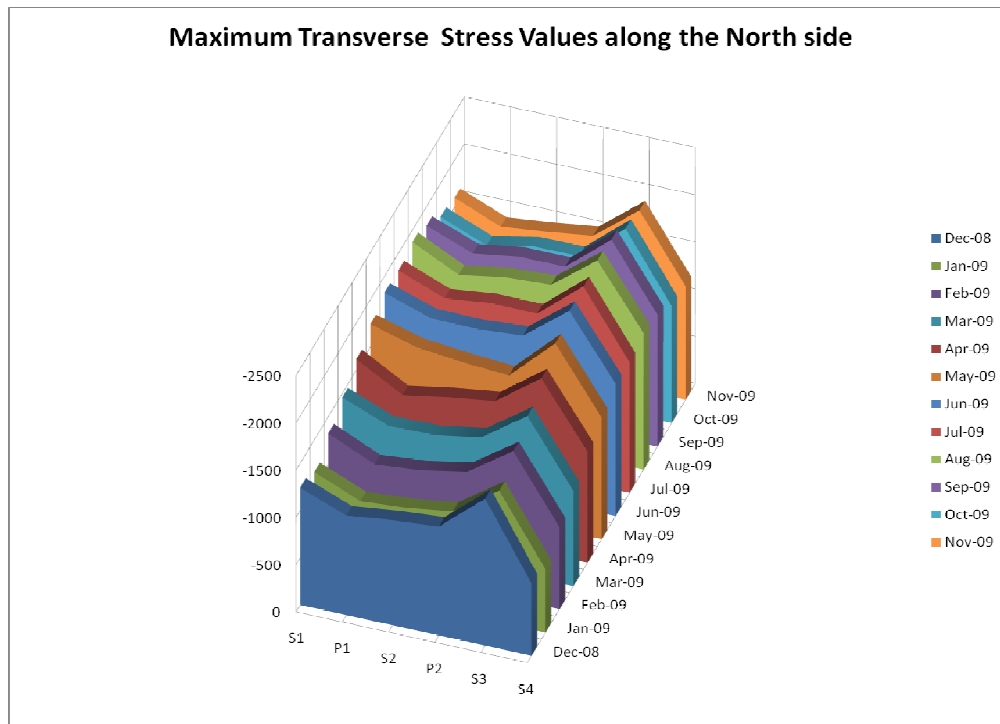


(a) Maximum

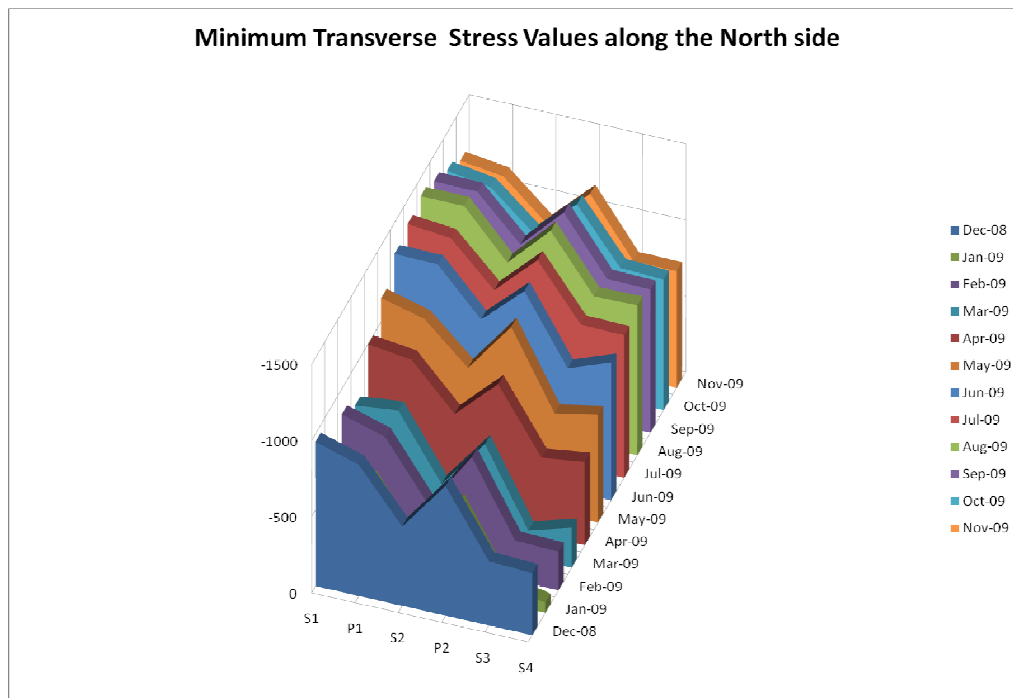


(b) Minimum

FIGURE 25: Maximum and Minimum Longitudinal Stresses – South Panels

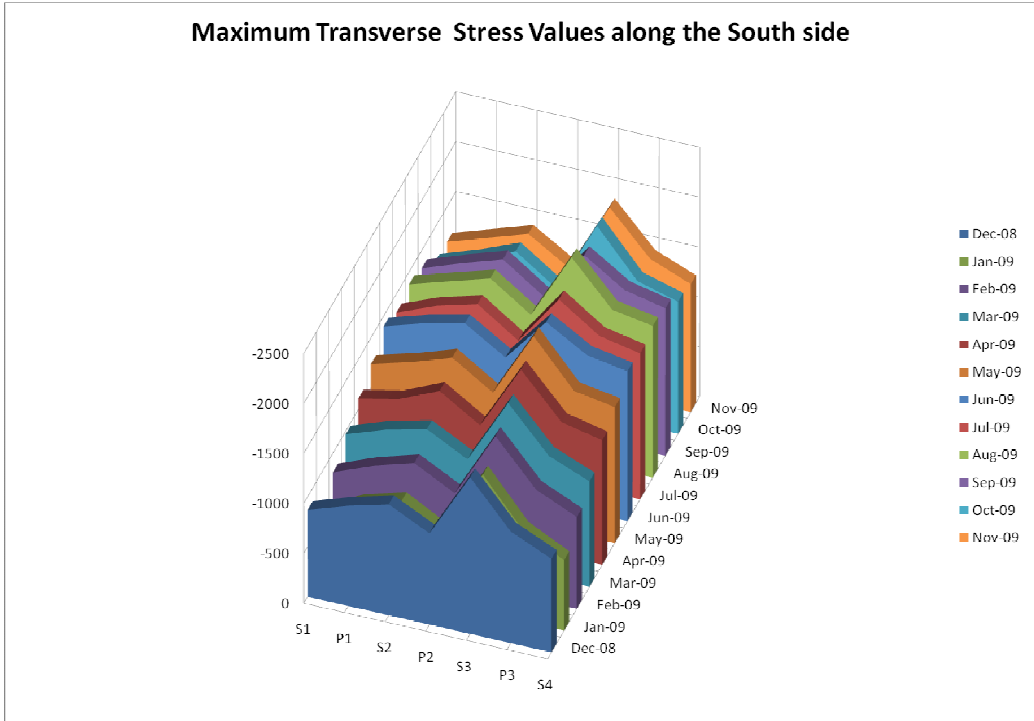


(b) Maximum

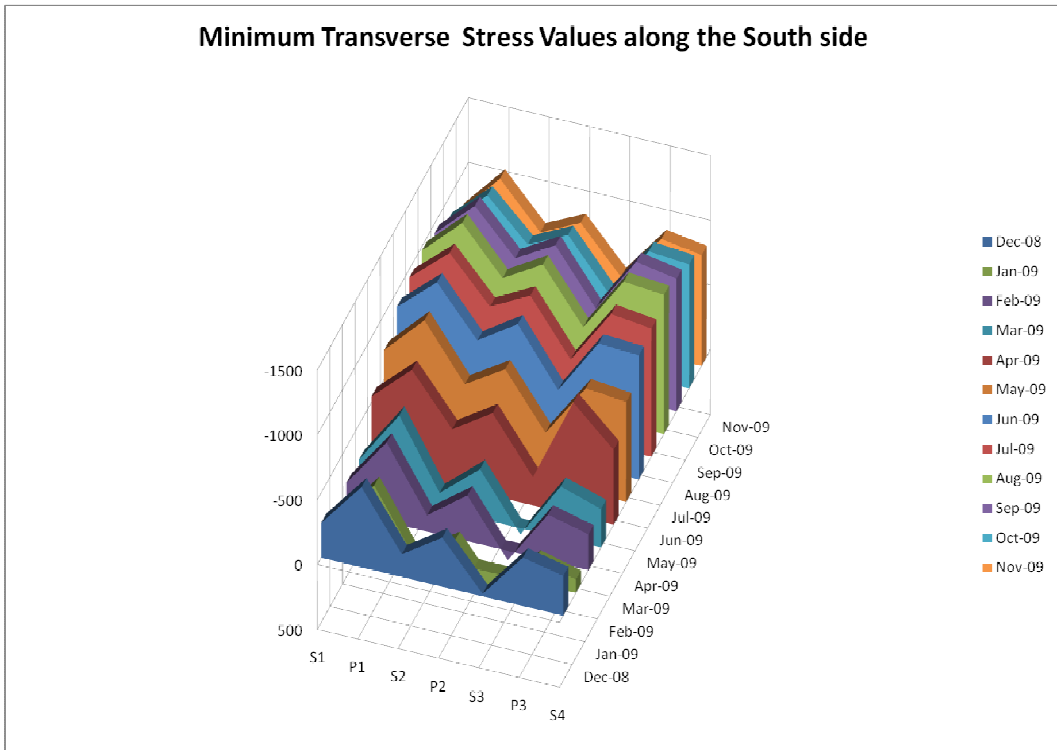


(b) Minimum

FIGURE 26: Maximum and Minimum Transverse Stresses – North Panels



(b) Maximum



(b) Minimum

FIGURE 27: Maximum and Minimum Transverse Stresses – South Panels

8.0 CONCLUSIONS

A health monitoring system was designed and deployed for the Parkview Bridge in Kalamazoo, Michigan. It is anticipated that this sensor-based health monitoring system would be capable of providing continuous monitoring of the bridge deck to determine its condition, assess the impacts from environmental factors such as temperature and from traffic loads, evaluate its deterioration rate by comparing to baseline stress envelopes at panel joints and critical stress sections, initiate maintenance and repairs when needed, and predict the remaining service life. Even after one year of in-service data measurement, meaningful observations regarding the bridge performance and the relationship between temperature and stress can be obtained. It was found that recorded stresses vary widely due to the combined effect from loading and temperature variations. However, it was concluded that temperature is the controlling factor in stress variations that are measured by the static sensors in this study. Variations in temperature cause the bridge's behavior to vary from season to season.

Evaluating the construction of the Parkview Bridge and the subsequent long-term monitoring of the structural behavior of its full depth precast deck panels will help MDOT in evaluating the implementation of the rapid bridge deck replacement technique. This phase of the research project resulted in the following outcomes and conclusions.

- The development of specifications (see Appendix B) for the selection and construction of bridge health monitoring instrumentation. The selection of the sensors was based on the analysis of existing SHM case studies, comparison of the specifications of available sensor technologies, and the cost of sensor systems. These were discussed in Chapters 2 and 4.
- In assessing the rapid bridge deck replacement technique we found that it can considerably save bridge construction time and consequently result in a large saving on user travel time. This travel time saving is significant enough that it can justify the relatively higher initial cost of the RBC technique.
- Considered together with other advantages of RBC, such as high quality and low maintenance cost, the technique offers a more efficient and economic alternative to the conventional method. While we strongly believe that RBC techniques should be implemented state-wide, more assessment studies such as the one presented in this report will need to be conducted to fully understand and realize the advantages of RBC techniques.

A few lessons were learned in this study during the design and construction of the sensor network. The first lesson is related to the installation of sensors which is found to need a formal quality control procedure. The method used for securing sensors worked fine, but could be further improved. For example, the foam spacers, which are tightened by zip ties, would occasionally fall out if disturbed before casting, especially when the workers were in contact with the reinforcement or stepping on the zip ties securing the sensors. To improve on this problem, workers should be prevented from standing over the reinforcement mesh when pouring concrete. A second lesson deals with sensor wire connections which present another challenge. Due to the large volume of sensors and wires being connected and spliced, strict supervision needs to be provided. The integrity of the project relies on proper sensor readings from known locations and orientations. The labeling and splicing processes must be carefully supervised to avoid errors in labeling sensors. A third lesson deals with the location of the cabinets that house the data loggers. While the cabinets are installed at the top of the pier, 16 feet high, to prevent

unwanted access to the expensive equipment, this has posed an access challenge for maintenance when needed, particularly that the pier is very close to live highway traffic, requiring extra safety measures. A better approach would be to provide secured cabinets at the ground level for easy access.

Since the sensors use analog signals via telephone lines to communicate data, electrical noise interference can significantly degrade the signal. Strain data recorded by the sensors may show out-of-range values that are caused by signal interference. Long cable lengths have been found to weaken and degrade the analog signal as well. When using a large volume of vibrating wire strain gages, it is recommended to use a minimum time of ten-minute intervals for continuous monitoring. Using shorter increments were found to cause several erroneous readings. Furthermore, depending on the number of arrays and frequency of data collection, capacity limitations of the data logger must also be determined. Prior estimates of capacity were determined to be two weeks when the actual capacity was closer to one. This has caused data to be overwritten and lost for that week.

We recognize at this time that the bridge is still new and is not expected to have problems. However, as time goes by, data covering a relatively long period of time will be collected and, when combined with a bridge deterioration model, can help predict bridge performance and call for timely preventative maintenance. We believe that three years worth of monitoring data would provide sufficient baseline information to create behavior envelopes that can be used for future prediction of bridge condition and can be the basis of a bridge deck deterioration prediction model.

9.0 RECOMMENDATIONS FOR FUTURE WORK

Due to loading and temperature variations, recorded stresses vary significantly. These variations, particularly in temperature, cause the bridge's behavior to vary from season to season. To further enhance the health monitoring of bridge decks using sensor networks, the following is a list of suggested future research and development studies that can add more models and tools for the analysis of the deck behavior:

- *Stress Envelopes*: Once large amounts of data have been collected and processed for a minimum recommended period of three years, envelopes can be developed to determine normal performance patterns and condition. This can provide fast and efficient assessment means for periodically evaluating the condition of the bridge deck in comparison to the design and behavioral limits.
- *Deck Performance and Health Condition Predictive Modeling*: Since the bridge is new, it is too early to begin to understand how weather and traffic will impact the bridge's deck over time. The deck was a unique design composed of forty eight pre-cast concrete panels, post-tensioned once installation was completed. Further analysis can be performed on the overall integrity of the deck providing valuable information on the performance and durability of the bridge's deck over time under current local traffic and weather conditions. Finite element modeling using actual strain data from the sensor network can shed additional insight on the health of the bridge deck. As more and more data is collected each year, these models could

be adjusted, calibrated, and validated using the known behavioral strain data. These current models for existing conditions could be used to develop health condition predictive models for bridge decks.

- *Database Design and Data Mining Algorithm*: While data is continuously monitored and stored, many further analyses can be performed over different periods of time. Since data collection and analysis were performed manually, database design may improve the efficiency and organization of the data. It is often difficult and time consuming to manually remove erroneous data. The design of an efficient automated system may be very beneficial when organizing and analyzing the large amounts of data. Data mining algorithms can also help in identifying trends in the data stored in the database which would then facilitate more advanced trend analyses.

10.0 REFERENCES CITED

- AASHTO (2000), American Association of State Highway and Transportation Officials, *Manual for Condition Evaluation of Bridges*, 2nd Edition, Washington, D.C.
- Aktan, A., Catbas, F., Grimmelsman, K., and Pervizpour, M. (2002), "Development of a model health monitoring guide for major bridges." Drexel Intelligent Infrastructure and Transportation Safety institute, FHWA Report No. DTFH61-01-P-00347.
- Boart Longyear (2006), <http://www.interfels.com>.
- BTS (2007a), Bureau of Transportation Statistics, "BTS Special Report: Highway Bridges in the US: an Overview," http://www.bts.gov/publications/bts_special_report/2007_09_19/.
- BTS (2007b), Bureau of Transportation Statistics, "Transportation Statistics Annual Report 2007," http://www.bts.gov/publications/transportation_statistics_annual_report/2007/.
- Casas, J. R. and Cruz, P. J. S. (2003), "Fiber Optic Sensors for Bridge Monitoring," *Journal of Bridge Engineering*, ASCE, Volume 8, Number 6, 362-373.
- CPPCI (2002), Canadian Precast Prestressed Concrete Institute, "Prestressed Girder Bridges." <http://www.cpci.ca/?sc=bs&pn=prestressedgirderbridges>.
- Chajes, M. et al. (2000), "Bridge-condition Assessment and Load Rating Using Nondestructive Evaluation Methods," *Transportation Research Record*, 2(1696), 83-91.
- Chen, Z., Liang, Y., and Ansari, F. (2003), "Remote Structural Control health Monitoring with serially multiplexed fiber optic acoustic emission sensors," *J. of Earthquake Engineering and Engineering Vibration*, vol. 2, issue 1pp. 141-146, June.
- Cheung, M., Li, W., Noruziaan, B. (2004), "Data acquisition, processing and management systems for a Canadian bridge monitoring project," *International Conference on Computing in Civil and Building Engineering (ICCCBE)*, 10, 2004.06.02-04, Weimar , Bauhaus-Universität, http://e-pub.uni-weimar.de/volltexte/2004/128/pdf/icccbe-x_012.pdf.
- Daher, B. (2004), *Use of Sensors in Monitoring Civil Structures*, Massachusetts Institute of Technology, Cambridge, September.
- Dunker, K. and Rabbat (1992), "Performance of Prestressed Concrete Highway Bridges in the United States – The First 40 Years," *PCI Journal*, V. 41, No. 5, May, pp. 59-65.
- FHWA (2008a), Federal Highway Administration, "FHWA Bridge Programs NBI Data," <http://www.fhwa.dot.gov/bridge/defbr07.cfm>.
- FHWA (2008b), Federal Highway Administration, "Prefabricated Bridge Elements and Systems," <http://www.fhwa.dot.gov/bridge/prefab>.

- FHWA (2007), Federal Highway Administration, *Deficient Bridges by State and Highway System*, <http://www.fhwa.dot.gov/bridge/defbr07.cfm>.
- FHWA (2006), Federal Highway Administration, "Guidelines for instrumentation of bridges," <http://www.fhwa.dot.gov/BRIDGE/hpcinstr.htm>.
- FHWA (2005), Federal highway administration, "Framework for prefabricated bridge elements and systems (PBES) decision making," <http://www.fhwa.dot.gov/bridge/prefab/if06030.pdf>.
- FHWA (2004), Federal Highway Administration, "Prefabricated Bridge Elements and Systems in Japan and Europe," FHWA International Technology Exchange Programs.
- Fu, G. and Moosa, A. (2002), "An Optical Approach to Structural Displacement Measurement and its Applications," *Engineering Mechanics*, V. 128, No. 5, pp. 511-520.
- Geokon (2006), <www.Geokon.com>.
- Georgia Department of Transportation (2002), "Forming the Concrete Columns." <http://www.dot.state.ga.us/specialsubjects/roadconstruction/sidney/approach/column.shtml>.
- Hieber, D., Wacker, J., Eberhard, M., and Stanton, J. (2005), "State-of-the-art Report on Precast Concrete Systems for Rapid Construction of Bridges," Final Technical Report, Contract T2695, Task 53, Washington Department of Transportation.
- Hou, T. and Lynch, P.J. (2006), "Rapid-to-Deploy Wireless Monitoring Systems for Static and Dynamic Load Testing of Bridges: Validation on the Grove Street Bridge," *SPIE 13th Annual International Symposium on Smart Structures and Materials*, San Diego, CA, February.
- Howell, D. A. and Shenton, H. W. (2006), "System for In-Service Strain Monitoring of Ordinary Bridges," *Journal of Bridge Engineering*, ASCE, Volume 11, Number 6, 673-680.
- Kim, S. Culler, D., and Demmel, J. (2006), "Structural health monitoring using wireless sensor network," University of California, Berkeley, http://www.cs.berkeley.edu/~binetude/course/cs294_1/paper.pdf.
- Kleinhans, D., Myers, J., and Nanni, A. (2007), "Assessment of Load Transfer and Load Distribution in Bridges Utilizing FRP Panels," *Journal of Composites for Construction*, American Society of Civil Engineers, Volume 11, Number 5, 545-552.
- Ko, J. and Ni, Y. (2005), "Technology developments in structural health monitoring of large-scale bridges," *Engineering Structures*, Elsevier Ltd., 27, 1715-1725.
- Lewis, A., Weinmann, T., and Telang, N. (2003), "Advances in Bridge Materials and Structural Health Monitoring Systems With Case Studies," *Proceedings of the 2nd New York city bridge Conference*, New York, NY, pp 301-316.
- Lin, M., Thaduri, J., and Gopu, V. (2003), "A Distributed Strain Sensor for Bridge Monitoring," *UTCA report 02304*, University of Alabama, Huntsville, AL.
- Lynch, J., Law, K., Straaser, E., Kiremiduian, A, Kenny, T. (2001), "The development of a wireless modular health monitoring system for civil structures," *Proceedings of the 2nd Workshop on Mitigation of Earthquake Disaster by Advanced Technologies*, Las Vegas, NV.
- Lynch, J. and Loh, K. (2006), "A summery review of wireless sensors and sensor networks for structural health monitoring," *Shock and Vibration Digest*, Vol. 38, No. 2, pp 91-128.
- Matsumoto, E. Waggoner, M. Sumen, G. Kreger, M, and Breen, J. (2001), "Development of a Precast Bent Cap System", University of Texas at Austin, Project summary report 1748-S.
- Merzbacher, C., Kersey, A., and Friebele, E. (1996), "Fiber Optic Sensors in Concrete Structures: a Review," *Smart Material Structure*, Vol 5., pp 196 – 208.

- NCHRP (2003), National Cooperative Highway Research Program, “Prefabricated bridge elements and systems to limit traffic disruption during construction,” (Synthesis Report 324).
- NCHRP(1998), National Cooperative Highway Research Program, *Manual for Bridge Rating Through Load Testing*, Research Results Digest, November, Number 234, Transportation Research Board, National Research Council, Washington, DC.
- Olund J. and DeWolf J. (2007), “Passive Structural Health Monitoring of Connecticut’s Bridge Infrastructure,” *Journal of Infrastructure Systems*, ASCE, V. 13, No. 4, 330-339.
- OPSens (2006), <http://www.opsens.com>.
- PCI (2003), *Bridge Design Manual*, Precast/Prestressed Concrete Institute, Chicago, IL.
- Parsons Transportation Group (2007), “Parkview Avenue Over US 131 – Design Calculation,” Prepared by Parsons Transportation Group, Jon No. 646403, January.
- Phares, B., Wipf, T., Greimann, L., and Lee, Y. (2005), *Health Monitoring of Bridge Structures and Components Using Smart-Structure Technology*, Wisconsin Highway Research Program, WHRP 05-03, Report No. 0092-04-14.
- Ravisankar, K., Sreeshlam, P., and Sridhar, S. (2005), “Assessment of long term performance of EFPI fiber optic sensors,” *International conference on smart materials structures and systems*.
- Robertson, I. (2005), “Prediction of vertical deflections for a long-span prestressed concrete bridge structure,” *Engineering Structures*, Elsevier Ltd., 27 (2005) 1820-1827.
- Roctest (2006), <http://www.roctest.com>.
- Shah, S., Popovics, J., Subramaniam, K., and Aldea, C. (2000), “New Directions in Concrete Health Monitoring Technology,” *J. of Engineering Mechanics*, V. 126, Issue 7, pp. 754-760.
- Sawyer T., “Sensor-Laced Concrete Promises to be Strong and Smart,” *Engineering News Record*, Vol. 254, No.2, January 2005.
- Shenton, H., Chajes, M., and Holloway, E. (2001), “A System for Long Term Monitoring of Live Load Strain in Bridges,” Report No. DTI 123, University of Delaware, Newark, DE.
- Xia, Y., Fujino, Y., Abe, M., and Murakoshi, J. (2005), “Short Term and Long Term Health Monitoring Experience of a Short Highway Bridge: Case Study”, *Bridge Structures. Assessment, Design and Construction*, Vol. 1, Issue 1, pp. 43-53.
- Yang, Y., Myers, J. (2003), “Live Load Test Results of Missouri’s First High Performance Concrete Superstructure Bridge,” *Transportation Research Board*, Paper No. 03-3717.

APPENDIX A: LIST OF ACRONYMS, ABBREVIATIONS, AND SYMBOLS

Abbreviation	Description
AASHTO	American Association of State Highway and Transportation Officials
CPM	Critical Path Method
FBG	Fiber Bragg Gratings
FHWA	Federal Highway Administration
FE	Finite Element
FOS	Fiber Optic Sensor
FWS	Future Wearing Surface
RBC	Rapid Bridge Construction
SHM	Structural Health Monitoring
VWSG	Vibrating Wire Strain Gages
WBS	Work Breakdown Structure

APPENDIX B: SENSORS CONSTRUCTION SPECIFICATIONS
MICHIGAN
DEPARTMENT OF TRANSPORTATION

SPECIAL PROVISION
FOR
PRECAST DECK PANEL INSTRUMENTATION AND DATA COLLECTION

C&T:SCK

1 of 3

C&T:APPR:RJZ:EMB:08-03-07

a. Description. This work includes furnishing all labor, materials, and equipment necessary to properly install housing and hardware for the instrumentation and data collection devices. In addition, the contractor shall coordinate work activities with the Western Michigan University (WMU) research team involving instrumentation placement, data collection, load testing, and all other related activities needed to monitor the performance of the bridge deck precast panels.

b. Materials. The following list of materials shall conform as specified in the current Standard Specifications for Construction and as outlined herein.

3/4 inch diameter (Dayton F-5 or equivalent) galvanized ferrule inserts.....	908
3/4 inch diameter galvanized threaded rod.....	908
Steel plate, galvanized.....	908
Conduit, Schedule 40 PVC, 3 inch.....	918
Electrical wire and cable.....	918

The 12 inch x 12 inch x 6 inch PVC junction boxes (Allied Moulded Products P/N AMJB12126 or equivalent) shall meet NEMA type 4x requirements.

Electrical cable shall be UL listed, AWG gauge, single conductor annealed copper insulated with high-heat and moisture resistant PVC, jacketed with abrasion, moisture, gasoline and oil resistant nylon, of the size indicated on the plans. Cable shall be Type USE, RHH, or RHW suitable for operations at 600 volts or less in wet or dry locations, including direct burial in the earth. Wire shall meet or exceed all applicable ASTM specifications, UL standard 44 (for RHH or RHW), UL standard 854 (for USE), Federal Specification J-C 30, IPCEA specifications, and requirements of Current State of Michigan Electrical Code. Wire in conduit shall be THHW or XHHW.

Electrical materials and equipment shall be new and be the standard products of manufacturers regularly engaged in the production of such materials. Material and equipment shall be the manufacturer's latest standard design and shall be free from all defects and imperfections that might affect the serviceability of the finished product. Manufacturer's trade names and equipment specified indicate the quality and description only. Comparable products of other manufacturers of the same quality and equal to that specified may be accepted. Should the cost of alternate or substitute equipment proposed by the Contractor require redesign, all costs incurred shall be borne by the Contractor, and the redesign approved by the Engineer prior to construction. The Contractor shall remain responsible for a complete and functional system.

c. Construction. The contractor shall coordinate the installation of the instrumentation and data collection devices with the fabricator and Western Michigan University (WMU) personnel as specified herein. All electrical work shall comply with Section 819 of the Standard Specifications for Construction, the latest applicable rules of the Construction Code Commission of the State of Michigan, the NEC, the special provision, and local codes as their jurisdiction applies.

1. REQUIREMENTS DURING FABRICATION: Coordinate the manufacturing of the precast deck panels with Dr. Sherif Yehia at WMU (269-276-3218) by providing a minimum of two weeks notification, and allow for the following work on 28 precast deck panels identified on the plans:

- A. Provide access to WMU staff for installation of embedded instrumentation on the precast deck panel reinforcement, and allow sufficient time for routing and securing instrumentation cabling prior to casting concrete. It is anticipated that this task will require 2 to 4 hours per panel to complete the installation.
- B. Provide access to WMU staff for data collection before casting and before storage.
- C. Allow WMU staff to sample the deck panel concrete during placement.

The instrumentation and securing devices shall be provided by WMU. The contractor shall provide and install two Dayton F-5 or equivalent galvanized ferrule 3/4 inch diameter inserts per precast deck panel at spacing identified in the plans for all of the precast deck panels.

2. REQUIREMENTS DURING ERECTION OF PRECAST DECK PANELS: The Contractor shall coordinate activities related to the precast deck panel installation with Dr. Sherif Yehia at WMU (269-276-3218) by providing a minimum of 2 weeks notification and provide the following:

- A. Install junction boxes, main panel boxes (supplied by WMU), conduit, cables, and wiring after the post tensioning operations are completed. Modify the boxes as needed to accommodate conduits and cables. A licensed electrician is required for electrical connections and cable splicing.
- B. Install three inch Schedule 40 PVC conduit runs with supports and connections as shown on the plans and route instrumentation cables (supplied by WMU) from each deck panel junction box to the main panel locations.
- C. Install two 110V/10A permanent GFCI electric outlets inside one main panel box, and conduit for supply connection as shown on the plans. Arrange for supply connection and meter installation with the utility company.
- D. Install two phone lines inside one main panel box, and route to the main line and arrange for connection by the telecommunication utility company.
- E. Install the main panels (supplied by WMU) on the pier cap of Pier 3 facing the slope paving, as shown in the plans.

F. Send a copy of the post tensioning report to Dr. Sherif Yehia at WMU (fax number 269-276-3218).

3. **REQUIREMENTS AFTER CONSTRUCTION:** The Contractor shall provide a minimum of 2 weeks notification to Dr. Sherif Yehia at WMU (269-276-3218) and allow for load testing operations by WMU prior to opening the structure to traffic. It is anticipated that the load testing will require up to 3 days.

d. **Measurement and Payment.** The completed work as described will be measured and paid for using the following contact item (pay item):

Contract Item (Pay Item)	Pay Unit
Precast Deck Panel Instrumentation and Data Collection.....	Lump Sum

Payment for **Precast Deck Panel Instrumentation and Data Collection** includes all the necessary labor, materials and equipment necessary to properly install and connect external junction boxes, wiring, panels, conduit, and electrical and phone lines, and coordination with the electric and phone utility companies. Payment includes an allowance for up to 10 percent overrun on quantities listed herein and on the plans. Items not specifically mentioned in the Standard Specifications for Construction or noted on the plans, but which are obviously necessary to make a complete working installation, shall be included. Payment will be made only when the Engineer has verified proper installation. No additional compensation will be given for any delays in operations or equipment use for providing access and coordination with WMU.

Concrete and steel reinforcement work will be paid for separately.

The following list of materials is provided for **information only**.

ITEM	QUANTITY
Conduit, Schedule 40 PVC, 3 inch	750 Foot
Coupling, Schedule 40 PVC, 3 inch	84 Each
U bolt 1/2 inch x 4 inch x 5 1/2 inch	20 Each
NEMA 4x 12 inch x 12 inch x 6 inch PVC junction box	28 Each
3/4 inch diameter galvanized ferrule inserts (Dayton F5 or equivalent)	96 Each
1/2 inch diameter galvanized ferrule inserts (Dayton F5 or equivalent)	12 Each
3/4 inch diameter galvanized threaded rod, nut and washer, 7 inch	40 Each
3/4 inch diameter galvanized threaded rod, nut and washer, 2 inch	56 Each
Steel plate, galvanized, 12 inch x 4 inch x 1/2 inch	20 Each
600 v Electrical wiring, 12 AWG	100 Foot
Electrical Outlet box, duplex GFCI receptacle	1 Each
Electrical conduit, galvanized steel	100 Foot
Phone line and jack (2 outlet)	2 Each

APPENDIX C: LOAD TEST SPREADSHEETS AND FORMULAS

C.1 Simulated Load Testing Scenarios

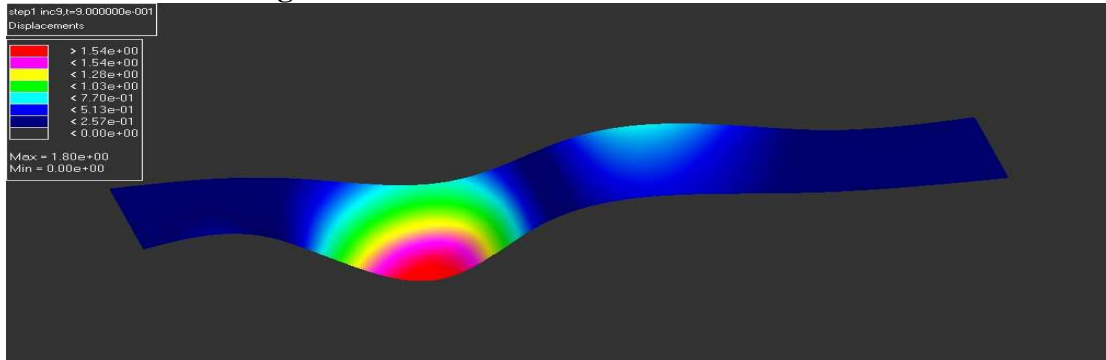


Figure C.1: Simulated Scenario 1

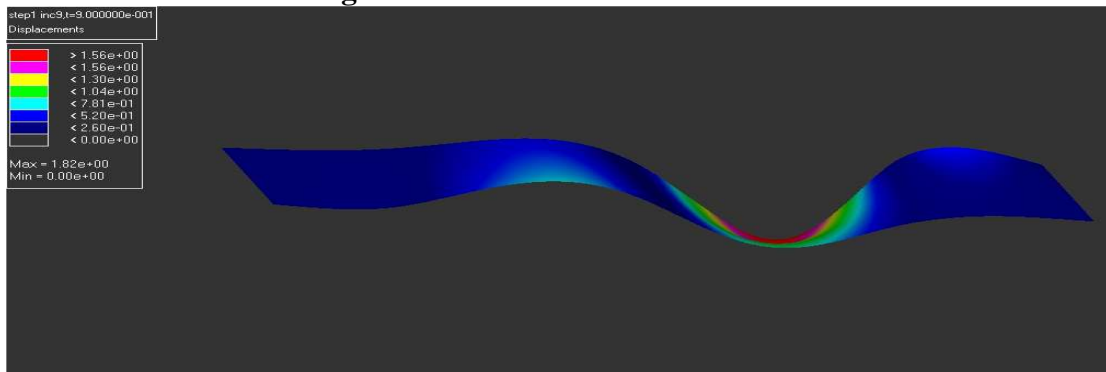


Figure C.2: Simulated Scenario 2

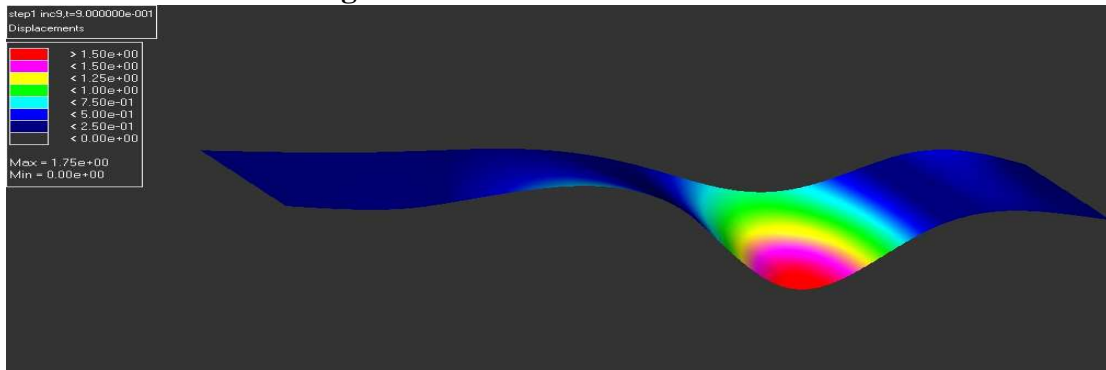


Figure C.3: Simulated Scenario 3

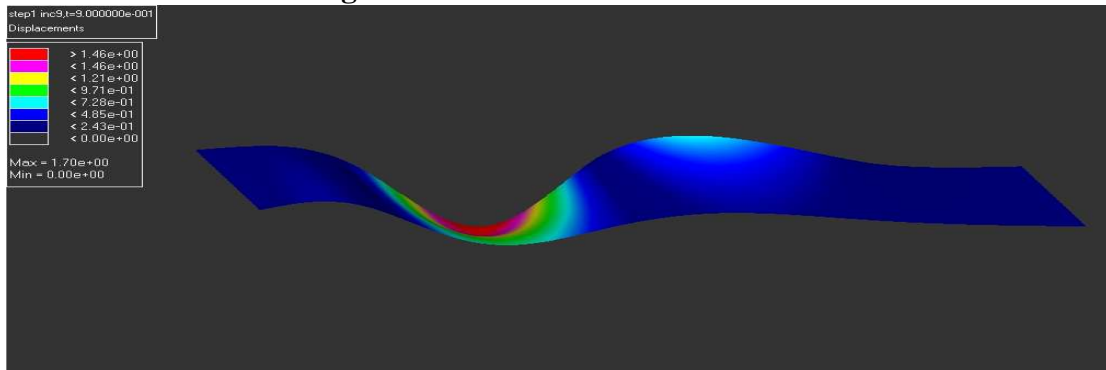


Figure C.4: Simulated Scenario 4

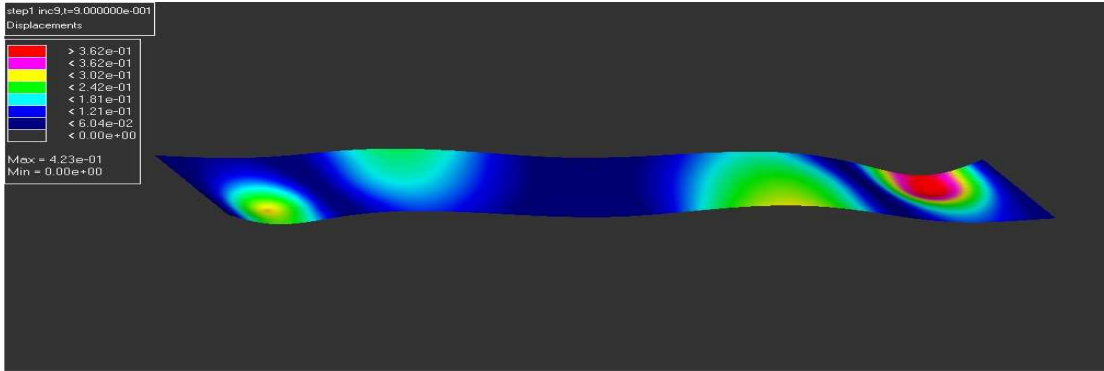


Figure C.5: Simulated Scenario 5

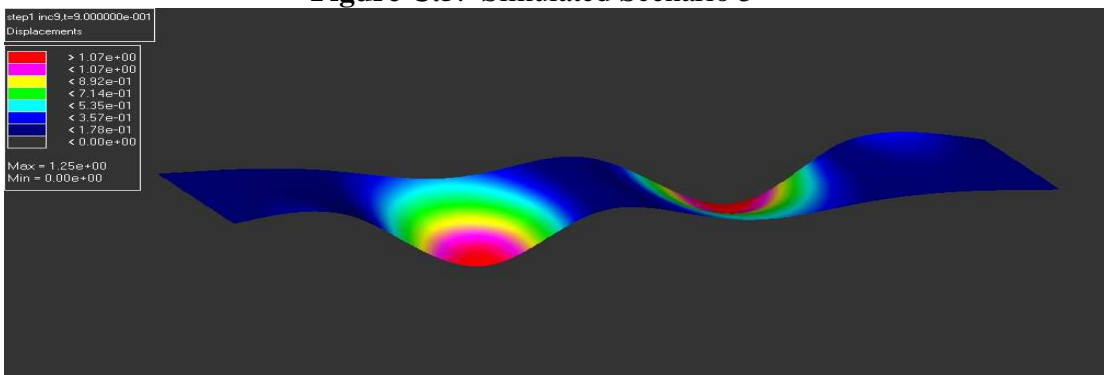


Figure C.6: Simulated Scenario 6

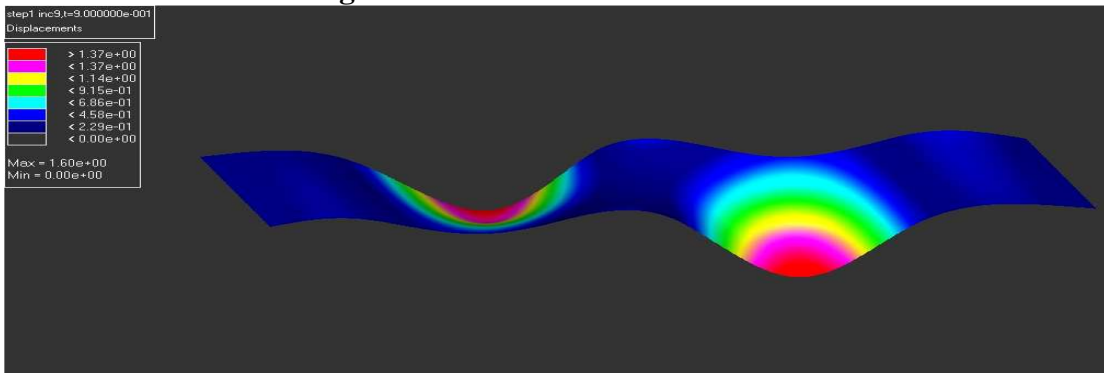


Figure C.7: Simulated Scenario 7

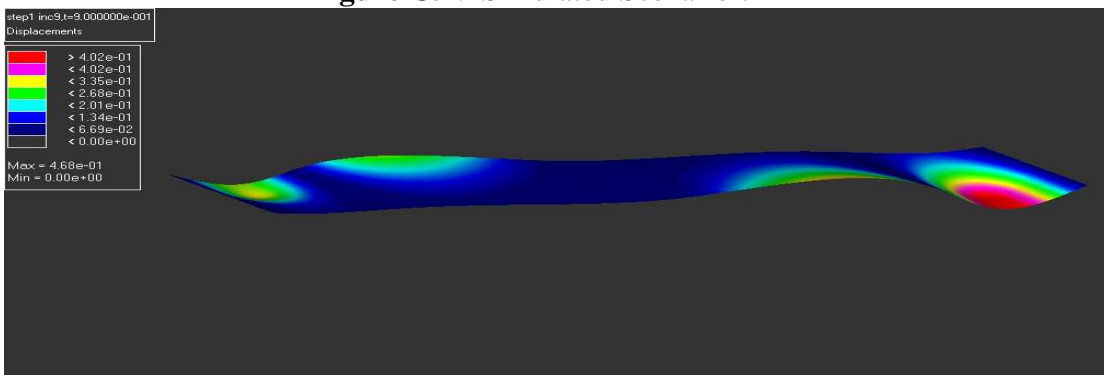


Figure C.8: Simulated Scenario 8

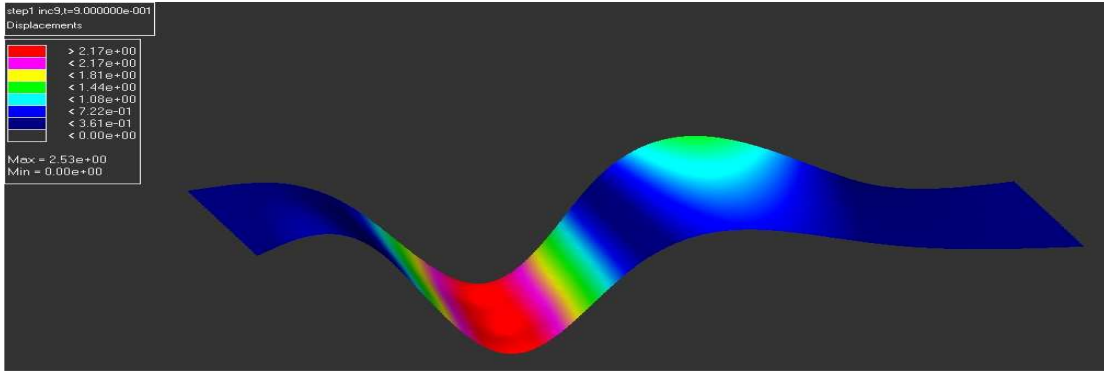


Figure C.9: Simulated Scenario 9

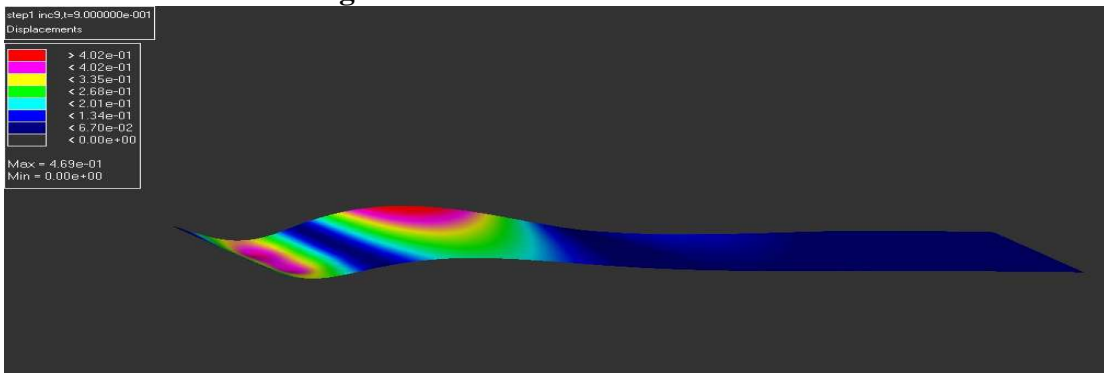


Figure C.10: Simulated Scenario 10

C.2 Load Test 1

C.2.1 Deflected Shape Bridge Models Using Survey Data

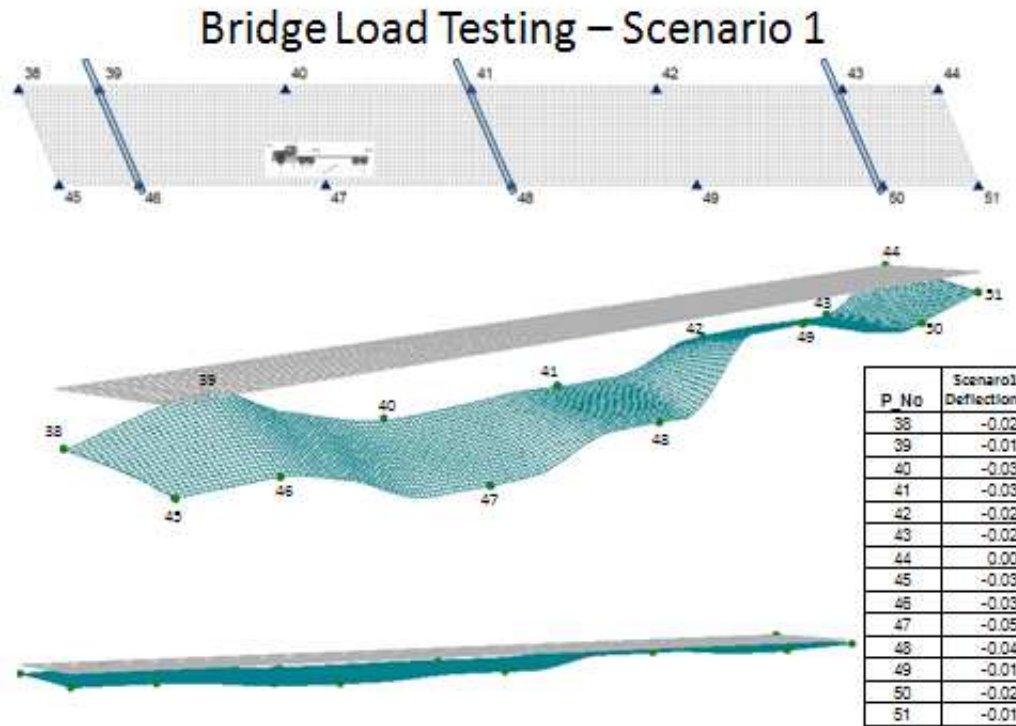


Figure C.11: Deflected Shape Model for Scenario 1

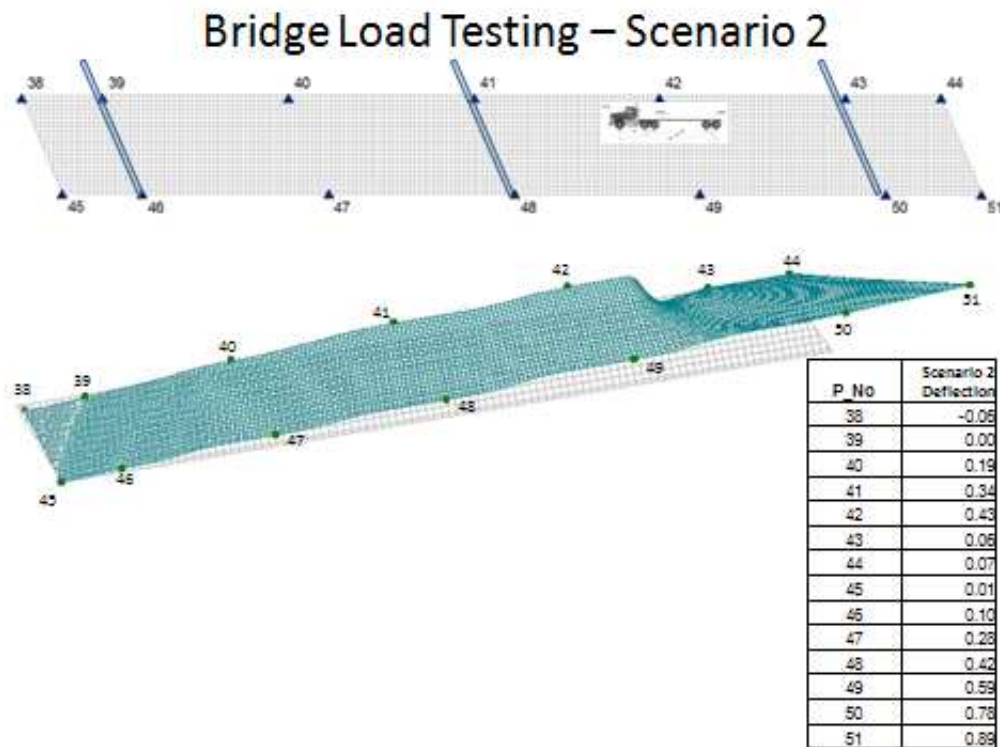


Figure C.12: Deflected Shape Model for Scenario 2

Bridge Load Testing – Scenario 3

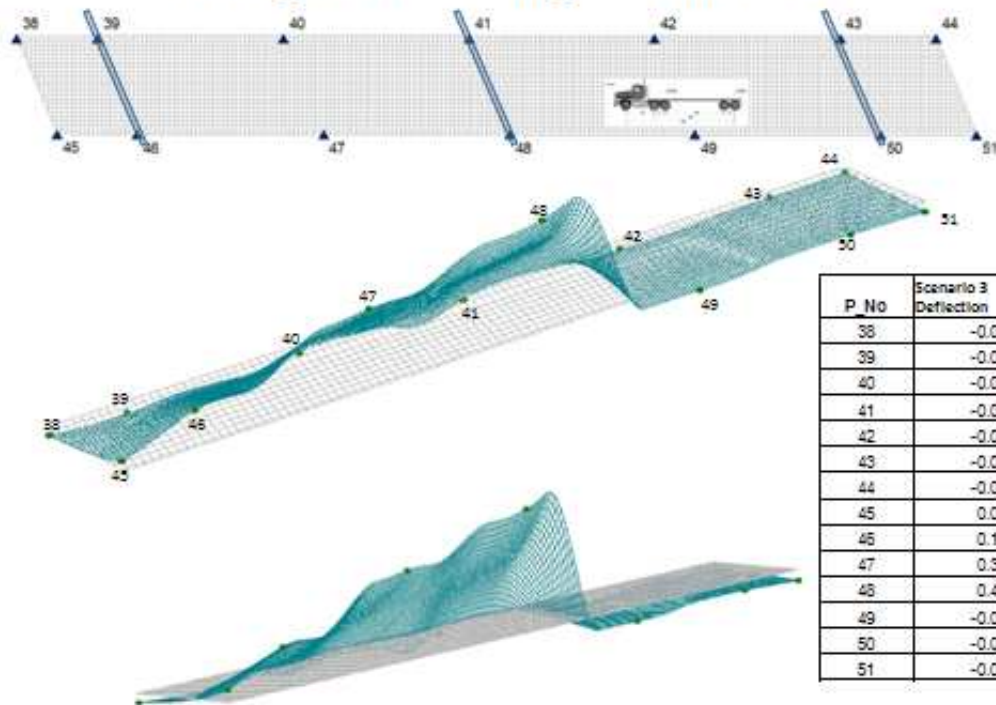


Figure C.13: Deflected Shape Model for Scenario 3

Bridge Load Testing – Scenario 4

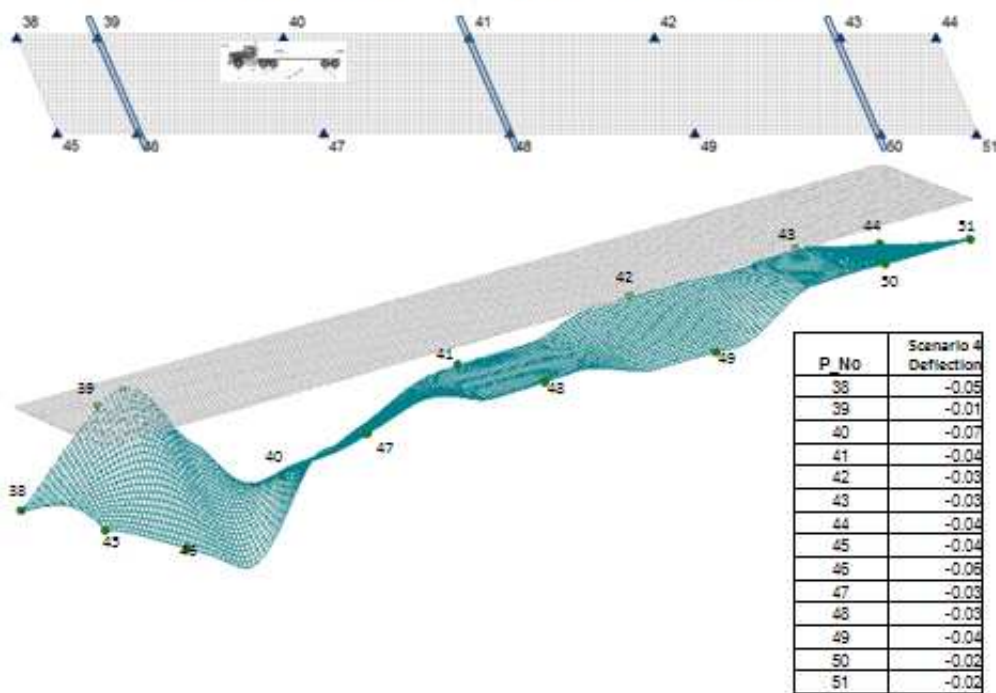


Figure C.14: Deflected Shape Model for Scenario 4

Bridge Load Testing – Scenario 5

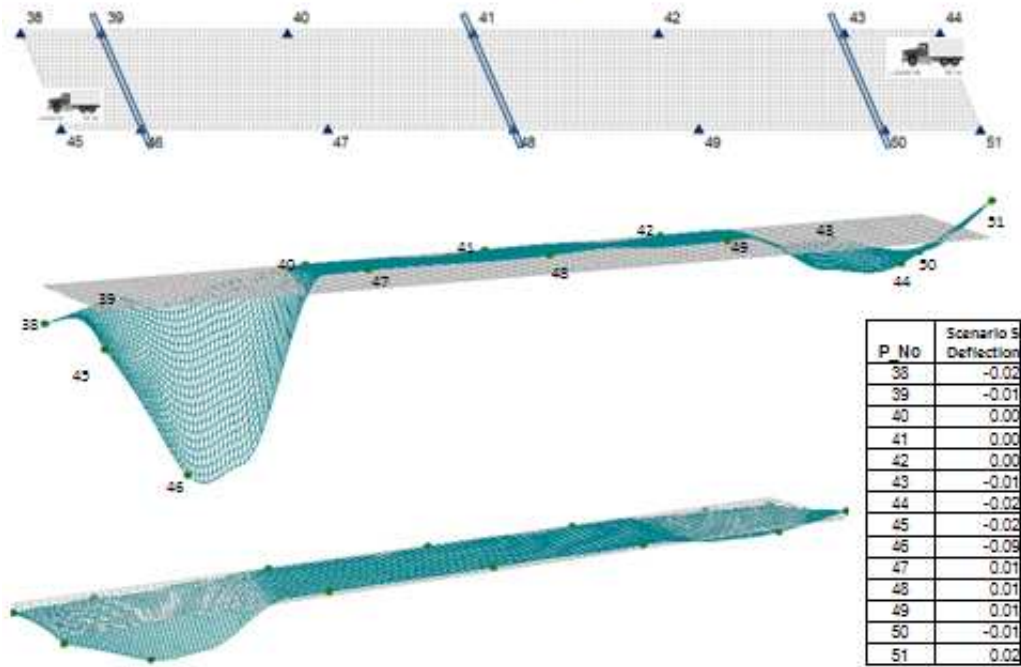


Figure C.15: Deflected Shape Model for Scenario 5

Bridge Load Testing – Scenario 6

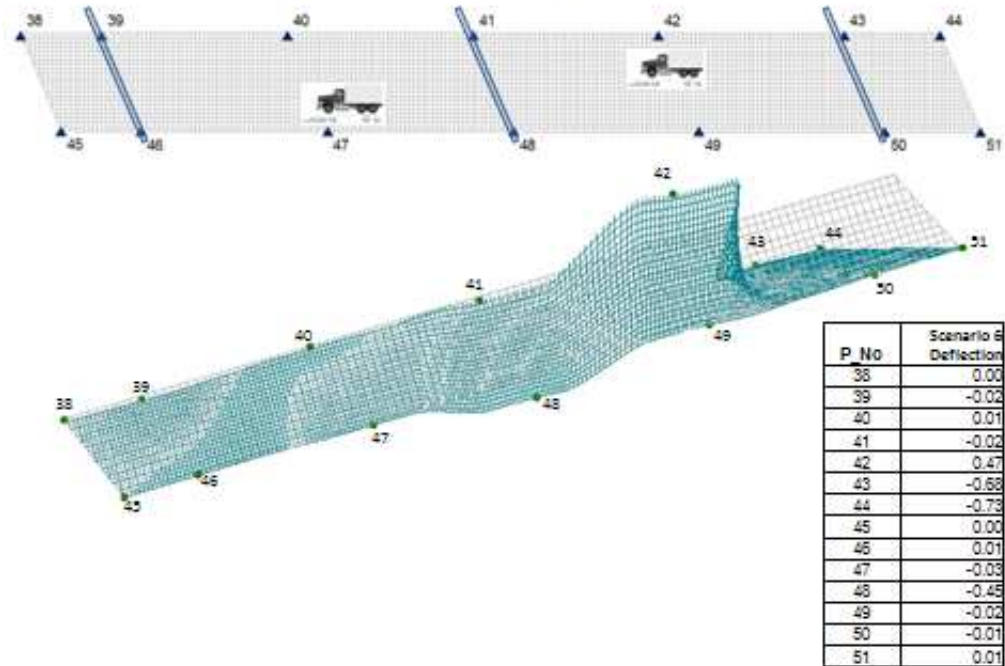


Figure C.16: Deflected Shape Model for Scenario 6

Bridge Load Testing – Scenario 7

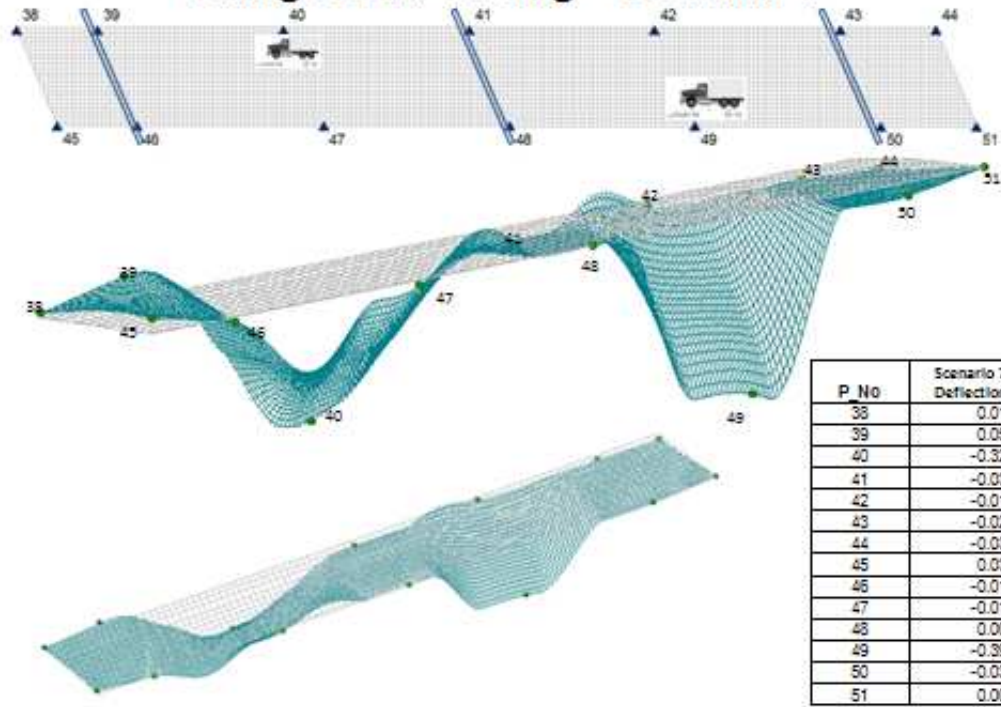


Figure C.17: Deflected Shape Model for Scenario 7

Bridge Load Testing – Scenario 8

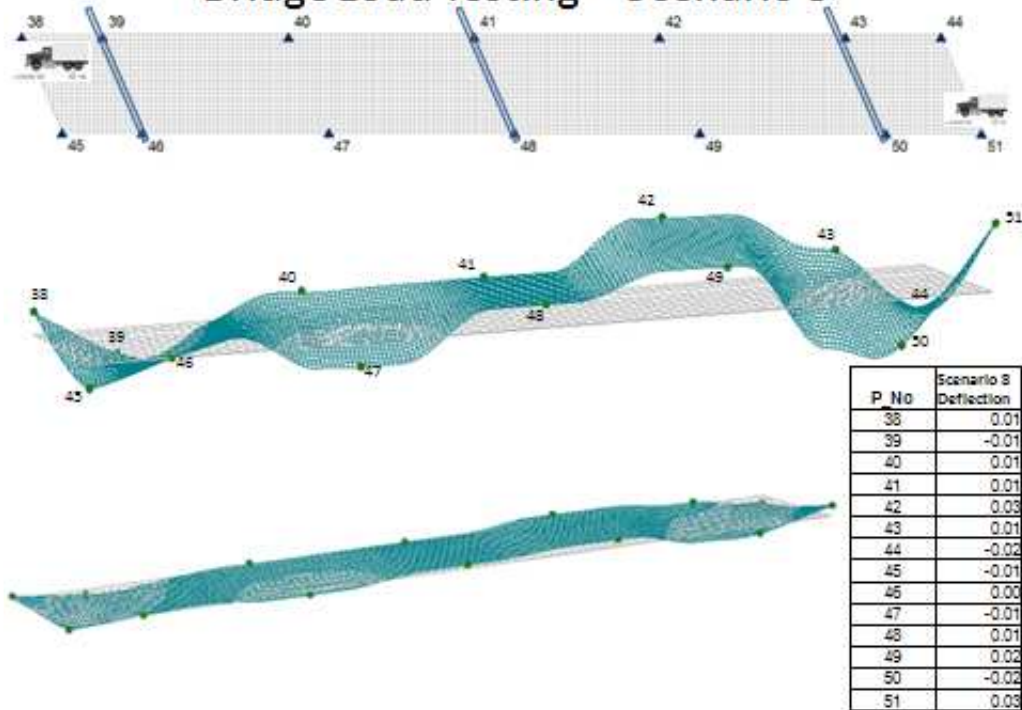


Figure C.18: Deflected Shape Model for Scenario 8

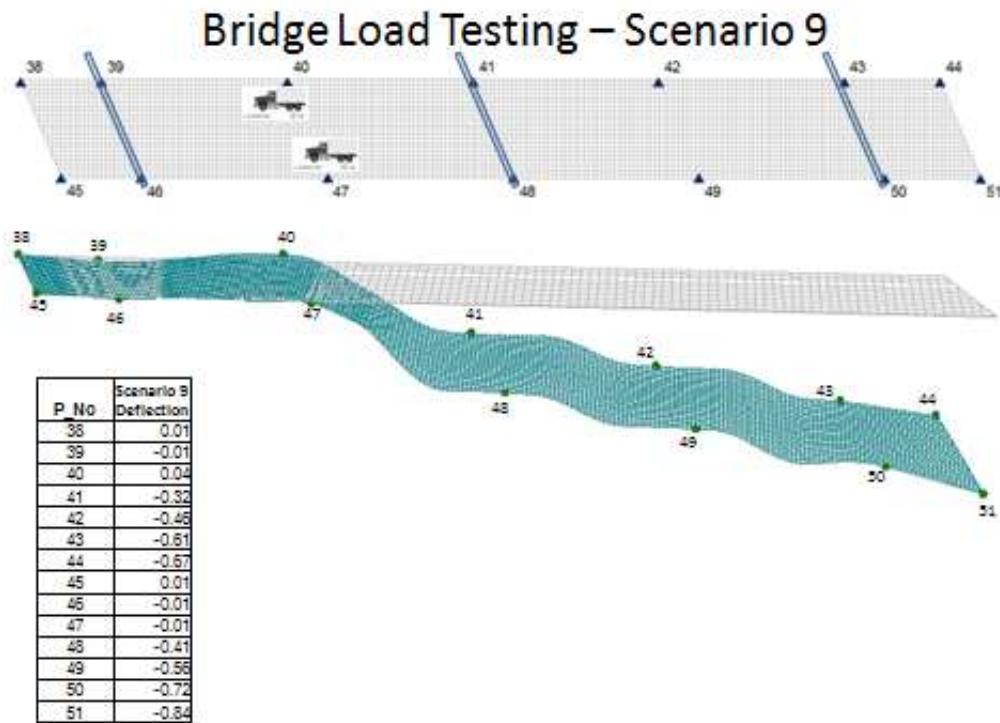


Figure C.19: Deflected Shape Model for Scenario 9

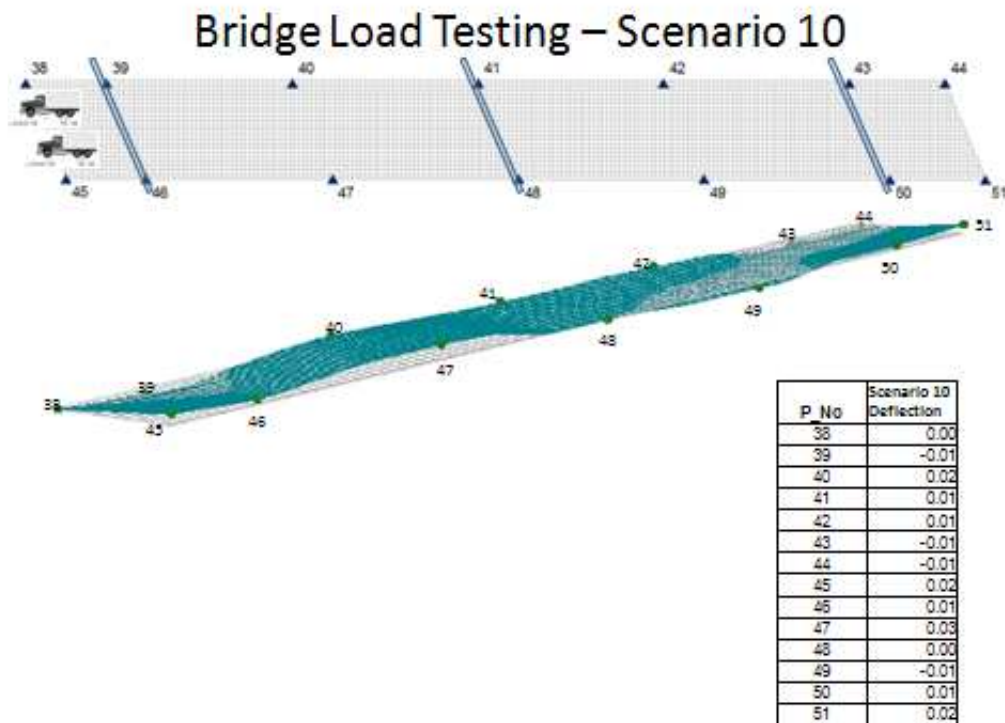


Figure C.20: Deflected Shape Model for Scenario 10

C.2.2 Load Testing 1 Scenario Stress Tables

Table C.1: Scenario 1 East Bound Lane Top Fiber Stress

Scenario 1 East Bound: Top Fiber Stresses									
Location ID	West Abut.	Midspan (45)	Pier 1 (46)	Midspan (47)	Pier 2 (48)	Midspan (49)	Pier 3 (50)	Midspan (51)	East Abut.
L.L. (psi)	0	-117	-100	-40	-15	-8	-8	-28	0
L.L. (ksf)	0	-17	-14	-6	-2	-1	-1	-4	0
F.W.S. (ksf)	0	-63	-67	-111	-62	-109	-55	-62	0
F.W.S.+ L.L. (ksf)	0	-80	-81	-117	-64	-111	-56	-66	0
Design F.W.S.+L.L. (ksf)	0	-84	-77	-148	-66	-147	-60	-85	0

Table C.2: Scenario 1 West Bound Lane Top Fiber Stress

Scenario 1 West Bound: Top Fiber Stresses									
Location ID	East Abut	Midspan (44)	Pier 3 (43)	Midspan (42)	Pier 2 (41)	Midspan (40)	Pier 3 (39)	Midspan (38)	West Abut.
L.L. (psi)	0	0	0	-16	-6	-24	-23	-78	0
L.L. (ksf)	0	0	0	-2	-1	-3	-3	-11	0
F.W.S. (ksf)	0	-62	-55	-109	-62	-111	-67	-63	0
F.W.S.+ L.L. (ksf)	0	-62	-55	-112	-63	-115	-70	-74	0
Design F.W.S.+L.L. (ksf)	0	-83	-65	-146	-66	-149	-72	-86	0

Table C.3: Scenario 2 East Bound Lane Top Fiber Stress

Scenario 2 East Bound: Top Fiber Stresses									
Location ID	West Abut.	Midspan (45)	Pier 1 (46)	Midspan (47)	Pier 2 (48)	Midspan (49)	Pier 3 (50)	Midspan (51)	East Abut.
L.L. (psi)	0	39	33	224	81	471	454	2460	0
L.L. (ksf)	0	6	5	32	12	68	65	354	0
F.W.S. (ksf)	0	-63	-67	-111	-62	-109	-55	-62	0
F.W.S.+ L.L. (ksf)	0	-57	-62	-79	-50	-42	11	293	0
Design F.W.S.+L.L. (ksf)	0	-84	-77	-148	-66	-147	-60	-85	0

Table C.4: Scenario 2 West Bound Lane Top Fiber Stress

Scenario 2 West Bound: Top Fiber Stresses									
Location ID	East Abut	Midspan (44)	Pier 3 (43)	Midspan (42)	Pier 2 (41)	Midspan (40)	Pier 3 (39)	Midspan (38)	West Abut.
L.L. (psi)	0	194	165	0	0	152	146	-233	0
L.L. (ksf)	0	28	24	0	0	22	21	-34	0
F.W.S. (ksf)	0	-62	-55	-109	-62	-111	-67	-63	0
F.W.S.+ L.L. (ksf)	0	-34	-31	-109	-62	-89	-46	-96	0
Design F.W.S.+L.L. (ksf)	0	-83	-65	-146	-66	-149	-72	-86	0

Table C.5: Scenario 3 East Bound Lane Top Fiber Stress

Scenario 3 East Bound: Top Fiber Stresses									
Location ID	West Abut.	Midspan (45)	Pier 1 (46)	Midspan (47)	Pier 2 (48)	Midspan (49)	Pier 3 (50)	Midspan (51)	East Abut.
L.L. (psi)	0	155	133	240	87	-40	-38	-111	0
L.L. (ksf)	0	22	19	35	13	-6	-6	-16	0
F.W.S. (ksf)	0	-63	-67	-111	-62	-109	-55	-62	0
F.W.S.+ L.L. (ksf)	0	-40	-48	-77	-49	-115	-60	-78	0
Design F.W.S.+L.L. (ksf)	0	-84	-77	-148	-66	-147	-60	-85	0

Table C.6: Scenario 3 West Bound Lane Top Fiber Stress

Scenario 3 West Bound: Top Fiber Stresses									
Location ID	East Abut	Midspan (44)	Pier 3 (43)	Midspan (42)	Pier 2 (41)	Midspan (40)	Pier 3 (39)	Midspan (38)	West Abut.
L.L. (psi)	0	-55	-47	-24	-9	-24	-23	-117	0
L.L. (ksf)	0	-8	-7	-3	-1	-3	-3	-17	0
F.W.S. (ksf)	0	-62	-55	-109	-62	-111	-67	-63	0
F.W.S.+ L.L. (ksf)	0	-70	-61	-113	-63	-115	-70	-80	0
Design F.W.S.+L.L. (ksf)	0	-83	-65	-146	-66	-149	-72	-86	0

Table C.7: Scenario 4 East Bound Lane Top Fiber Stress

Scenario 4 East Bound: Top Fiber Stresses									
Location ID	West Abut.	Midspan (45)	Pier 1 (46)	Midspan (47)	Pier 2 (48)	Midspan (49)	Pier 3 (50)	Midspan (51)	East Abut.
L.L. (psi)	0	-155	-133	-24	-9	-32	-31	-55	2
L.L. (ksf)	0	-22	-19	-3	-1	-5	-4	-8	0
F.W.S. (ksf)	0	-63	-67	-111	-62	-109	-55	-62	0
F.W.S.+ L.L. (ksf)	0	-85	-86	-115	-63	-114	-59	-70	0
Design F.W.S.+L.L. (ksf)	0	-84	-77	-148	-66	-147	-60	-85	0

Table C.8: Scenario 4 West Bound Lane Top Fiber Stress

Scenario 4 West Bound: Top Fiber Stresses									
Location ID	East Abut	Midspan (44)	Pier 3 (43)	Midspan (42)	Pier 2 (41)	Midspan (40)	Pier 3 (39)	Midspan (38)	West Abut.
L.L. (psi)	0	-111	-94	-24	-9	-56	-54	-194	0
L.L. (ksf)	0	-16	-14	-3	-1	-8	-8	-28	0
F.W.S. (ksf)	0	-62	-55	-109	-62	-111	-67	-63	0
F.W.S.+ L.L. (ksf)	0	-78	-68	-113	-63	-119	-75	-91	0
Design F.W.S.+L.L. (ksf)	0	-83	-65	-146	-66	-149	-72	-86	0

Table C.9: Scenario 5 East Bound Lane Top Fiber Stress

Scenario 5 East Bound: Top Fiber Stresses									
Location ID	West Abut.	Midspan (45)	Pier 1 (46)	Midspan (47)	Pier 2 (48)	Midspan (49)	Pier 3 (50)	Midspan (51)	East Abut.
L.L. (psi)	0	-78	-66	8	3	8	-8	55	0
L.L. (ksf)	0	-11	-10	1	0	1	-1	8	0
F.W.S. (ksf)	0	-63	-67	-111	-62	-109	-55	-62	0
F.W.S.+ L.L. (ksf)	0	-74	-77	-110	-61	-108	-56	-54	0
Design F.W.S.+L.L. (ksf)	0	-84	-77	-148	-66	-147	-60	-85	0

Table C.10: Scenario 5 West Bound Lane Top Fiber Stress

Scenario 5 West Bound: Top Fiber Stresses									
Location ID	East Abut	Midspan (44)	Pier 3 (43)	Midspan (42)	Pier 2 (41)	Midspan (40)	Pier 3 (39)	Midspan (38)	West Abut.
L.L. (psi)	0	-55	-47	0	0	0	0	-78	0
L.L. (ksf)	0	-8	-7	0	0	0	0	-11	0
F.W.S. (ksf)	0	-62	-55	-109	-62	-111	-67	-63	0
F.W.S.+ L.L. (ksf)	0	-70	-61	-109	-62	-111	-67	-74	0
Design F.W.S.+L.L. (ksf)	0	-83	-65	-146	-66	-149	-72	-86	0

Table C.11: Scenario 6 East Bound Lane Top Fiber Stress

Scenario 6 East Bound: Top Fiber Stresses									
Location ID	West Abut.	Midspan (45)	Pier 1 (46)	Midspan (47)	Pier 2 (48)	Midspan (49)	Pier 3 (50)	Midspan (51)	East Abut.
L.L. (psi)	0	0	0	-24	-9	-16	-15	28	0
L.L. (ksf)	0	0	0	-3	-1	-2	-2	4	0
F.W.S. (ksf)	0	-63	-67	-111	-62	-109	-55	-62	0
F.W.S.+ L.L. (ksf)	0	-63	-67	-115	-63	-112	-57	-58	0
Design F.W.S.+L.L. (ksf)	0	-84	-77	-148	-66	-147	-60	-85	0

Table C.12: Scenario 6 West Bound Lane Top Fiber Stress

Scenario 6 West Bound: Top Fiber Stresses									
Location ID	East Abut	Midspan (44)	Pier 3 (43)	Midspan (42)	Pier 2 (41)	Midspan (40)	Pier 3 (39)	Midspan (38)	West Abut.
L.L. (psi)	0	-2018	-1724	375	-136	8	-8	0	0
L.L. (ksf)	0	-291	-248	54	-20	1	-1	0	0
F.W.S. (ksf)	0	-62	-55	-109	-62	-111	-67	-63	0
F.W.S.+ L.L. (ksf)	0	-352	-303	-55	-82	-110	-68	-63	0
Design F.W.S.+L.L. (ksf)	0	-83	-65	-146	-66	-149	-72	-86	0

Table C.13: Scenario 7 East Bound Lane Top Fiber Stress

Scenario 7 East Bound: Top Fiber Stresses									
Location ID	West Abut.	Midspan (45)	Pier 1 (46)	Midspan (47)	Pier 2 (48)	Midspan (49)	Pier 3 (50)	Midspan (51)	East Abut.
L.L. (psi)	0	117	-100	-8	3	-312	-300	0	0
L.L. (ksf)	0	17	-14	-1	0	-45	-43	0	0
F.W.S. (ksf)	0	-63	-67	-111	-62	-109	-55	-62	0
F.W.S.+ L.L. (ksf)	0	-46	-81	-112	-61	-154	-98	-62	0
Design F.W.S.+L.L. (ksf)	0	-84	-77	-148	-66	-147	-60	-85	0

Table C.14: Scenario 7 West Bound Lane Top Fiber Stress

Scenario 7 West Bound: Top Fiber Stresses									
Location ID	East Abut	Midspan (44)	Pier 3 (43)	Midspan (42)	Pier 2 (41)	Midspan (40)	Pier 3 (39)	Midspan (38)	West Abut.
L.L. (psi)	0	-83	-71	-8	-3	-256	246	39	0
L.L. (ksf)	0	-12	-10	-1	0	-37	35	6	0
F.W.S. (ksf)	0	-62	-55	-109	-62	-111	-67	-63	0
F.W.S.+ L.L. (ksf)	0	-74	-65	-111	-62	-148	-32	-57	0
Design F.W.S.+L.L. (ksf)	0	-83	-65	-146	-66	-149	-72	-86	0

Table C.15: Scenario 8 East Bound Lane Top Fiber Stress

Scenario 8 East Bound: Top Fiber Stresses									
Location ID	West Abut.	Midspan (45)	Pier 1 (46)	Midspan (47)	Pier 2 (48)	Midspan (49)	Pier 3 (50)	Midspan (51)	East Abut.
L.L. (psi)	0	-39	33	-8	3	16	-15	83	0
L.L. (ksf)	0	-6	5	-1	0	2	-2	12	0
F.W.S. (ksf)	0	-63	-67	-111	-62	-109	-55	-62	0
F.W.S.+ L.L. (ksf)	0	-68	-62	-112	-61	-107	-57	-50	0
Design F.W.S.+L.L. (ksf)	0	-84	-77	-148	-66	-147	-60	-85	0

Table C.16: Scenario 8 West Bound Lane Top Fiber Stress

Scenario 8 West Bound: Top Fiber Stresses									
Location ID	East Abut	Midspan (44)	Pier 3 (43)	Midspan (42)	Pier 2 (41)	Midspan (40)	Pier 3 (39)	Midspan (38)	West Abut.
L.L. (psi)	0	-55	47	24	9	8	-8	39	0
L.L. (ksf)	0	-8	7	3	1	1	-1	6	0
F.W.S. (ksf)	0	-62	-55	-109	-62	-111	-67	-63	0
F.W.S.+ L.L. (ksf)	0	-70	-48	-106	-61	-110	-68	-57	0
Design F.W.S.+L.L. (ksf)	0	-83	-65	-146	-66	-149	-72	-86	0

Table C.17: Scenario 9 East Bound Lane Top Fiber Stress

Scenario 9 East Bound: Top Fiber Stresses									
Location ID	West Abut.	Midspan (45)	Pier 1 (46)	Midspan (47)	Pier 2 (48)	Midspan (49)	Pier 3 (50)	Midspan (51)	East Abut.
L.L. (psi)	0	39	-33	-8	-3	-447	-431	-2322	0
L.L. (ksf)	0	6	-5	-1	0	-64	-62	-334	0
F.W.S. (ksf)	0	-63	-67	-111	-62	-109	-55	-62	0
F.W.S.+ L.L. (ksf)	0	-57	-72	-112	-62	-174	-117	-396	0
Design F.W.S.+L.L. (ksf)	0	-84	-77	-148	-66	-147	-60	-85	0

Table C.18: Scenario 9 West Bound Lane Top Fiber Stress

Scenario 9 West Bound: Top Fiber Stresses									
Location ID	East Abut	Midspan (44)	Pier 3 (43)	Midspan (42)	Pier 2 (41)	Midspan (40)	Pier 3 (39)	Midspan (38)	West Abut.
L.L. (psi)	0	-1852	-1582	-367	-134	32	-31	39	0
L.L. (ksf)	0	-267	-228	-53	-19	5	-4	6	0
F.W.S. (ksf)	0	-62	-55	-109	-62	-111	-67	-63	0
F.W.S.+ L.L. (ksf)	0	-328	-282	-162	-81	-107	-72	-57	0
Design F.W.S.+L.L. (ksf)	0	-83	-65	-146	-66	-149	-72	-86	0

Table C.19: Scenario 10 East Bound Lane Top Fiber Stress

Scenario 10 East Bound: Top Fiber Stresses									
Location ID	West Abut.	Midspan (45)	Pier 1 (46)	Midspan (47)	Pier 2 (48)	Midspan (49)	Pier 3 (50)	Midspan (51)	East Abut.
L.L. (psi)	0	78	66	24	9	-8	8	55	0
L.L. (ksf)	0	11	10	3	1	-1	1	8	0
F.W.S. (ksf)	0	-63	-67	-111	-62	-109	-55	-62	0
F.W.S.+ L.L. (ksf)	0	-52	-58	-108	-61	-111	-53	-54	0
Design F.W.S.+L.L. (ksf)	0	-84	-77	-148	-66	-147	-60	-85	0

Table C.20: Scenario 10 West Bound Lane Top Fiber Stress

Scenario 10 West Bound: Top Fiber Stresses									
Location ID	East Abut	Midspan (44)	Pier 3 (43)	Midspan (42)	Pier 2 (41)	Midspan (40)	Pier 3 (39)	Midspan (38)	West Abut.
L.L. (psi)	0	78	66	24	9	-8	8	55	0
L.L. (ksf)	0	11	10	3	1	-1	1	8	0
F.W.S. (ksf)	0	-62	-55	-109	-62	-111	-67	-63	0
F.W.S.+ L.L. (ksf)	0	-50	-45	-106	-61	-112	-66	-55	0
Design F.W.S.+L.L. (ksf)	0	-83	-65	-146	-66	-149	-72	-86	0

C.3 Load Test 2

C.3.1 Deflected Shape Bridge Models Using Survey Data



Figure C.11: Deflected Shape Model for Scenario 1

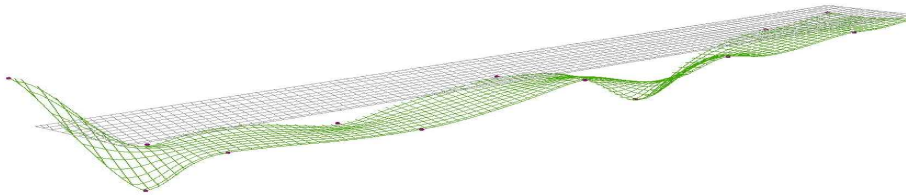


Figure C.12: Deflected Shape Model for Scenario 2

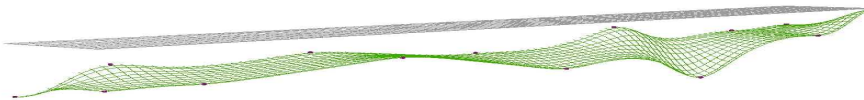


Figure C.13: Deflected Shape Model for Scenario 3

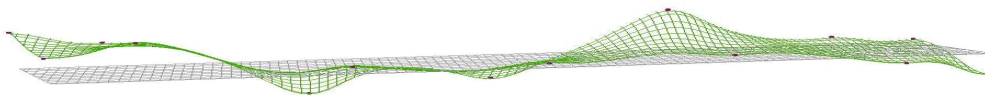


Figure C.14: Deflected Shape Model for Scenario 4



Figure C.15: Deflected Shape Model for Scenario 5

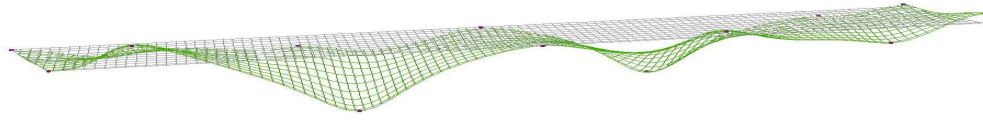


Figure C.16: Deflected Shape Model for Scenario 6



Figure C.17: Deflected Shape Model for Scenario 7

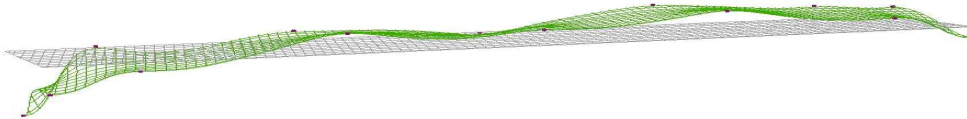


Figure C.18: Deflected Shape Model for Scenario 8

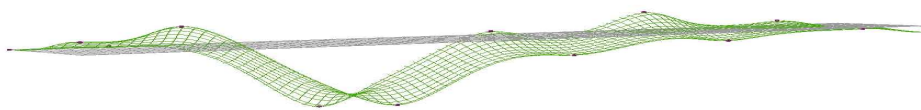


Figure C.19: Deflected Shape Model for Scenario 9

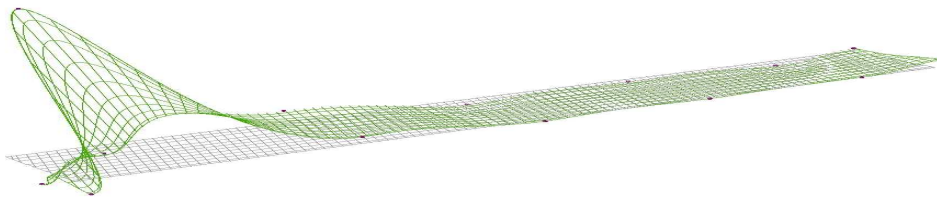


Figure C.20: Deflected Shape Model for Scenario 10

C.3.2 Load Testing Scenario Stresses from Deflection Tables

Table C.21: Scenario 1 East Bound Lane Top Fiber Stress

Scenario 1 East Bound: Top Fiber Stresses									
Location ID	West Abut.	Midspan (45)	Pier 1 (46)	Midspan (47)	Pier 2 (48)	Midspan (49)	Pier 3 (50)	Midspan (51)	East Abut.
L.L. (psi)	0	47	40	-34	12	10	-9	-50	0
L.L. (ksf)	0	7	6	-5	2	1	-1	-7	0
F.W.S. (ksf)	0	-63	-67	-111	-62	-109	-55	-62	0
F.W.S.+ L.L. (ksf)	0	-56	-61	-116	-60	-108	-56	-69	0
Design F.W.S.+L.L. (ksf)	0	-84	-77	-148	-66	-147	-60	-85	0

Table C.22: Scenario 1 West Bound Lane Top Fiber Stress

Scenario 1 West Bound: Top Fiber Stresses									
Location ID	East Abut	Midspan (44)	Pier 3 (43)	Midspan (42)	Pier 2 (41)	Midspan (40)	Pier 1 (39)	Midspan (38)	West Abut.
L.L. (psi)	33	-66	-57	0	0	0	0	47	0
L.L. (ksf)	5	-10	-8	0	0	0	0	7	0
F.W.S. (ksf)	0	-62	-55	-109	-62	-111	-67	-63	0
F.W.S.+ L.L. (ksf)	0	-71	-63	-109	-62	-111	-67	-56	0
Design F.W.S.+L.L. (ksf)	0	-83	-65	-146	-66	-149	-72	-86	0

Table C.23: Scenario 2 East Bound Lane Top Fiber Stress

Scenario 2 East Bound: Top Fiber Stresses									
Location ID	West Abut.	Midspan (45)	Pier 1 (46)	Midspan (47)	Pier 2 (48)	Midspan (49)	Pier 3 (50)	Midspan (51)	East Abut.
L.L. (psi)	0	-186	-159	-29	-10	-11	-10	-17	0
L.L. (ksf)	0	-27	-23	-4	-2	-2	-1	-2	0
F.W.S. (ksf)	0	-63	-67	-111	-62	-109	-55	-62	0
F.W.S.+ L.L. (ksf)	0	-90	-90	-115	-63	-111	-56	-64	0
Design F.W.S.+L.L. (ksf)	0	-84	-77	-148	-66	-147	-60	-85	0

Table C.24: Scenario 2 West Bound Lane Top Fiber Stress

Scenario 2 West Bound: Top Fiber Stresses									
Location ID	East Abut	Midspan (44)	Pier 3 (43)	Midspan (42)	Pier 2 (41)	Midspan (40)	Pier 1 (39)	Midspan (38)	West Abut.
L.L. (psi)	0	-27	-23	-68	-25	-38	-37	186	0
L.L. (ksf)	0	-4	-3	-10	-4	-6	-5	27	0
F.W.S. (ksf)	0	-62	-55	-109	-62	-111	-67	-63	0
F.W.S.+ L.L. (ksf)	0	-65	-58	-119	-65	-117	-72	-36	0
Design F.W.S.+L.L. (ksf)	0	-83	-65	-146	-66	-149	-72	-86	0

Table C.25: Scenario 3 East Bound Lane Top Fiber Stress

Scenario 3 East Bound: Top Fiber Stresses									
Location ID	West Abut.	Midspan (45)	Pier 1 (46)	Midspan (47)	Pier 2 (48)	Midspan (49)	Pier 3 (50)	Midspan (51)	East Abut.
L.L. (psi)	0	-140	-119	-19	-7	-57	-55	-7	0
L.L. (ksf)	0	-20	-17	-3	-1	-8	-8	-1	0
F.W.S. (ksf)	0	-63	-67	-111	-62	-109	-55	-62	0
F.W.S.+ L.L. (ksf)	0	-83	-84	-114	-63	-118	-62	-63	0
Design F.W.S.+L.L. (ksf)	0	-84	-77	-148	-66	-147	-60	-85	0

Table C.26: Scenario 3 West Bound Lane Top Fiber Stress

Scenario 3 West Bound: Top Fiber Stresses									
Location ID	East Abut	Midspan (44)	Pier 3 (43)	Midspan (42)	Pier 2 (41)	Midspan (40)	Pier 1 (39)	Midspan (38)	West Abut.
L.L. (psi)	0	-70	-60	-12	-5	-19	-18	-186	0
L.L. (ksf)	0	-10	-9	-2	-1	-3	-3	-27	0
F.W.S. (ksf)	0	-62	-55	-109	-62	-111	-67	-63	0
F.W.S.+ L.L. (ksf)	0	-72	-63	-111	-63	-114	-70	-90	0
Design F.W.S.+L.L. (ksf)	0	-83	-65	-146	-66	-149	-72	-86	0

Table C.27: Scenario 4 East Bound Lane Top Fiber Stress

Scenario 4 East Bound: Top Fiber Stresses									
Location ID	West Abut.	Midspan (45)	Pier 1 (46)	Midspan (47)	Pier 2 (48)	Midspan (49)	Pier 3 (50)	Midspan (51)	East Abut.
L.L. (psi)	0	93	80	6	2	6	-6	-63	2
L.L. (ksf)	0	13	11	1	0	1	-1	-9	0
F.W.S. (ksf)	0	-63	-67	-111	-62	-109	-55	-62	0
F.W.S.+ L.L. (ksf)	0	-49	-56	-110	-62	-109	-55	-71	0
Design F.W.S.+L.L. (ksf)	0	-84	-77	-148	-66	-147	-60	-85	0

Table C.28: Scenario 4 West Bound Lane Top Fiber Stress

Scenario 4 West Bound: Top Fiber Stresses									
Location ID	East Abut	Midspan (44)	Pier 3 (43)	Midspan (42)	Pier 2 (41)	Midspan (40)	Pier 1 (39)	Midspan (38)	West Abut.
L.L. (psi)	0	10	9	35	-13	-28	27	140	0
L.L. (ksf)	0	1	1	5	-2	-4	4	20	0
F.W.S. (ksf)	0	-62	-55	-109	-62	-111	-67	-63	0
F.W.S.+ L.L. (ksf)	0	-60	-53	-105	-64	-115	-63	-43	0
Design F.W.S.+L.L. (ksf)	0	-83	-65	-146	-66	-149	-72	-86	0

Table C.29: Scenario 5 East Bound Lane Top Fiber Stress

Scenario 5 East Bound: Top Fiber Stresses									
Location ID	West Abut.	Midspan (45)	Pier 1 (46)	Midspan (47)	Pier 2 (48)	Midspan (49)	Pier 3 (50)	Midspan (51)	East Abut.
L.L. (psi)	0	70	60	-7	-2	-6	-6	-10	0
L.L. (ksf)	0	10	9	-1	0	-1	-1	-1	0
F.W.S. (ksf)	0	-63	-67	-111	-62	-109	-55	-62	0
F.W.S.+ L.L. (ksf)	0	-53	-59	-112	-62	-110	-55	-63	0
Design F.W.S.+L.L. (ksf)	0	-84	-77	-148	-66	-147	-60	-85	0

Table C.30: Scenario 5 West Bound Lane Top Fiber Stress

Scenario 5 West Bound: Top Fiber Stresses									
Location ID	East Abut	Midspan (44)	Pier 3 (43)	Midspan (42)	Pier 2 (41)	Midspan (40)	Pier 1 (39)	Midspan (38)	West Abut.
L.L. (psi)	0	-95	81	5	-2	-4	4	47	0
L.L. (ksf)	0	-14	12	1	0	-1	1	7	0
F.W.S. (ksf)	0	-62	-55	-109	-62	-111	-67	-63	0
F.W.S.+ L.L. (ksf)	0	-75	-43	-109	-62	-112	-67	-56	0
Design F.W.S.+L.L. (ksf)	0	-83	-65	-146	-66	-149	-72	-86	0

Table C.31: Scenario 6 East Bound Lane Top Fiber Stress

Scenario 6 East Bound: Top Fiber Stresses									
Location ID	West Abut.	Midspan (45)	Pier 1 (46)	Midspan (47)	Pier 2 (48)	Midspan (49)	Pier 3 (50)	Midspan (51)	East Abut.
L.L. (psi)	0	0	0	-58	21	5	-5	33	0
L.L. (ksf)	0	0	0	-8	3	1	-1	5	0
F.W.S. (ksf)	0	-63	-67	-111	-62	-109	-55	-62	0
F.W.S.+ L.L. (ksf)	0	-63	-67	-120	-59	-109	-55	-57	0
Design F.W.S.+L.L. (ksf)	0	-84	-77	-148	-66	-147	-60	-85	0

Table C.32: Scenario 6 West Bound Lane Top Fiber Stress

Scenario 6 West Bound: Top Fiber Stresses									
Location ID	East Abut	Midspan (44)	Pier 3 (43)	Midspan (42)	Pier 2 (41)	Midspan (40)	Pier 1 (39)	Midspan (38)	West Abut.
L.L. (psi)	0	10	-9	-58	21	-10	-9	0	0
L.L. (ksf)	0	1	-1	-8	3	-1	-1	0	0
F.W.S. (ksf)	0	-62	-55	-109	-62	-111	-67	-63	0
F.W.S.+ L.L. (ksf)	0	-60	-56	-118	-59	-113	-68	-63	0
Design F.W.S.+L.L. (ksf)	0	-83	-65	-146	-66	-149	-72	-86	0

Table C.33: Scenario 7 East Bound Lane Top Fiber Stress

Scenario 7 East Bound: Top Fiber Stresses									
Location ID	West Abut.	Midspan (45)	Pier 1 (46)	Midspan (47)	Pier 2 (48)	Midspan (49)	Pier 3 (50)	Midspan (51)	East Abut.
L.L. (psi)	0	0	0	0	0	-35	34	-3	0
L.L. (ksf)	0	0	0	0	0	-5	5	0	0
F.W.S. (ksf)	0	-63	-67	-111	-62	-109	-55	-62	0
F.W.S.+ L.L. (ksf)	0	-63	-67	-111	-62	-115	-50	-62	0
Design F.W.S.+L.L. (ksf)	0	-84	-77	-148	-66	-147	-60	-85	0

Table C.34: Scenario 7 West Bound Lane Top Fiber Stress

Scenario 7 West Bound: Top Fiber Stresses									
Location ID	East Abut	Midspan (44)	Pier 3 (43)	Midspan (42)	Pier 2 (41)	Midspan (40)	Pier 1 (39)	Midspan (38)	West Abut.
L.L. (psi)	0	36	31	-12	-4	-5	-5	47	0
L.L. (ksf)	0	5	4	-2	-1	-1	-1	7	0
F.W.S. (ksf)	0	-62	-55	-109	-62	-111	-67	-63	0
F.W.S.+ L.L. (ksf)	0	-56	-50	-111	-63	-112	-68	-56	0
Design F.W.S.+L.L. (ksf)	0	-83	-65	-146	-66	-149	-72	-86	0

Table C.35: Scenario 8 East Bound Lane Top Fiber Stress

Scenario 8 East Bound: Top Fiber Stresses									
Location ID	West Abut.	Midspan (45)	Pier 1 (46)	Midspan (47)	Pier 2 (48)	Midspan (49)	Pier 3 (50)	Midspan (51)	East Abut.
L.L. (psi)	0	-93	-80	14	5	20	19	-30	0
L.L. (ksf)	0	-13	-11	2	1	3	3	-4	0
F.W.S. (ksf)	0	-63	-67	-111	-62	-109	-55	-62	0
F.W.S.+ L.L. (ksf)	0	-76	-79	-109	-61	-107	-52	-66	0
Design F.W.S.+L.L. (ksf)	0	-84	-77	-148	-66	-147	-60	-85	0

Table C.36: Scenario 8 West Bound Lane Top Fiber Stress

Scenario 8 West Bound: Top Fiber Stresses									
Location ID	East Abut	Midspan (44)	Pier 3 (43)	Midspan (42)	Pier 2 (41)	Midspan (40)	Pier 1 (39)	Midspan (38)	West Abut.
L.L. (psi)	0	27	23	19	-7	7	6	-233	0
L.L. (ksf)	0	4	3	3	-1	1	1	-34	0
F.W.S. (ksf)	0	-62	-55	-109	-62	-111	-67	-63	0
F.W.S.+L.L. (ksf)	0	-58	-51	-107	-63	-110	-66	-96	0
Design F.W.S.+L.L. (ksf)	0	-83	-65	-146	-66	-149	-72	-86	0

Table C.37: Scenario 9 East Bound Lane Top Fiber Stress

Scenario 9 East Bound: Top Fiber Stresses									
Location ID	West Abut.	Midspan (45)	Pier 1 (46)	Midspan (47)	Pier 2 (48)	Midspan (49)	Pier 3 (50)	Midspan (51)	East Abut.
L.L. (psi)	0	47	40	-51	-19	-8	-7	-23	0
L.L. (ksf)	0	7	6	-7	-3	-1	-1	-3	0
F.W.S. (ksf)	0	-63	-67	-111	-62	-109	-55	-62	0
F.W.S.+L.L. (ksf)	0	-56	-61	-119	-65	-111	-56	-65	0
Design F.W.S.+L.L. (ksf)	0	-84	-77	-148	-66	-147	-60	-85	0

Table C.38: Scenario 9 West Bound Lane Top Fiber Stress

Scenario 9 West Bound: Top Fiber Stresses									
Location ID	East Abut	Midspan (44)	Pier 3 (43)	Midspan (42)	Pier 2 (41)	Midspan (40)	Pier 1 (39)	Midspan (38)	West Abut.
L.L. (psi)	0	-10	9	10	4	-59	57	0	0
L.L. (ksf)	0	-1	1	1	1	-9	8	0	0
F.W.S. (ksf)	0	-62	-55	-109	-62	-111	-67	-63	0
F.W.S.+L.L. (ksf)	0	-63	-53	-108	-61	-120	-59	-63	0
Design F.W.S.+L.L. (ksf)	0	-83	-65	-146	-66	-149	-72	-86	0

Table C.39: Scenario 10 East Bound Lane Top Fiber Stress

Scenario 10 East Bound: Top Fiber Stresses									
Location ID	West Abut.	Midspan (45)	Pier 1 (46)	Midspan (47)	Pier 2 (48)	Midspan (49)	Pier 3 (50)	Midspan (51)	East Abut.
L.L. (psi)	0	-96	82	9	-3	-2	2	36	0
L.L. (ksf)	0	-14	12	1	0	0	0	5	0
F.W.S. (ksf)	0	-63	-67	-111	-62	-109	-55	-62	0
F.W.S.+ L.L. (ksf)	0	-77	-55	-110	-62	-110	-54	-56	0
Design F.W.S.+L.L. (ksf)	0	-84	-77	-148	-66	-147	-60	-85	0

Table C.40: Scenario 10 West Bound Lane Top Fiber Stress

Scenario 10 West Bound: Top Fiber Stresses									
Location ID	East Abut	Midspan (44)	Pier 3 (43)	Midspan (42)	Pier 2 (41)	Midspan (40)	Pier 1 (39)	Midspan (38)	West Abut.
L.L. (psi)	0	23	-20	-3	-1	15	-15	-143	0
L.L. (ksf)	0	3	-3	0	0	2	-2	-21	0
F.W.S. (ksf)	0	-62	-55	-109	-62	-111	-67	-63	0
F.W.S.+ L.L. (ksf)	0	-58	-57	-110	-62	-109	-69	-83	0
Design F.W.S.+L.L. (ksf)	0	-83	-65	-146	-66	-149	-72	-86	0

APPENDIX D: SENSOR STRESS CHARTS AND DATA (CD-ROM)

One year worth of sensor stress charts and data are provided on the attached CD organized in two separate folders:

- Stress Charts
- Raw Data Spreadsheets

The organization of the stress charts and the raw data folders are shown in the following two illustrations.

